”Adaptive mutations” in the S/MAPK pathways provide selective advantage in quiescent fission yeast

Rostyslav Makarenko

Sorbonne University

Ecole Doctorale : Complexité du Vivant

Laboratoire : Dynamique du génome

« Adaptive mutations » in the S/MAPK pathways provide a selective advantage in quiescent fission yeast

Thèse de doctorat en Complexité du Vivant

Présentée par :

Rostyslav Makarenko

Dirigée par : Benoit Arcangioli et Serge Gangloff

Présentée et soutenue publiquement le 29 avril 2019

Devant un jury composé de :
Président : Ivan Matic
Rapporteur : Geneviève Thon
Rapporteur : Isabelle Sagot
Examinatrice : Jenny Wu
Examinatrice : Nathalie Dostatni
Directeur de thèse : Benoit Arcangioli
Co-Directeur de thèse : Serge Gangloff

Remerciements.

I would like first to give a message of thanks to Dr Isabelle Sagort and Dr Geneviève Thon for finding the time to provide corrections to my manuscript and participate in my thesis committee. I would like to say thanks to Ivan Matic, Nathalie Dostatni and Jenny Wu for participation in my thesis committee and for a productive discussion.

Thanks to my family: my father Olexander Makarenko, my mother Hanna Makarenko, my brother Anton Makarenko and my brother Olexander Makarenko. My family is my harbour, I Love you all. I can always count on you, whatever happens in Life.

A big thanks to the members of the Dynamique du Genome Unit! Thank you, Benoit and Serge, amazing scientists for teaching me during my PhD studies. I am proud to have you as my supervisors! Thank you, Stefania and Catherine, for your professional help as the scientists and researcher during my PhD.

An incredible thanks to Claire, every time I need to find something somewhere, I knew who should I ask. Thank you for the lemon cakes and praise for the help dealing with S. pombe cells in quiescence.

I would like to say thanks to Dr Valentyn Oksenych, my Ukrainian friend, currently Professor in NTNU, Trondheim, Norway. Thank you for sharing your knowledge and experience. Thank you for helping me during my initial steps in searching for PhD position. Also, thank you for your hospitality in Norway on Aug 2016. Looking forward to meet you during our carrier paths.

An incredibly big thanks for people from France, accepting me, entrager from Ukraine, almost European, as your friend: Simon, Valentin, Celia, Lena, Olivia, Wilhelm, Claire, David, Elodie and Antonin, Alicia and Quentin (and of course Hugo), Lucie and Maxim.

Sorry for my level of the French language, I have not improved it to the level I wish, but I fell in love with this language. Thank for all the time we have spent together: watching GoT, hiking in Fontainebleau, celebrating birthdays, weddings and New Years, sharing the meals and incredible emotions.

Special thanks to Luccie Poggi, my bench neighbour for incredible nice time for healthy atmosphere, for awesome jokes and great smiles (no more nasty jokes, just the nice ones ;-)).

Thank you, Olivia, Wilhem and Léna for sharing a beer, GoT series and a big fun during this PhD.

Thank you Samia and Celia. You two understand and support me like nobody else in this world. I have no words to express how your support was vital for me during this time. The warm of Hearts is the thing that allowed me to push this job till the end. I wish you could have so much more Luck in your Lifes. I want to you so much Happiness and so much Luck in your Futures as it could be imagined!

Thank you all!

Thanks to Bioinformatics Institut and all the beautiful people I met there. You have provided a knowledge that really matters in the modern world, and you have open a door into a Big world. Thanks to Yuriy Aulchenko from RSSSO for choosing me for that summer school.

A special thanks goes to German Demidov, whose joke have costed me so much, but whose lesson taught me the real matters of things in this world. I wish you Herostratic fame!

Thank you GRAND RANDOM for this chance!

I am a completely adult now.

Abstract

Quiescence and proliferation reflect two fundamentally different cellular stages, yet very limited information exists on how cells maintain their genome stability in quiescence. Using nitrogen-starved fission yeast as a model for quiescence, our laboratory has demonstrated that cells are not only subject to DNA damage in G_0 but also accumulate replication-independent mutations linearly with time. In our current work, we have demonstrated that mutations accumulating in growth-arrested phase undergo a selection process in quiescence similar to that observed in *E. coli*. Selection favors mutations that affect functions of the genes of the MAP-kinase (*mkh1*, *pek1*, *pmk1*) and SAP-kinase pathways (*win1*, *wis1*, *sty1*), and their downstream targets (*pmc1*, *sgf73*, *tif452*). These genes represent core cellular signaling that regulates cell proliferation, cell differentiation, and cell death conserved among all eukaryotic species from yeast to human. Mutations in components of the S/MAPK pathways and their regulators are associated with multiple diseases in humans, primary cancer and degenerative neuronal death accumulated with ageing. In this work, we have demonstrated that wild-type cells dying in quiescence release traces of nitrogen that triggers the viable population to exit from quiescence. The wild-type cells are dying during their entry into S-phase releasing more nitrogen. Thus, mutants in the S/MAPK pathways are better scavengers and selection in quiescence is characterized by the ability of the mutant to resume cycling in quiescence coupled with a resistance to programed cell death.

Résumé

La quiescence et la prolifération reflètent deux stades cellulaires fondamentalement différents, mais il existe très peu d'informations sur la manière dont les cellules maintiennent la stabilité de leur génome en quiescence. En utilisant des levures de fission privées d'azote comme modèle de quiescence, notre laboratoire a démontré que les cellules subissent non seulement les dommages de l'ADN au stade G_0, mais accumulent également des mutations indépendantes de la réplication linéairement avec le temps. Dans les travaux en cours, nous avons démontré que les mutations accumulées au cours de la phase d'arrêt de la croissance subissent un processus de sélection en quiescence similaire à celui observé chez *E. coli*. La sélection favorise les mutations qui affectent les fonctions des gènes des voies de la MAP-kinase (*mkh1*, *pek1*, *pmk1*) et de la SAP-kinase (*win1*, *wis1*, *sty1*) et de leurs cibles en aval (*pmc1*, *sgf73*, *tif452*). Ces gènes sont impliqués dans la signalisation cellulaire centrale qui régule la prolifération, la différenciation et la mort cellulaire conservée chez toutes les espèces eucaryotes, de la levure à

l'homme. Des mutations dans des composants de la voie S/MAPK ou dans ses régulateurs sont associées à de multiples maladies chez l'homme, dont certains cancers et une mort neuronale dégénérative en fonction de l'âge. Les cellules libèrent des traces d'azote lors de leur mort, ce qui déclenche l'entrée dans le cycle cellulaire des cellules encore en vie. Les cellules sauvages ne peuvent compléter un cycle et meurent, libérant davantage d'azote. Les mutants de la voie S/MAPK sont caractérisés par une capacité d'entrée dans le cycle différente en fonction de la concentration d'azote disponible ce qui entraine une résistance à la mort cellulaire.

Table of Contents

List of figures

List of tables

List of equations

List of codes

List of abbreviations

(encountered more than 5 times in the manuscript)

bp – Base Pair

CLS – Chronological Life Span

DNA – DeoxyriboNucleic Acid

EMM – Edinburgh Minimal Medium

EMM-N – Edinburgh Minimal Medium without Nitrogen

GASP – Growth Advantage in Stationary Phase

MAP kinase – Mitogen Activated Protein kinase

PCR – Polymerase Chain Reaction

RLS – Replicative Life Span

RNA – RiboNucleic Acid

S. cerevisiae – *Saccharomyces cerevisiae*

S. pombe – *Schizosaccharomyces pombe*

YES – Yeast extract with supplement

INTRODUCTION

1 INTRODUCTION

Quiescence and proliferation reflect two fundamentally different cellular stages, yet the right decision between proliferation and non-proliferation should provide survival adaptation in a changing environment. In multicellular organisms, fluctuations between quiescence and proliferation are critical for development and tissue homeostasis in adults. Cell proliferation usually includes the following characteristics: cell division (increase in the number of the cells), full-genome replication of DNA and cell growth. Quiescence is a physiological stage when cells temporary or permanently exit from the cell cycle, arrest in G_0 but remain metabolically active.

Quiescence is widespread among both multicellular and unicellular organisms. More than 25 years ago, it has been proposed that quiescence is one of the most common stages in Nature among unicellular organisms (Lewis and Gattie, 1991). Quiescence is probably the most common form of the plankton and it is estimated that 60% of the earth's biomass is composed of resting microorganisms (Dassow and Montresor, 2010; Johnston et al., 2004).

In multicellular organisms, quiescent cells are present in two different forms regarding their ability to resume cycling. The first type of quiescent cells is temporarily arrested in quiescence with the ability to resume cycling under a given stimulus. Embryonic cells during diapause and many adult cells as stem cells, progenitor cells, fibroblasts, lymphocytes, hepatocytes and some epithelial cells are an example of temporarily arrested mammalian cells (Yao, 2014). In plants, temporarily arrested cells are found in the form of meristematic stem cell progenitors or suppressed seeds and buds (Velappan et al., 2017).

The second category is post-mitotic quiescent cells that have lost the ability to exit from G0 (myocytes, neurons). The experiments that attempted to exit differentiated cells from G0 in vitro reported that it results in cell death (Kruman, 2004). However, upon reprograming into a dedifferentiated stage, post-mitotic cells can lose their status and acquire the ability to resume cycling. This type of behavior was found both in plant and animal tissues. Under wounding damage, dedifferentiation can be a signal of early-stage cancer (Friedmann-Morvinski and Verma, 2014; Sell, 1993).

The decision between the proliferation and quiescence, quiescence entry, maintenance and exit in mammalian is under the control of many pathways: retinoblastoma Rb-E2F pathway, various

MAP-kinase signal pathways (Notch-HES1), stress response pathways (p53 and p38), metabolic pathways (PI3K and mTOR), pathways implicated in autophagy and epigenetic regulation (microRNAs, histone methylation) (Yao, 2014). Importantly, many of these pathways are found in unicellular eukaryotes suggesting that genes controlling quiescence are conserved from yeast to humans (Yanagida, 2009). MAP kinase pathways are the core cellular modules in eukaryotes regulating the fundamental properties of the cell (proliferation and mitosis, stress response and gene expression, differentiation, cell survival and apoptosis), allowing to adapt rapidly to the changing environment (Pearson et al., 2001). Somatic mutations in these pathways are the usual hallmarks of cancer and multiple other human diseases (Dhillon et al., 2007; Kim and Choi, 2010).

There is little information existing on how quiescent cells maintain genome stability. The key difference between these cellular stages is DNA replication. Replication, and in particular DNA polymerase activity on the one hand, is a source of mutations (Ganai and Johansson, 2016). On the other hand, replication is coupled with the DNA damage response necessary for efficient repair (Branzei and Foiani, 2005). Increasing evidence that quiescent cells can accumulate mutations independently from the replication process will allow understanding better the development of age-related diseases like cancer or neurodegenerative diseases. (Leija-Salazar et al., 2018).

During growth arrest in response to stress, prokaryotic cells activate a mechanism inducing mutagenesis and genome instability called stress-induced mutagenesis (Foster, 2007). It is possible that similar mechanisms of genome instability are implicated in cancer development (Fitzgerald et al., 2017).

1.1 The different states of non-dividing cells

Quiescence is only one possible type among the various non-dividing stages of the cell. Definition of the quiescence stage distinguishes it from other non-dividing cellular stages: *dormancy* - metabolically inactive cells, for instance in plant seed or microbiologic spores, also used in the context of cancer dormancy (reviewed in (Lennon and Jones, 2011; Rittershaus et al., 2013); *senescence* - irreversible cell cycle arrest of the aberrant cells that are under certain stress stimuli, usually associated with cellular damage appearing with aging often linked to telomere length and oncogenic suppression (reviewed in, (Campisi and d'Adda di Fagagna, 2007; Fridlyanskaya et al., 2015; Hernandez-Segura et al., 2018; Rodier and Campisi, 2011;

van Deursen, 2014); *persistence* - growth-limiting stage that refers to the bacterial or fungal resistance to antibiotics) (reviewed in (Harms et al., 2016; Lewis, 2007; Yaakov et al., 2017) (Figure 1)

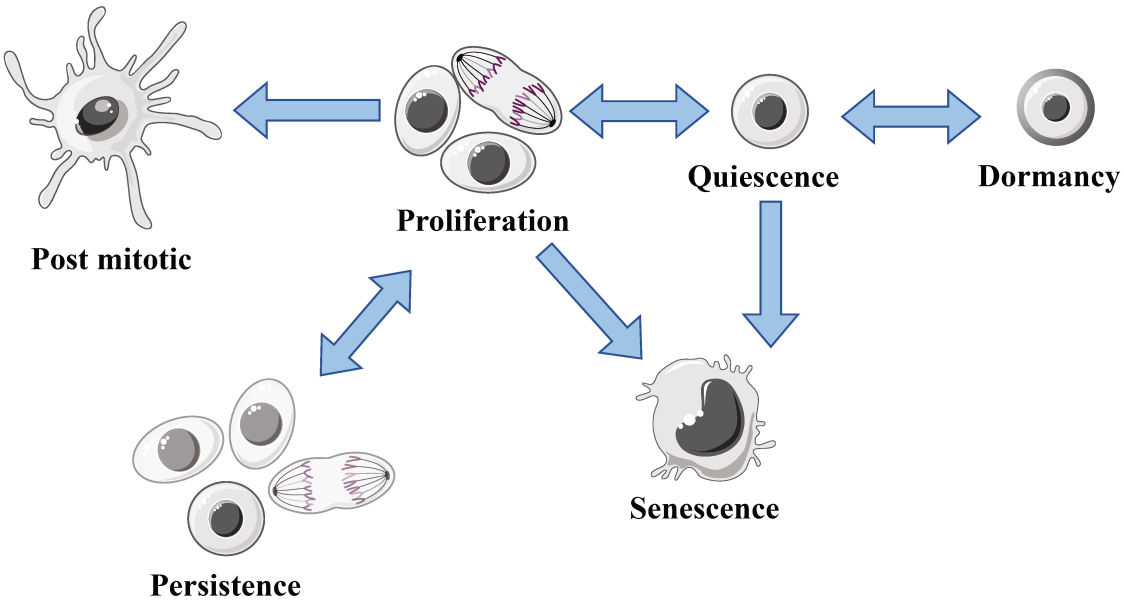

Figure 1: Various non-dividing stages of cells and their relationship.

Proliferating cells can arrest in various non-dividing stages. Post-mitotic and senescent cells are irreversible, whereas quiescence, persistence and dormancy are reversible stages.

1.1.1 Senescence

Senescence - is a permanent state of the cell cycle arrest usually associated with cellular damage over time. Senescence was first discovered *in vitro* human fibroblast cell culture by Leonard Hayflick as the fact that cells are permanently arrested after 50 cellular divisions with no ability to return into the cell cycle (Hayflick, 1965; Hayflick and Moorhead, 1961) due to constant shortening of the telomere length (Campisi, 1997). Thus, a decrease in proliferation potential observed after multiple cell divisions that ultimately leads to a complete arrest is named replicative senescence. Senescence as a progressive loss of the ability of the cells to proliferate has become one of the first theories of ageing (Herbig, 2006).

Senescent cells are characterized by a permanent cell cycle arrest, usually in G1 (Carnero, 2013), growth without cell division (hypertrophy) (Wright et al., 2013) and resistance to apoptotic stimuli (Carnero, 2013; Childs et al., 2014). Importantly, activation of the mTOR pathway in mammalian is necessary for the enlargement of the cell body of senescent cells, and

TOR pathways are known to integrate various stress signals and to modulate cell growth accordingly (Bent et al., 2016; Lloyd, 2013; Loffredo et al., 2013).

Based on the source of the damaging agent, cellular senescence can acquire various forms: *DNA damage-induced senescence*, *oxidative stress-induced senescence* (Colavitti and Finkel, 2005) *chemotherapy-induced senescence* (Ewald et al., 2010)**,** *postmitotic cellular senescence* (Sapieha and Mallette, 2018), *oncogene-induced senescence* (Chandeck and Mooi, 2010).

Oncogene-induced senescence (OIS) is an excellent example of a robust and sustained antiproliferative response resulting from aberrant mitogenic signaling that can lead to permanent cell cycle arrest and cellular senescence (DiMauro and David, 2010). OIS is a protective mechanism against cancerogenesis, and it is prevalent in pre-malignant tumors, and progression to malignancy requires evading senescence (Collado and Serrano, 2010)**.** OIS is a protective mechanism that allows multicellular organisms to counteract tumor formation at an initial stage of the oncogenic transformation.

The phenomenon of OIS was first discovered in an in vitro model in a lung fibroblast cell line where cells containing an activated form of RAS (HRAS-G12V) were arrested after six days of proliferation in G_1 and express the typical senescence markers (Serrano et al., 1997). In OIS, initial hyperactivation of the RAF-ERK MAP kinase pathway results in inhibition of cellular proliferation due to the presence of the classical negative feedback loop that counteracts the effect of oncogenic Ras on its downstream effectors (Courtois-Cox et al., 2006). This feedback loop is regulated by dual specificity MAPK phosphatases: the activated form of MAP kinase acquires affinity to the MAP phosphatase and binding causes conformation changes that turn the phosphatase into an active form. This complex, in turn, catalyzes the dephosphorylation of activated MAP kinases and deactivates them (Kidger and Keyse, 2016; Kondoh and Nishida, 2007).

Accordingly, the signaling produced by oncogenic Ras becomes tumorigenic only when the negative feedback loops are canceled or when they are bypassed by the upregulation of the oncogene. OIS is described in multiple in vitro and in vivo models (Collado and Serrano, 2010). Mutations and phenotypes associated with OIS are often found in melanomas (malignant transformed nevi) (Gray-Schopfer et al., 2006) and in neurofibrosarcoma (malignant transformed schwannoma and schwannoma) (Courtois-Cox et al., 2006).

Senescent cells may create a favorable microenvironment for surrounding cancer cells in heterogeneous tumors, stimulating proliferation by secreting growth chemokines and cytokines, remodeling the surrounding microenvironment both by autocrine or paracrine mechanisms. The ability of the cells to regulate senescent cell cycle arrest by secretion and taking up the secretory molecules was named senescence associated secretory phenotype (SASP) (Coppe et al., 2010). For example (Wajapeyee et al., 2008) has demonstrated that BRAFV600E melanoma cell lines secrete Insulin-like growth factor-binding protein 7, regulating the availability of insulin-like growth factors, and secreted molecules are taken up by senescent cells inhibiting the RAF-MEK1/2-ERK1/2 pathway. Similar regulation of the proliferation-quiescence decision by taking up the secretory molecules in unicellular organisms was called quorum sensing (Sprague, 2006). Quorum sensing has been confirmed in *E. coli* and *S. cerevisiae* stationary cultures. Thus, medium from stationary cell cultures of budding yeast triggers filament growth, providing an adaptation to adverse environmental conditions (Chen, 2006).

Aging is an equivalent of cellular senescence in unicellular organisms which is assayed primarily by measuring replicative or chronological lifespan. **Replicative life span** (RLS) is a measure of the number of divisions an individual cell can undergo before death mostly by tracking cells on a single-cell level. **Chronological life span** (CLS) is a calculation of the time length that cells can be maintained in a non-dividing stage when the whole population is tracked, by measuring the viability of non-dividing cells in the stationary phase or upon starvation. (Florea, 2017).

RLS has been confirmed in asymmetrically dividing species. *S. cerevisiae* is an excellent example of RLS, as proliferation in budding yeast is performed by growth and septation of a bud. An individual yeast cell can make approximately 20-25 cell divisions, after which they enter into a short post-proliferative stage followed by cell lysis (Mortimer and Johnston, 1959). In bacteria, RLS in asymmetrically dividing cells has been described on the example of *Caulobacter crescentus*. The generation capacity of an individual bacterial cell is constitutively declining with time (Ackermann, 2003). Stem cells are an example of asymmetrically dividing cells where one cell retains the properties of the stem cell while the other undergoes differentiation. The hypothesis of an asymmetric cell division in stem cells has proposed that the parental strand of DNA is sequestered in the daughter stem cell, while the newly synthesized DNA is segregated to the differentiated cell. Thus, the stem cell keeps the original DNA during its whole life, while differentiated cells inherit DNA that contains mutations due to replication

(Cairns, 1975). The hypothesis of the immortal DNA stand has been confirmed for muscle satellite cells (Conboy et al, 2007; Shinin et al, 2006), denied for hemopoietic stem cells (Kiel et al., 2007) and neither proven nor refuted yet in other systems (Yennek and Tajbakhsh, 2013).

In organisms dividing by fission (*S. pombe* and *E. coli*), mother and daughter cells are distinguished by the inheritance of the old or young pole. The "old" cell inherits damaged proteins fused into large aggregates due to the effect of macromolecular crowding and diffusion (Lindner et al., 2008; Stewart et al., 2005). Thus, cells that continuously receive the old pole experience a small but significant decreased division rate (Lindner et al., 2008; Stewart et al., 2005). Upon conditions of increased stress, the old pole lineage division rate can decrease continuously until death (Spivey et al., 2017). Despite the clear role of protein damage, aging in *E. coli* could not be explained by protein aggregates alone, and it is likely that factors other than protein damage are involved (Lindner et al., 2008). Thus, during proliferation, *E. coli* and *S. pombe* do not age in benign conditions but do age under stress.

Notably, both fission and budding yeast contain active telomerase. Hence, RLS in yeast is telomerase independent. However, like in mammals, telomeres from yeast cells with reduced telomerase activity progressively shorten with each cell division. At a late time point of senescence, most of the cells die or remain arrested (Nakamura et al., 1997). Similar results have been reported from budding yeast: *S. cerevisiae* cells exhibit progressive telomere shortening and lose viability after about 60–80 generations (Lustig and Petes, 1986).

The majority of the experiments on Chronological lifespan performed on *E. coli* or *S. cerevisiae* models were performed under conditions where the microbial population is grown in rich medium until saturation and maintained in the same medium without replenishing the nutrients (Fabrizio and Longo, 2003; 2007). Chronological lifespan also refers to multicellular eukaryotes, for terminally differentiated postmitotic cells such as neurons (MacLean et al., 2001). In both yeast and human fibroblasts, chronological age is known to influence the cells replicative capacities; the longer the time in quiescence, the fewer divisions a cell can undergo upon proliferation resumption (Ashrafi et al., 1999; Marthandan et al., 2014; Munro et al., 2001).

1.1.2 Dormancy

Dormancy – is a non-dividing cellular stage described by a significant decline of cellular metabolism up to almost a full restriction, developed as an adaptation to unfavorable environmental conditions. The term "dormancy" is in use regarding the following categories:

1) season dormancy of multicellular organisms: mammalian *hibernation* (Carey et al., 2003) and *aestivation* (Charlwood et al., 2000), *embryonic diapause* (Koštál, 2006; Poelchau et al., 2013), *plant seed dormancy* (Baskin and Baskin, 2004; Finkelstein et al., 2008).

Similar to unicellular organisms, dormancy in animals and plants is characterized by a significant depression of the metabolism and reduced or even ceased cellular proliferation (Carey et al., 2003; Lengwinat and Meyer, 1996). The molecular mechanisms of dormancy in multicellular species are very poorly studied, but an implication of the core signaling pathways (ERK and p38 MAP kinases in animals both in vertebrates and invertebrates) has been reported in several cases (Storey and Storey, 2012; Zhu et al., 2005). In the dormant stage, both animals and plants can survive a prolonged period: months, years and even decades (Powell, 2001).

2) dormancy of microorganisms as an adaptation to the unfavorable environmental conditions (reviewed in (Rittershaus et al., 2013)); Gram-positive bacteria, particularly *Bacillus*, *Clostridium*, *Sporohalobacter*, *Anaerobacter*, and *Heliobacterium*, form special structures in dormancy as endospores (Errington, 2003), cysts or conidia. Unlike persister cells, endospores are the result of a morphological differentiation process triggered by nutrient limitations in the environment. Endospore formation implicates activation of sigma factors that are general response transcription factors. Dormant cells often acquire resistance to various stressful agents. For instance, *Bacillus* spores exhibit resistance to heat, desiccation, chemicals, UV exposure (SETLOW, 1995)**.**

Gram-negative bacteria (including *E. coli*) do not form special dormant structures (Nicholson et al., 2000). Instead, non-sporulating bacteria can enter into a special state of dormancy called viable but non-cultivable stage (VBNC) – an in vitro discovered phenomenon (Xu et al., 1982), where bacteria fail to grow and proliferate on an optimal substrate under a subset of stressful conditions but remain viable with the potential for regrowth for a prolonged period of time (Figure 2). VBNC has been described for at least 85 bacterial species, but its abundance in Nature remains largely unknown (Li et al., 2014). Multiple factors can trigger VBNC in

different species: temperature downshift, non-optimal pH, low-oxygen availability, drying and others. VBNC cells generally acquire a spherical cell shape like that observed in quiescence in fission and budding yeast (Al-Bana et al., 2013; Costa et al., 1999).

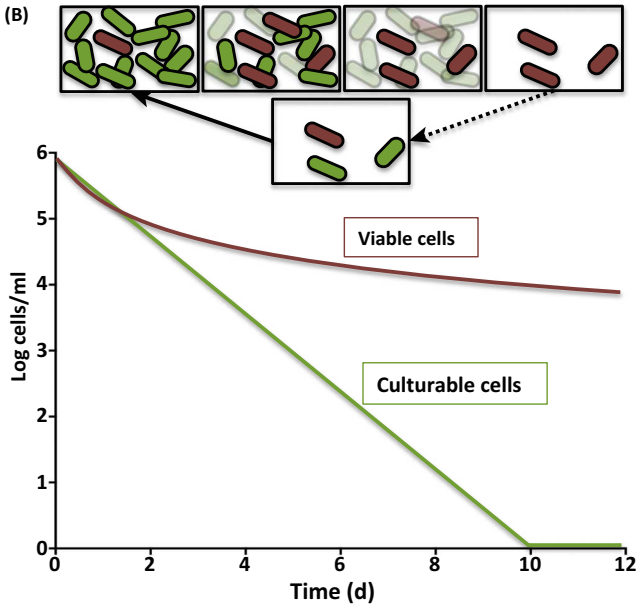

Figure 2: Viable cells are not necessarily culturable. From (Ayrapetyan et al., 2015).

Viable but not culturable cells are isolated by applying a lethal stress (e.g., cold temperature) to a growing culture. During this process, cells become undetectable on nutrient media (green line); however, a proportion of the population remains viable (red curve) as can be determined by a variety of viability assays. When the inducing stress is removed the population becomes culturable after a resuscitation period (broken arrow). When cells are provided with nutrients they give rise to a population that is similarly tolerant to the inducing stress as the original population (unbroken arrow).

3) dormancy of cancer cells (Aguirre-Ghiso, 2007; Gao et al., 2017; Gomis and Gawrzak, 2017; Marches et al., 2006) or dormancy as a form of latent infection of bacteria (*Mycobacterium tuberculosis* (Gengenbacher and Kaufmann, 2012) or yeast (Cryptococcus *neoformans* (Alanio et al., :2015))

Tumor dormancy reflects the capability of disseminated tumor cells, or micrometastases, to evade treatment and remain at a low number after primary tumor resection (Gomis and Gawrzak, 2017). Cancer dormancy can refer to two different types: tumor mass dormancy and cellular dormancy. Cellular dormancy is defined as an arrest in the cell cycle mediated by different signaling pathways. In tumor mass dormancy cell proliferation is balanced by apoptosis due to lack of nutrient supply and immune surveillance (Aguirre-Ghiso, 2007). Signaling mechanisms of cancer dormancy are poorly understood. However, there is evidence

that it is involved in the switch between proliferation and quiescence and in the regulation of cancer dormancy (Osisami and Keller, 2013; Ranganathan et al., 2006; Sosa et al., 2011). These signaling pathways are often activated in response to microenvironment factors and involve PI3K-AKT, p38 and ERK pathways. The microenvironment-induced stress also leads to p38 activation and ERK1/2 deactivation (Adam et al., 2009; Bragado et al., 2012). p38 activation has been shown to inhibit tumor progression, as it is implicated in promoting growth arrest through the activation of p53 and p16 signaling and the down-regulation of cyclin D1 (Bulavin et al., 2004; Demidov et al., 2006). It has also been implicated in reducing the expression and activation of the mitogenic signaling of ERK1/2. The ratio of ERK1/2 to p38 has been shown to predict if a tumor cell will proliferate or enter a dormant state upon dissemination, with a high ratio suggesting proliferation and a low ratio suggesting dormancy (Aguirre-Ghiso et al., 2003).

1.1.3 Persistence

Persistence **–** the ability of microorganisms (mainly bacteria) (Wuyts et al., 2018) stochastically or in response to stress enter a reversible slow-growth and low-metabolic stage in which cells acquire resistance to threatening damage (for instance – antibiotics). Persistence was first described in bacteria by Joseph W. Bigger in 1944 during the treatment of a staphylococcal infection with penicillin, in a context where a population of bacteria survives under antibiotic treatment and are capable of giving rise to a new population (Bigger, 1994). Importantly, this resistance is not inherited, because the surviving population of bacteria is as sensitive to the drug as the ancestor population. Nowadays, the term persistence has two meanings. In the strict sense, persistence is used for persistent infections, where the microorganisms (pathogenic bacteria and fungi) survive under the antibiotic treatment. In the broad sense, persistence is a general characteristic of any population in which cells survive under severe stress by generating slow-growing or non-growing cells (Glickman and Sawyers, 2012; Knoechel et al., 2014). Formation of persister cells is characterized by biphasic kinetics under treatment with antibiotics. A lethal dose of bactericidal antibiotics rapidly eradicates the sensitive portion of the population (Figure 3). The remaining viable cells in a population are only non-growing persister cells that are killed at a slower rate. The termination of antibiotic treatment enables the population to be replenished by the resuscitation of surviving persisters.

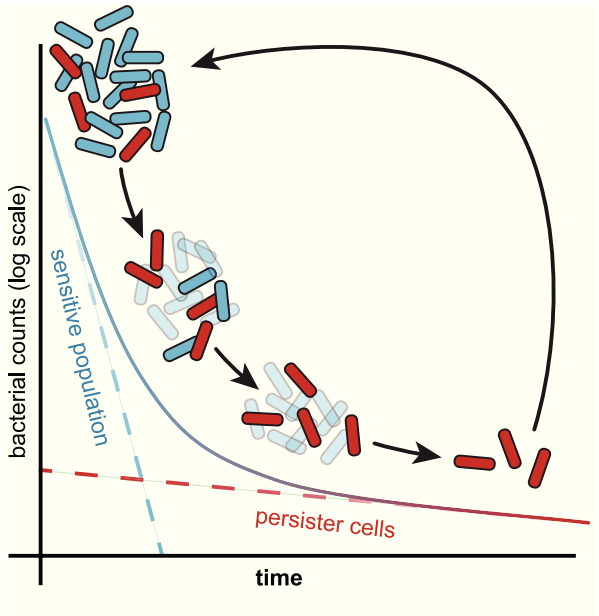

Figure 3: Biphasic killing kinetics of bactericidal antibiotic treatment. From (Harms et al., 2016)

A lethal dose of bactericidal antibiotic added at time zero rapidly eradicates the sensitive bulk of the population (blue) until only non- growing persister cells (red) that are killed at a slower rate remain. The slower killing has been interpreted to reflect the persister resuscitation rate, but this remains to be substantiated experimentally.The termi- nation of antibiotic treatment enables the population to be replenished by resuscitation of surviving persisters.

Activation of persistence beside antibiotic treatment has been reported in multiple environmental conditions. Persistence was reported both for planktonic and biofilms but the number of persistent cells is substantially higher in biofilms. For instance, *Pseudomonas aeruginosa* produces persistent cells at a 100-1000-fold higher rate in biofilms compared to the free-living form (Stewart et al., 2015). Therefore, persisters are likely just one face of a more general bacterial strategy to cope with dynamic and latently hostile environments. This hypothesis is in line with the finding that bacterial killing—not only by antibiotics but also by environmental hazards such as acid stress, toxic metals, or heat—displays biphasic kinetics (Gefen and Balaban, 2009).

Size and composition of the persister subpopulation in bacterial communities are controlled mainly by stress signaling pathways, such as the general stress response (RpoS) or the SOS response in conjunction with the second messenger (p)ppGpp that is almost always involved in persister formation (Harms et al., 2016). (p)ppGpp is an alarmone molecule, a part of the stringent response, a stress signaling pathway found in bacteria and plant chloroplasts that is a functional analogue of GTP signaling in animals.

Stringent response – is a bacterial stress response primary in reaction to amino-acid starvation (Haseltine and Block, 1973). Several other stresses like fatty acids, iron, or heat can trigger the stringent response as well. In *E. coli,* the stringent response is mediated by the alarmone, a (p)ppGpp guanosine pentaphosphate or tetraphosphate signal molecule (Jishage, 2002), causing inhibition of translation by targeting the tRNA regulon. Induction of the stringent response is usually found in parallel to upregulation of RpoS (Gentry et al., 1993). (p)ppGpp inhibits DNA, rRNA, nucleotides, and phospholipid synthesis, thereby arresting cell division and activating metabolic pathways that protect the vulnerable cells from environmental stress. Production of (p)ppGpp in *E. coli* is regulated by the (p)ppGpp synthetase RelA and the bifunctional synthetase/hydrolase enzyme SpoT. An implication of the stringent response in persistence formation has been shown in a series of experiments involving the gram-negative bacteria *E. coli* and *Pseudomonas aeruginosa* containing deactivation mutations in RelA/SpoT genes resulting in defective persistence formation under multiple conditions (Germain et al., 2015). Notably, mutations in genes responsible for amino acid synthesis cause defects in persistence, but a relation with the stringent response pathway has not been studied yet (Fung et al., 2010).

RpoS or σS factor – is a master regulator of the bacterial stress response that is activated upon different types of stimuli. Increase of RpoS is detected upon starvation for carbon, nitrogen or phosphate, hyperosmolarity (Muffler et al., 1996), abnormal temperatures (Sledjeski et al., 1996), pH (Bearson et al., 1996) or high density in the stationary phase (Lange et al., 1994). Sigma factors are proteins required for transcription initiation in bacteria. They are proteins that recruit RNA polymerase (RNAP) to the core promoters (Gruber and Gross, 2003). Together with RNA polymerase, sigma factors form a complex called RNA polymerase holoenzyme that directly or indirectly regulates the expression of 10% of the genes in *E. coli* (Hengge-Aronis, 2002).

The SOS-response can be activated under the perturbation of cellular homeostasis, extreme environmental conditions like oxidative stress, extreme pH, blocked DNA replication, and antibiotic treatment (Baharoglu and Mazel, 2014). The role of the SOS response in bacterial persistence is ambiguous. On the one hand, it serves as a stress response pathway that is necessary for persistence formation; on the other hand, induction of the SOS response is essential for DNA repair (Bernier et al., 2013). Thus, different stress signaling pathways involved in persister formation are known to enhance mutation rates, but leave open the possibility for an adaptive role of persistence in a given context (Kohanski et al., 2010).

Because both persistence and dormancy describe stress-induced phenotypes regulated by identical pathways, persistence can be considered as a dormant stage. Indeed, a phenotypic link between VBNC, persistence and dormancy in bacteria has been demonstrated recently (Kim et al., 2018).

Although persistence has been studied in the context of resistance to antibiotic treatment in pathogenic fungal infections (candidiasis (*Candida albicans*) (Erdogan and Rao, 2015) , meningitis (*Cryptococcus neoformans*) (Spitzer et al., 1993), and others, there is little information regarding the mechanisms of persistence formation in unicellular eukaryotes.

The first demonstration of persistence in eukaryotic cells has been reported by the Barkai laboratory in *S. cerevisiae* (Yaakov et al., 2017). This laboratory has developed an approach to detect persister cells based on the level of expression of the Hsp12 heat-shock protein in the rapidly growing, unstressed population. Hsp12 is part of the environmental stress response, whose induction by moderate stress protects cells from a range of severe stresses (Berry and Gasch, 2008). In these conditions, a small subpopulation of growing yeast (0.1%) produces high levels of Hsp12 protein and exhibits low proliferative potential (only 65% of the cells are able to form colonies) but becomes more resistant to almost all types of stress (temperature, chemical agents, etc.). Hsp12 induction in persistent cells of budding yeast correlates with DNA damage, as approximately half of the replication-blocked cells have a long-lived Rad52 focus, a marker of double strain break. Thus, severe DNA damage, such as DSB, triggers persistence in budding yeast. Prolonged DNA damage leading to persistence might culminate in mutations. Indeed, slow-growing cells significantly enriched in genetic mutations (mainly indels and SNVs) are found in the population. Finally, activation of the general stress response is important for yeast persistence, as the deletion of Msn2/4, a downstream target of the PKI pathway (Gasch et al., 2000), strongly reduces the persistent subpopulation.

1.1.4 Quiescence

Senescence, dormancy and persistence can be considered as extreme forms of cellular quiescence. The molecular links between quiescence establishment and cell cycle regulation are still unclear (Matson and Cook, 2016). Fascinating studies indicate that cells decide to enter quiescence long before they actually stop proliferating (Argüello-Miranda et al., 2018; Chassot et al., 2014; Hitomi and Stacey, 1999). Attempts to find quiescence-specific molecular markers are hampered by the complexity and the heterogeneity of the quiescence stages (Coller, 2011).

Unicellular organisms (bacteria and yeast) are commonly used as models for quiescence because its induction depends on a single factor in the medium. Laboratory systems exist that model the natural states of microbial quiescence based on growth inhibition at high cell density, on starvation for an essential nutrient or the combination of both. The first condition is reached by growing the culture to the stationary phase or a colony growing on solid surfaces. The second condition is reached by removing one of the essential nutrients from the medium: glucose, amino acids or nucleotides in auxotrophic strains, or macro elements (Sulfur, Phosphor) (Dykhuizen, 1990; Klosinska et al., 2011). Fission and budding yeast are well-developed systems for investigating quiescence.

By contrast, in *S. pombe*, the diauxic shift does not occur upon entry into the stationary phase because *S. pombe* lacks the glyoxylate cycle enzymes that are required for the utilization of ethanol for growth after glucose depletion. Thus, *S. pombe* cells arrest quickly under limited glucose conditions. Owing to the lack of diauxic shift, the fundamental properties of the stationary phase of *S. pombe* might be distinct from those of *S. cerevisiae*. *S. pombe* cell division ceases after cells reach a maximal concentration (2 x 10^8 /ml). Such cells are pear-shaped, 20% of them contain 1C DNA and lose viability rapidly. Fission yeast can grow and divide with 0.04% of glucose in the medium (by contrast, the standard concentration of glucose in EMM medium is 2% glucose and human blood contains 0.08% glucose (Tanaka and Yanagida, 1996; Yanagida, 2009) (Figure 4).

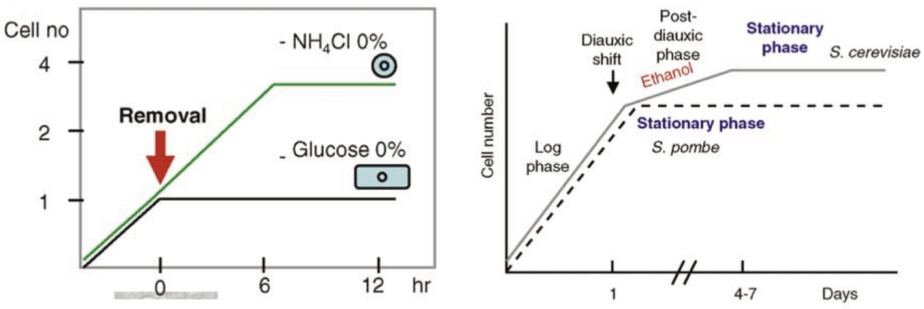

Figure 4: Comparison of quiescence models in *S. pombe* and *S. cerevisiae* (From (Yanagida, 2009)).

If glucose is completely eliminated from the growth medium, cells are arrested without further division. The resulting arrested cells are rod-shaped, similar to the growing cells. *S. pombe cells* can grow in 0.08% glucose in growth medium though the cell length is short. The stationary phase of *S. cerevisiae* is characterized by the diauxic shift, which is a metabolic shift from utilizing glucose to utilizing ethanol as an energy source.With this shift, *S. cerevisiae* cells slowly and continuously grow and reach the stationary phase after 6–7 days. In sharp contrast, *S. pombe* is not able to utilize ethanol because it lacks a glyoxylate cycle, and it enters the stationary phase within 1 day after finishing the log phase.

In *E. coli*, most of the models are based on stationary phase liquid cultures usually followed by depletion of a nutrient in the medium (Foster, 1999; Zinser and Kolter, 2004)}. Similar to eukaryotic cells passing into quiescence, stationary phase bacteria undergo a morphological adaptation. Cells become smaller and acquire a spherical form as the result of two processes, reductive division and dwarfing (Nyström, 2004). Dwarfing is a form of self-digestion and is the result of the degradation of endogenous cell material, especially from the cytoplasmic and the outer membranes that can be considered as a form of autophagy (Nyström, 2004). An alternative approach to block proliferation in *E. coli* and induce the resting state is to grow bacteria on a solid surface (agar plates) in the form of colonies or biofilms (Serra et al., 2013). Stationary phase entry is followed by activation of several global regulators and molecular pathways including RelA and SpoT – the master regulators of the starvation stringent response pathway (Magnusson et al., 2005) stress response factor RpoS. Detailed physiology of *E. coli* stationary phase cells is reviewed in (Nyström, 2004).

In more complex systems, like mammals, proliferating cells isolated from tissues in vitro can be induced into quiescence by serum deprivation, limitation of mitogens or by loss of adhesion and cell contact inhibition. The most frequently studied systems include fibroblasts (Mitra et al., 2018; Nishiyama et al., 1991), various neural cells (Vonlaufena et al., 2010), myoblasts (Sellathurai et al., 2013), myosatellite cells, hematopoietic stem cells, lymphocytes and others. Standard quiescence culture models in invertebrates include *D. melanogaster's* wing culture or *C. elegans*, where all the cells are arrested in a post-mitotic stage.

1.2 *Schizosaccharomyces pombe* (fission yeast)

Schizosaccharomyces pombe is a haploid unicellular eukaryotic organism originating from East Africa and discovered by Paul Linder in 1893 from millet beer. *S. pombe* belongs to the group of the Ascomycota fungi – the most diverse and widespread ecological group of yeast that comprises 64 000 species (1988). Based on a set of morphological and genomic features, the clade of fission yeast *Schizosaccharomyces* is divided into 4 species: *S. pombe*, *S. japonicus*, *S. octosporus* and *S. cryophilus* (Rhind et al., 2011). *S. pombe* is "domestic" species found in the ecological niches connected to human activity, and approximately 160 fission yeast strains have been collected worldwide from cultivated fruits like grapes, apples, cocoa; alcoholic beverages like tequila, rum, wine; kombucha (traditional fermented tea from Australian natives) and several others. However, the natural ecology remains largely unknown (Jeffares, 2018). Genomic sequencing of these strains has demonstrated moderate genetic diversity, indicating

that all known strains have a common ancestor, who lived approximately 2 300 years ago (Jeffares et al., 2015).

1.2.1 *S. pombe* genome

The 13.8 Mb genome of *S. pombe* is organized into three chromosomes: chromosomes I (5.7 Mb), II (4.6 Mb) and III (3.5 Mb) and has roughly 5000 protein-coding genes (Smith et al., 1987; Wood et al., 2002). According to the Pombase database, 69% of them have human orthologues, and over 500 of these genes are associated with a human disease (McDowall et al., 2014; Wood et al., 2011). Some of its genomic features make this yeast particularly suited to the study particular processes (Table 1). Both fission and budding yeast contain a genome of approximately the same size and gene number, but *S. pombe* genes have a more mosaic structure: 43% of the genes contain introns of a total number of about 5 000, while only 250 introns have been reported in budding yeast (Goffeau et al., 1996). Both species share genes with higher eukaryotes, but they do not share them with each other. *S. pombe* has an RNAi machinery similar to vertebrates, while it is missing from *S. cerevisiae*. As a consequence, fission yeast has a more complex heterochromatin organization (Grunstein and Gasser, 2013; Martienssen et al., 2005). Conversely, the *S. cerevisiae* genome encodes a family of PEX genes, responsible for peroxisome formation found virtually in all eukaryotic cells while *S. pombe* does not (Sibirny, 2016). *S. cerevisiae* has a small centromere of 125 bp in length, rarely found in eukaryotic cells. By contrast, *S. pombe* has large, repetitive centromeres (40–100 kb) more similar to the mammalian ones (Clarke et al., 1993; Furuyama and Biggins, 2007). Except for gametes, all or nearly all mammalian cells are diploid. While *S. cerevisiae* cells can be maintained as both haploids or diploids (Herskowitz, 1988), *S. pombe* is almost exclusively haploid: diploid forms of *S. pombe* are unstable in laboratory conditions, and only one natural diploid isolate has been reported so far (Jeffares et al., 2015)}. Both fission and budding yeast as well as mammalian form protective structures at the telomeric ends called t-loops. Where in vertebrates there are two complexes involved in t-loops formation (shelterin and trimeric complexes), fission yeast contains only the shelterin complex and budding yeast the trimeric complex (Price et al., 2014).

Table 1: Some features of the genomes of the two yeast *S. pombe* and *S. cerevisiae* in comparison with human

	H. sapiens	***S. pombe***	***S. cerevisiae***
Genome size	3 234.8 Mb	13.6 Mb	12.1 Mb
Protein-coding genes	20 000	5 000	6 000
RNAi	+	+	-
Type of centromeres	repetitive	repetitive	point
Number of chromosomes	23	3	16
Ploidy	diploid	haploid	diploid/haploid
Introns	common	common	rare
Peroxisome genes	+	-	+
Telomere complexes	shelterin/ trimeric complex	shelterin	trimeric complex

1.2.2 *S. pombe* cell cycle

Starting from the pioneering work of Paul Nurse, *S. pombe* is used as a model organism to investigate the genetics of cell cycle. The genes that regulate cell cycle progression in eukaryotes (cyclin and cyclin-dependent kinases) were primarily discovered in fission yeast (Nurse et al., 1976). In nutrient-rich medium *S. pombe* cells are rod-shaped, approximately 3 µm in diameter and 7.5-15 µm lengthwise (depending on the cell cycle stage), and grow by elongation at the ends. As in a typical eukaryotic cell, *S. pombe* genome duplication in S phase is separated from its segregation in M-phase when cell division occurs by an intermediate gap phase called G_2. Another gap phase called G_1 precedes S phase.

Fission yeast spends 70% of its time in G_2, and 30% of the remaining time is approximately equally split between G_1, S and M phases. *S. pombe* divides by fission, a symmetrical process in which a septum grows across the center of a long cylindrical cell, dividing the old cell into two equal new cells. Under optimum conditions, fission yeast doubles every 3 hours (rich medium). A time in G_1, called START in yeast is equivalent to the restriction point in mammalian cells (Pardee, 1974; Woollard and Nurse, 1995). Once cells have passed START,

they are committed and must complete the ongoing cell cycle. The second major decision point that determines the rate of progression through the cell division cycle is the timing of commitment to mitosis (M phase) at the G_2/M boundary, and is the major control point in fission yeast (Nurse, 1975). Under most laboratory conditions, fission yeast cells have already passed the size threshold to pass START before dividing. As a consequence, the next round of DNA replication is initiated before completion of the cytokinesis of the ongoing cell cycle.

The critical regulatory molecule during eukaryotic cell cycle progression is the cyclin-depended kinase (CDK). In budding and fission yeast, Cdc2 is the only cyclin-dependent kinase present (called Cdc28 in budding yeast). The activity of the Cdc2 is required for the onset of DNA replication and mitosis (Stern and Nurse, 1996). Cdc2 activity is low in G_1, increases during S-phase and G_2 and reaches a maximum in the M-phase. In *S. pombe,* Cdc2 activity is positively regulated through its association with the four cyclins: Cig1, Cig2, Puc1 and Cdc13 and negatively by Rum1. Cyclins are small proteins that do not have an enzymatic activity but have specific sites that recruit the CDK to specific substrates to activate downstream targets. The amount of Cdc2 during the cell cycle remains constant while the level of cyclins oscillates. Thus, the concentration of the cyclins in the cell cycle determines the function of Cdc2. G_0 cells have no S-phase cyclin (Cig2) but contain low levels of Cdc13, a mitotic cyclin B, and high levels of the CDK inhibitor Rum1 (Nurse, 1975).

1.2.3 *S. pombe* quiescence

The pioneering work on quiescence in fission yeast has been started in Mitsuhiro Yanagida's laboratory where it was shown that upon nitrogen starvation, heterothallic *S. pombe* strains enter quiescence instead of conjugation in the absence of a mating partner (Tanaka and Yanagida, 1996). Quiescence entry in fission yeast is followed by two cell divisions without growth and an arrest in G_0 with a 1C DNA content (Sajiki et al., 2009) (Figure 5). Unlike meiotic spores, the quiescent cells remain metabolically active and intensively exchange with the environment: cells take up glucose and vitamins, and lose viability rapidly in the absence of the nutrients. After 12 hours in quiescence, *S. pombe* cells lose the ability to mate but remain viable for weeks and months if the medium is refreshed every other week and can resume cycling upon nitrogen addition.

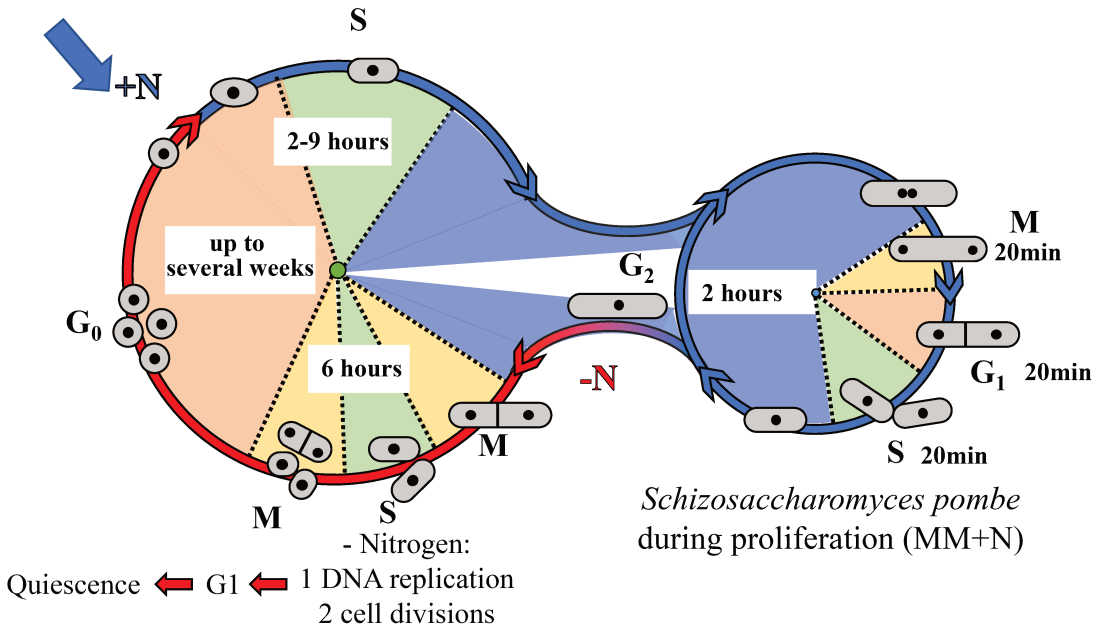

Figure 5: Schematic representation of the *S. pombe* life cycle. Adapted from (Yanagida, 2009).

When exponentially growing *S. pombe* cells are shifted to quiescence medium that lacks a nitrogen source, two rounds of cell division are induced before the arrest (~6 h after the shift). The cells are able to mate and go into meiosis if there are sexual partners of a different mating type. If not, the cells become long-lived, quiescent G0 cells that are not able to mate (>12 h). Cells of the G0 phase are small and round, differing from those of the rod-shaped dividing cells of variable length (micrographs are the merged image taken by transmission and DAPI stain; the nuclear chromatin is white). The *S. pombe* G0 phase here is defined to be a cell state in which cells never divide but remain viable. Such G0 cells are in a reversible state, and can restore the ability to initiate cell growth and division upon application of a growth stimulus (e.g. replenishment of the nitrogen source). Three distinct control windows exist: entry into, maintenance of, and exit from the G0 phase. The G0-phase cells are completely arrested, showing no signs of cell growth, thus they differ from prereplicative G1 or postreplicative G2 phase cells that traverse the cell-cycle stages.

Quiescent cells differ from growing ones by morphological features. Quiescent cells are spherical with an approximate size of 3.5 µm in diameter and quiescence entry is followed by a volume reduction of 40%–50% within 12 hr of nitrogen removal. The change in cell shape during the transition from dividing to non-dividing cells is reminiscent of the wide morphological change of higher eukaryotic differentiated cells. This round cell shape implies isometric actin localization and concomitant endosome formation. Vacuoles (similar to vertebrate lysosomes) are abundant, and the cell wall is thicker than that of vegetative cells. These G0 cells are resistant to heat and have a long chronological life span (Tanaka and Yanagida, 1996).

Transcriptome, proteome and metabolome of proliferating and quiescent cells are different qualitatively and quantitatively in *S. pombe*. Transcriptome shrinks globally after quiescence

entry: the total RNA mass is reduced by 85% to that of proliferating cells. With the consideration of smaller cellular volume, quiescent cells contain only 19.6% rRNA and 31.3% mRNA compared to proliferating cells. The protein-coding transcriptome shrinks to 18% of proliferating cells, but mRNAs are retaining 72% of the diversity in proliferating cells. Only 81 mRNAs (1.6% of the total) are more than 2-fold more abundant in quiescent than in proliferating cells, with mRNAs involved in cell maintenance, such as adaptation to stress and nutrient limitations. Thus, quiescent cells harbor a diminished but diverse transcriptome, with the majority of mRNAs being expressed at only one copy/cell (Marguerat et al., 2012). Upon G0 exit, prior to DNA replication, quiescent cells exhibit two principal transitions in transcript levels (Shimanuki et al., 2007). In the first immediate transition, the levels of approximately 1000 transcripts (~20% of the *S. pombe* genome) either increased or decreased more than fourfold. This extensive transition might reduce and replace many G_0-active transcripts with those required for the exit from G_0 or those leading to the initiation of cell growth.

By contrast, the proteome does not shrink globally after quiescence entry. The protein content of arrested cells is approximately one fifth that of proliferating cells in growth medium (Shimanuki et al., 2007), representing 51.7% of the protein number measured in proliferating cells (Marguerat et al., 2012). The proteome is substantially remodeled during quiescence, with 47% of all proteins changing their copy numbers more than 2-fold. Quiescent cells upregulate proteins implicated in a quiescence lifestyle such as stress response, nitrogen starvation, DNA repair, vacuoles and cell wall, while maintaining strongly reduced translational machinery and proteins implicated in growth similar to those strongly repressed at the mRNA level (Marguerat et al., 2012). To conclude, entry into quiescence thus consists of a rapid adaptation where selected genes are induced and a global, but differential, repression of most genes.

Immediately after removing nitrogen from the medium, within the first 15 min, *S. pombe* proceeds a partial remodeling of the cellular metabolome (Sajiki et al., 2013). These changes involve an increase in trehalose, 2-oxoglutarate, and succinate levels with rapid depression of purine biosynthesis intermediates. This time interval is quite short for gene expression and translation, suspecting that a substantial part of the N-starvation response might be implemented by enzymes already present in the vegetative cell. Within 1 hour after quiescence entry, the number of free amino acids decreases, although several modified amino acids—including hercynylcysteine sulfoxide, a precursor to ergothioneine—accumulates. The level of the high-energy metabolites such as ATP, S-adenosyl-methionine or NAD+ remain constant. The

metabolic changes during quiescence entry reflect adaptation to environmental stress by the accumulation of trehalose and ergothioneine, both of which have protective functions.

Epigenetic plasticity is essential for quiescence regulation and RNAi is a major requirement for quiescence. *S. pombe* has one copy of each of the key enzymes involved: Dicer (Dcr1), Argonaute (Ago1) and RNA-dependent RNA polymerase (Rdp1). RNAi null mutants lose viability in both entry into and long-term maintenance of quiescence (Roche et al., 2016). RNAi promotes RNA polymerase release in both cycling and quiescent cells: RNA pol II release mediates heterochromatin formation at centromeres, allowing proper chromosome segregation during mitotic growth and G_0 entry, and RNA pol I release results in heterochromatin formation at rDNA during quiescence maintenance.

Fission yeast has to maintain the stability of telomeres in quiescent cells and *S. pombe* is an excellent model to investigate the dysfunctional telomeres in non-proliferating cells. Although telomeres attrition is correlated with cell division, telomere shortening has been also observed in somatic cells of brain regions or skeletal muscle, regardless of their replicative activity (Daniali et al., 2013; Mamdani et al., 2016). Thus, eroded telomeres are rearranged in quiescence. These rearrangements, named STEEx, correspond to the amplification of subtelomeric blocks delineated by an HRS and are promoted by transcription and these rearranged telomeres prevent cells to exit properly from quiescence. This model represents a mode of telomeres repair mechanism specific to post-mitotic cells that is likely promoted by transcription (Maestroni et al., 2017).

1.2.4 Genetic regulation of *S. pombe* quiescence

Many features regarding quiescence exit are shared among fission yeast and mammalian cells: nutrient signal sensing to start division, proper regulation of CDK, change in cell shape, replication is preceded by the initiation of cell growth, regulation of DNA replication, massive scale limitations in ribosome biogenesis and protein synthesis. For the exit, TORC1, which promotes protein translation and ribosome biogenesis, is required, suggesting that the diminished protein biosynthesis might be important for maintaining the G_0 phase. Among other mechanisms, it was indicated the role of the RNA-mediated interference (Joh et al., 2016; Roche et al., 2016). The autophagy pathway is activated, and some of the genes of the autophagy pathway are essential for quiescence maintenance (Takeda and Yanagida, 2010).

Regarding the genetic regulation of proliferation and quiescence, all the genes can fit into the following categories: genes essential for proliferation (housekeeping genes) and not for quiescence; genes essential for quiescence and not for proliferation and genes essential both for proliferation and quiescence ("superhousekeeping genes"). In quiescence, genes can be classified as essential for quiescence entry, necessary for quiescence maintenance and required for an exit from quiescence.

The study of the superhousekeeping genes and genes essential for quiescence are based on Yanagida's pilot screens with haploid deletion stains and temperature sensitive strains constructed by random mutagenesis. Approximately 20% of deletion mutants (50 strains were examined) and 25% of temperature-sensitive mutants (610 strains tested) lose viability in quiescence (Yanagida, 2009). Taking into consideration that there are 3700 haploid deletion mutants with 1300 essential genes for proliferation, around 1065 genes might be essential in quiescence.

Genes that regulate cell cycle during proliferation control G_0 entry and maintenance as well. Thus, in Yanagida's laboratory, it has been shown that the main regulator of the cycle, the *cdc2-cdc13* complex, is necessary for quiescence maintenance as *cdc2*-I35N and *cdc13*-563 mutants lose viability upon nitrogen starvation (Yanagida, 2009). Deletion of *rum1*, an inhibitor of *cdc2* during G_1, controls the DNA content in quiescence cells as *rum1*Δ arrest as round cells with a 2C DNA content (Yanagida, 2009).

Multiple cellular complexes and metabolic pathways are implicated in regulation of G_0 in fission yeast. Superhousekeeping genes require genes implicated in MAPK-mediated stress responsive-protein phosphorylation, Rab5-mediated and HOPS-mediated (homotypic fusion and vacuole protein sorting) vacuole-fusion dynamics, cortical actin interacting WASP (Wiskott-Aldrich syndrome protein) and Huntington-interacting End4/Sla2 mediated endosome formation. Methylation is essential both for proliferation and quiescence. Methylation is one of the most important and universal biochemical reactions in cells. It is involved in numerous cellular processes, such as transcriptional control, lipid metabolism, and signal transduction. The *sam1* gene encoding the S-adenosylmethionine synthetase is part of the superhousekeeping genes, and mutations in this gene affect both proliferation and quiescence. During proliferation, mutations in *sam1* affect cell growth and cell cycle progression at two transition points: the G_2/M transition in vegetative cultures and the G_1/S

transition after release from nitrogen-starvation-induced G_0 phase. Mutations in *sam1* block cell growth and cell cycle progression in vegetative cultures and also cause failure to exit from nitrogen starvation-induced G_0. Furthermore, *sam1* mutants lose cell viability during G_0. These metabolic changes appear to cause defects of both cell growth and cell cycle progression (Hayashi et al., 2018).

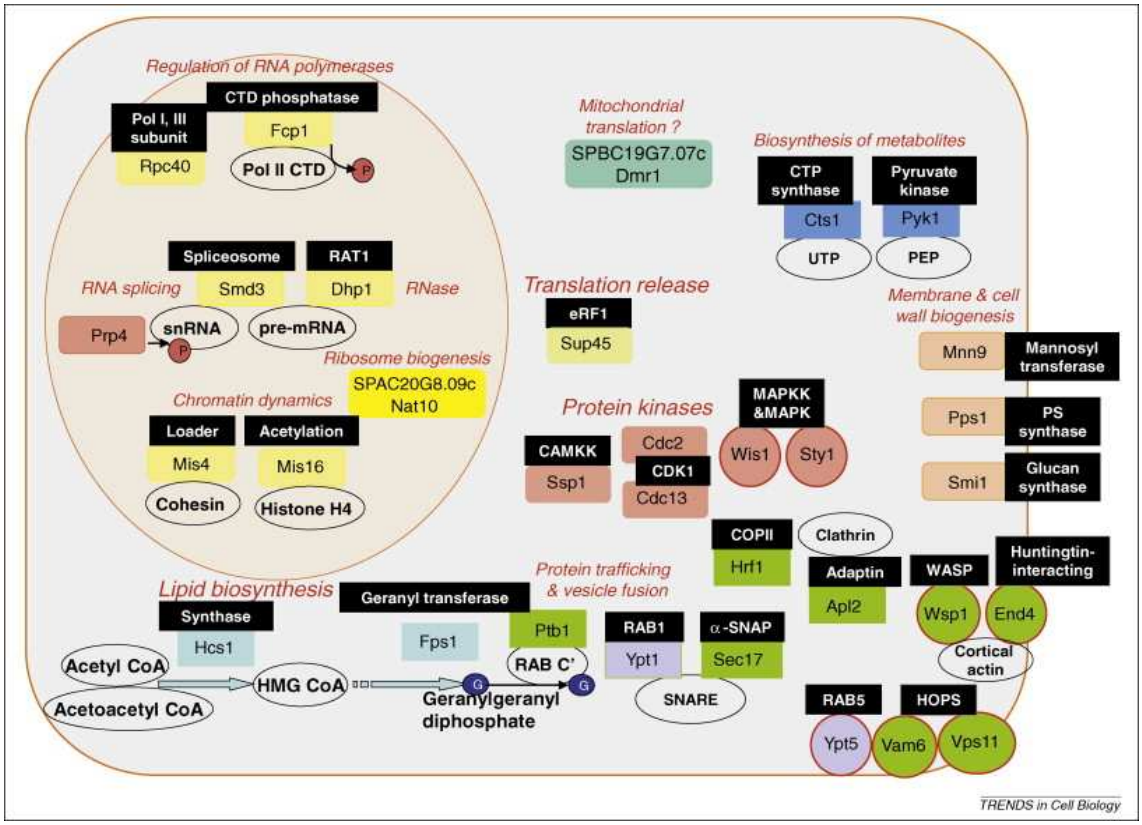

Figure 6: Superhousekeeping gene products that are required for both quiescence and proliferation. From (Yanagida, 2009).

Temperature-sensitive (ts) mutants (n=610) whose cell division was blocked in growth medium were evaluated for their viability in nitrogen-deficient quiescence medium. Of these, 160 mutants had a significant loss of viability. A pilot study that included gene cloning, genetic linkage and phenotypic analyses identified 34 gene products, which collectively are called superhousekeeping genes, because of their requirement in both quiescence and proliferation. The entry into G0 quiescence requires 7 of these 34 superhousekeeping genes (red circles) that are implicated in MAPK-mediated stress responsive-protein phosphorylation, Rab5- and homotypic fusion and vacuole protein sorting (HOPS)-mediated vacuole-fusion dynamics, and cortical-actin interacting Wiskott-Aldrich syndrome protein (WASP)- and Huntington-interacting End4/Sla2-mediated endosome formation. Common names for the gene products are shown in black boxes, and the S. pombe-specific protein names are denoted by three letters followed by a number. The remaining 27 proteins that appeared to be required for maintaining G0 quiescence have broad cellular functions in the nucleus, cytoplasm, cell envelope and various subcellular organelles. Seven of them are protein kinases known to be involved in nuclear RNA metabolism (Prp4), cell cycle control (CDK1), stress response (p38-like MAPK and MAPKK) and glucose utilization (Ssp1/CaMKK). Two metabolic enzymes, cytidine 5'-triphosphate (CTP) synthase Cts1 and pyruvate kinase Pyk1, produce high-energy compounds [CTP, phosphoenol pyruvate (PEP) respectively]. Three proteins Mnn9, Pps1 and Smi1, which are involved in cell wall metabolism, mannosyl transfer, phosphatidyl serine and glucan synthesis, respectively, are essential to

maintain the cell wall and the intracellular homeostatic environment. Three enzymes, the HMG-CoA synthase Hcs1, the geranyl transtransferase Fps1 and the geranyl geranyl transferase subunit Ptb1 are involved in the pathway that leads to the geranyl geranylation of the carboxyterminus of small G proteins, such as Ypt1 (similar to Rab1) and Ypt5 (similar to Rab5). Several essential proteins are involved in trafficking and vesicle fusion. They are Ypt1 (Rab1-like GTPase), Sec17 (SNARE interacting alpha protein (SNAP), Hfr1 (COPII component) and Apl2 (clathrin-interacting adaptin). In the nucleus, superhousekeeping Rpc40 is the subunit of RNA polymerases I and III, whereas Fcp1 is a CTD phosphatase that appears to have a key role in differentiating quiescence from proliferation.Smd3 and Dhp1, and Prp4, are involved in RNA splicing and pre-mRNA processing, whereas Nat10 and Sup45 are involved in ribosome biogenesis and protein translation. Mis4, similar to S. cerevisiae Scc2, is required for the loading of cohesin in proliferating cells and is the causal gene for human disease Cornelia de Lange syndrome. Mis16, similar to mammalian RbAP, is a histone H4 chaperone.

These genes include the function of the ATP metabolism, protein trafficking and cell-wall morphogenesis, suggesting that quiescence require a large set of the cell program rebuilding. (Sajiki et al., 2009). These genes are conserved from fungi to mammals and cover wide broad of functions including MAPKK-MAPK signaling pathways, actin-interacting endosome formation, lipid formation and ATP biosynthesis through sugar catabolism, RNA transcription, splicing, processing and protein translation metabolism, protein trafficking, chromatin remodeling and dynamics, cell-wall morphogenesis.

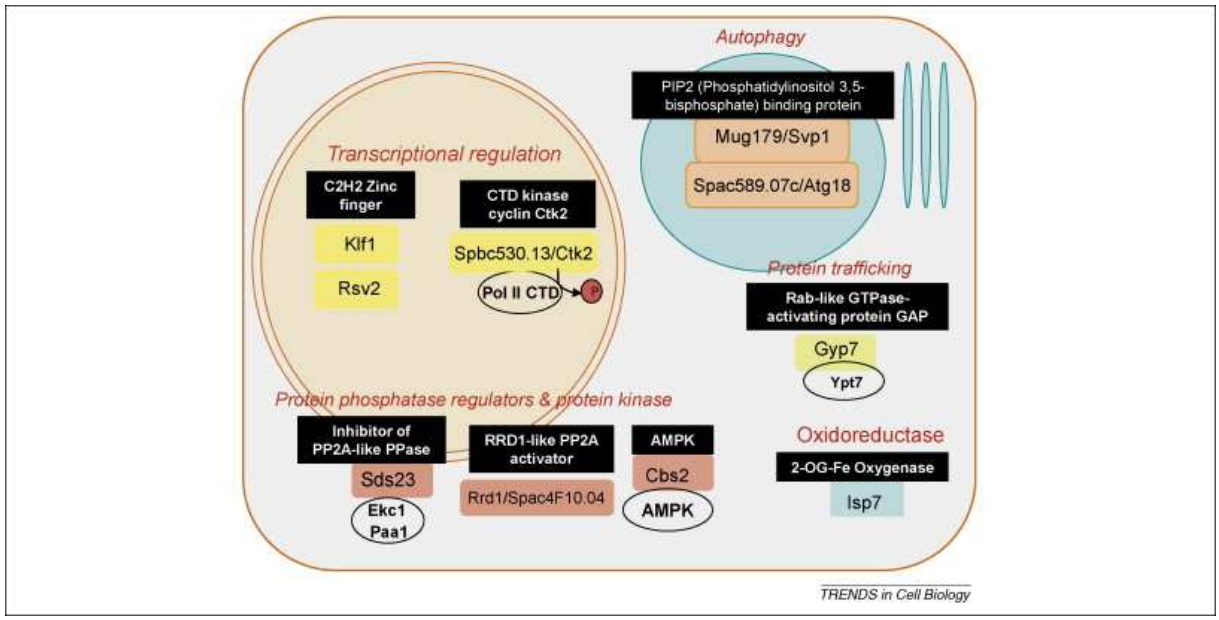

Figure 7: G0-lethal but normal proliferation mutations in *S. pombe* genes (From (Yanagida, 2009)).

A pilot study was conducted to identify mutants that become lethal in the quiescence medium. Of 50 deletion mutant strains constructed and tested, approximately 20% lost viability in the quiescence medium, but grew in the growth medium. These deletion mutants might represent defects in G0-specific functions Klf1 and Rsv2 are C2H2-type zinc-finger transcription factors. Ctk2-like cyclin (SPBC530.13) is the presumed subunit of Ctk1 kinase that regulates RNA polymerase II through phosphorylation of the largest subunit C-terminal repeat domain (CTD). Two proteins, Mug179 and SPAC589.07c, having motifs of PIP2 (phosphatidyl inositol 3, 5-bisphosphate) binding and membrane spanning, are similar to Atg18, thus they might be implicated in autophagy. Gyp7 is a GAP (GTPase activating protein) that targets Ypt7, a Rab-like GTPase implicated in vacuole and protein trafficking. Isp7 is an oxygenase highly expressed in response to

oxidative stress. The three remaining proteins are related to protein phosphorylation and dephosphorylation. Cbs2 is the gamma-subunit of AMPK that has diverse roles and is required for sensing the intracellular energy state and acts as the upstream factor of the TSC-Rheb-TOR signal transduction pathways. It has four CBS domains. Sds23 has also four CBS domains and was recently reported to be the inhibitor for type 2A-like protein phosphatase. SPAC4F10.04 is similar to budding yeast Rrd1 that activates type 2A phosphatase (PTPA type PPIase).

Vacuole dynamics are essential for quiescence entry and the strains with mutations in *vps11*, *vam6 and ypt5* genes lose viability after quiescence entry. G_0-lethal mutations are in control of transcription, phosphorylation, autophagy and trafficking. Genes required for quiescence maintenance cover a broad range of cellular activities involving the cell surface, cytosol, cytoplasmic organelles and nucleus. Four genes encode cell-cycle-related protein phosphorylation and dephosphorylation, and two are implicated in sister chromatid cohesion and chromatin remodeling. Two, eight and three gene functions are required, respectively, for ATP metabolism, protein trafficking and cell-wall morphogenesis, although six genes are implicated in RNA metabolism. The group of genes, essential for quiescence maintenance includes a significant number of genes related to protein phosphorylation signaling. Most were phosphatase-related genes rather than kinases (11:1), implying that dephosphorylation is a primary means of maintaining mitotic competence in quiescence (Yanagida, 2009).

1.2.5 The TOR Complexes

The decision to switch from quiescence to proliferation and back in eukaryotes is under the control of TOR (target of rapamycin) that regulates mRNA translation in response to nutrient availability (Crespo and Hall, 2002; Loewith et al., 2002; Ma and Blenis, 2009). The activity of the TOR pathway relies on two complexes, TORC1 and TORC2, that are evolutionarily conserved in eukaryotes (Figure 8). Rapamycin is a macrolide that inactivates the TOR kinase indirectly (Vézina et al., 1975). In budding yeast, rapamycin arrests cells in G_1. However, it does not affect the vegetative growth of wild-type fission yeast (Weisman et al., 1997). In mammalian, rapamycin inhibits the G_1-S transition in T-lymphocytes, and this feature is used in immune suppression during organ transplantation. mTORC1 signaling is hyperactive in the majority of cancers and rapamycin is used as an inhibitor of cancer cell proliferation. mTOR integrates the input from upstream pathways, including insulin, growth factors, and amino acids (Hay, 2004). The two complexes have different functions in the cell: TORC1 controls cell growth and metabolism while TORC2 controls cell survival and proliferation. TORC1 is the only target of rapamycin and is in charge of translation regulation as well as nutrition and stress response (Wullschleger et al., 2006).

While human cells contain one catalytic subunit *mtor*, both budding and fission yeast contain two: *tor1* (component of the TORC2) and *tor2* (component of TORc1). *S. pombe* and human TORC1 (but not *S. cerevisiae*) are under the control of TSC-Rheb signaling, which is under the control of AMPK, MAPK and Akt/PKB pathways.

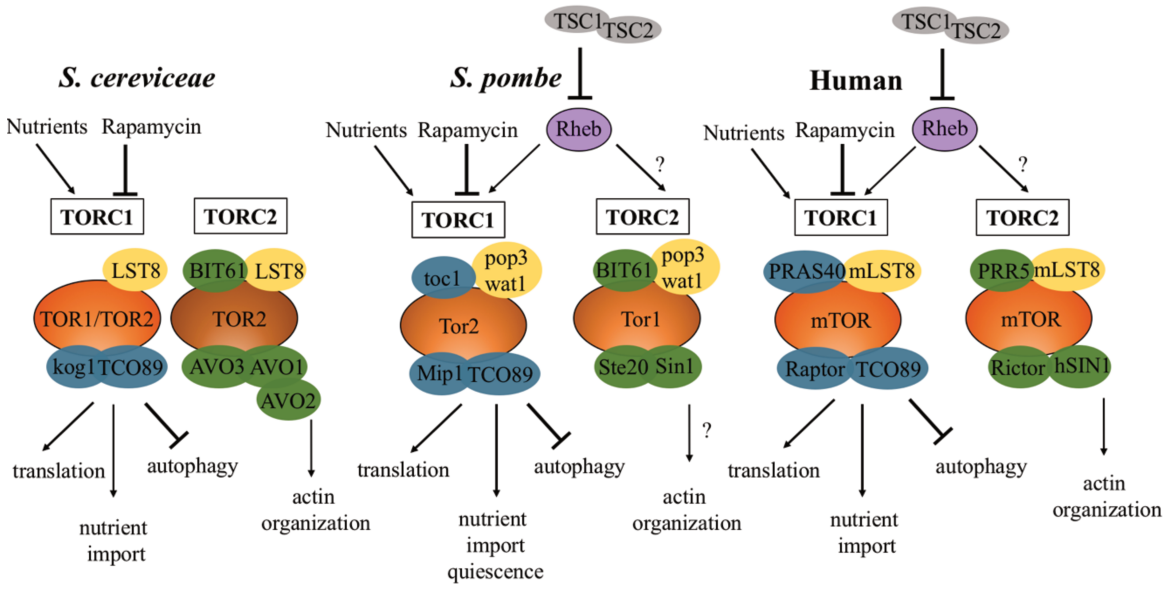

Figure 8: TOR complexes are conserved among different species – modified from (Yanagida, 2009).

TOR signaling plays a central role in nutrient cell growth. Depleting TOR kinases, which can be achieved by mutations and by drugs such as rapamycin, seems to be a prerequisite for cellular quiescence. (a) Evolutionarily distant *S. cerevisiae*, *S. pombe* and human cells have two functionally distinct TOR complexes, TORC1 and TORC2. Yeasts have a dual catalytic subunit, but humans have only one catalytic subunit. *S. pombe* and human TORC1 (but not *S. cerevisiae*) are under the control of TSC-Rheb signaling, which is under the control of AMPK, MAPK and Akt/PKB. The main target for rapamycin is TORC1. TORC-associated proteins are depicted by the nomenclature of these three organisms. *S. pombe* TORC1 consists of four non-catalytic subunits (Mip1, Tco89, Toc1 and Pop3/Wat1) and the catalytic subunit Tor2. Mip1 is similar to human Raptor and *S. cerevisiae* Kog1. Toc1 has not been found in other organisms' TORC1, whereas Tco89 is conserved in TORC1. Pop3/Wat1 similar to human and *S. cerevisiae* Lst8, however, this is a common subunit also present in TORC2. Lst8 is present in TORC2. *S. pombe* Pop3/Wat1 is a Lst8 homolog. *S. pombe* TORC2 contains four non-catalytic subunits (Ste20, Sin1, Bit61 and Pop3/Wat1) and the catalytic subunit Tor1. Ste20 is similar to human Rictor and *S. cerevisiae* Avo3. Cellular functions assigned for TORC1 and TORC2 are indicated. The question marks indicate that the relationship is not settled.

The *tor2* gene, a core component of TORC1, is essential for growth and serves as a nutrient sensor in fission yeast. Deletion of *tor2* mimics nitrogen starvation and activates the sexual pathway in fission yeast. (Alvarez and Moreno, 2006). Loss of function in *tor2* is followed by an upregulation of all the repressed genes in quiescence, supporting a role for TORC1 in the induction of quiescence (Matsuo et al., 2007).

In mammalian, mTOR function is essential both for cell differentiation and quiescence maintenance. mTOR-/- in mice results in early death during embryonic development accompanied by an aberrant morphogenesis and inability to establish stem cells (Murakami et al., 2004). Tissue-specific inactivation of mTOR results in corresponding diseases. Thus, it was shown in mouse models that mTOR regulates skin morphogenesis and epidermal barrier formation (Ding et al., 2016). Inactivation of mTOR in muscle tissues leads to the muscle myopathy and early-age death (Risson et al., 2009). mTOR deletion in hematopoietic stem cells results in loss of quiescence and bone narrow failure (Guo et al., 2013). mTOR deletion in neural stem cells results in the inhibition of neurogenesis and differentiation (Hartman et al., 2013). Constitutive activation of mTOR leads to the depletion of the stem cell pool (Chen et al., 2008; Haller et al., 2017).

Hyperactivation of TOR activity in both yeast and mammals results in an increase in cell growth that can force cells to enter the cell cycle. Indeed, almost all cancer cell lines demonstrate constitutive activation of mTORC1 and lower dependence on exogenous growth factors (Menon and Manning, 2009). Activation mutations in *mtor* are found in a variety of cancers, primarily in melanomas, consistent with a role for mTOR in tumorigenesis (Grabiner et al., 2014; Sato et al., 2010). Mutations in mTOR are never present alone and are accompanied by mutations in genes involved in cell cycle and MAP-kinase pathway but their influence on the phenotype is unknown (Sato et al., 2010). In contrast to the other quiescent states considered, in dormant tumor cells, TOR is activated and contributes to cancer cell survival (Schewe and Aguirre-Ghiso, 2008).

Inhibition of TORC1 by rapamycin and caffeine prolongs CLS in stationary phase fission yeast (Rallis et al., 2013). Similarly, rapamycin extends CLS in budding yeast and organismal lifespan in worms, flies, and mice (Fontana et al., 2010).

In fission yeast, TORC1 couples cell growth with cell division via Sty1, a mitogen-activated protein kinase (MAPK) that recruits the Polo kinase to the spindle pole bodies that trigger Cdc2 activation to advance mitotic onset. This mitotic onset is abolished in cells depleted of Gcn2, Pyp2, or Sty1 or on blockage of Sty1-dependent Polo spindle pole bodies recruitment. Therefore, TOR signaling modulates mitotic onset through the stress MAPK pathway via the Pyp2 phosphatase.

1.3 MAP Kinases and Their Role in Quiescent Cells

MAP kinases or mitogen-activated protein kinases are signaling enzymes. They are activated by phosphorylation on serine/threonine residues in active sites and they phosphorylate downstream kinases in response to their activation. MAP kinase genes are conserved and found in all eukaryotes. They constitute core signaling pathways and they cover a broad range of functions in the cells, including response to growth stimuli and stress, control of apoptotic signals, proliferation and differentiation (Pearson et al., 2001). Classical MAP kinase cascades are composed of a 3-step system: MAPKKK->MAPKK->MAPK. The last MAP kinase in the series is activated by dual phosphorylation on specific threonine and tyrosine residues in Thr-X-Tyr motifs, where X is an arbitrary amino-acid.

Components of the MAP kinase cascades are all located in the cytosol, but the final MAPK is transported into the nucleus upon activation. MAP kinases are typically activated by a small GTPase and/or phosphorylated by protein kinases downstream of cell surface receptors (Cuevas et al., 2007). Upon activation, MAP kinases phosphorylate various substrates in the cytosol or/and nucleolus, primarily transcriptional factors, changing protein function, gene expression and activating the appropriate genetic program in response to the biological stimulus (Morrison, 2012).

In fission yeast, the 3 MAP kinase pathways have been identified (Figure 9). The pheromone-responsive MAPK signaling pathway byr2->byr1->spk1, the MAPK cell wall integrity stress response pathway mkh1->pek1->pmk1 and the SAPK win1/wis4->wis1->sty1 general stress response pathway. In budding yeast, there are 5 MAP kinase pathways: ste11->ste7->fu3, ste11->ste7->kss1, ssk2/22->pbs2->hog1 (homologues of the fission yeast SAPK pathway), bck1->mkk1/2->mpk1 pathway (homologue of the fission yeast MAPK pathway) and the non-canonical cak1->smk1 pathway. Mammals express a large variety of the protein kinases depending on the cell type, but the MAP kinase pathways in humans can be reduced to 4 major categories (Morrison, 2012). The Ras-activated pathway Raf-MEK1-ERK which is mainly characterized as an inductor of cell growth and proliferation in response to growth factors, hormones or mitogens. The structural homologues of the ERK pathway in fission and budding yeast are *mpk1* and *pmk1* pathways. Whereas the ERK pathway is responsible for mitogenic signals in mammalian, both are implicated in the cell wall integrity during stress response in yeast. The two SAPK stress response pathways are present in mammalian cells: the p38 and JNK (Janus kinase) pathways are important both under physiological and stress conditions and

are activated upon extracellular and intracellular signals. The structural and functional homologues of the p38 pathway are budding and fission yeast Hog1 and Sty1 pathways, respectively. Activation of these pathways in mammalian can be triggered by stress, growth signals, cytokine controls and hormones. Stress response pathways control cell differentiation, cell fate (survival or death) and apoptosis, inflammation, and cell cycle arrest (Morrison, 2012). A third MAP kinase pathway is known as an atypical ERK pathway that can be activated by cytokines. Despite the considerable variability in MAP kinase types and functions, they regulate the core cellular functions; therefore, unicellular organisms like yeast can provide a simple and convenient model for studying fundamental features.

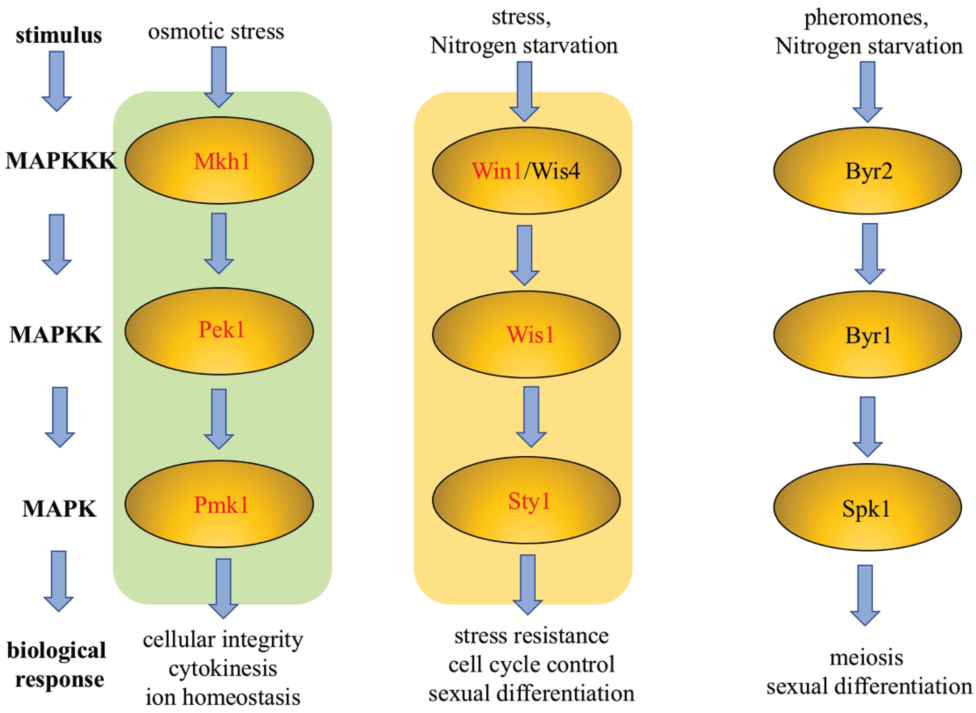

Figure 9: MAP kinase pathways in fission yeast *S. pombe*. Genes identified in this study are highlighted in red.

In *S. pombe*, three distinct MAPK pathways have been identified. These include the Mating Pheromone-responsive Spk1 MAPK pathway, the stress-sensing Sty1/Spc1/Phh1 MAPK pathway, and the Pmk1/Spm1 MAPK pathway, which regulates cell integrity. In response to starvation, the mating pheromone-responsive Spk1 MAPK pathway is required for mating and sporulation and includes the MAP kinase Spk1, the MAPKK Byr1, the MAPKKK Byr2 and the small GTPase. sty1 is a member of the Stress-Activated Protein Kinase family, an evolutionary conserved subfamily of MAPKs and was identified as a regulator of the Osmotic Response and Cell Cycle. Sty1 is activated by the Wis1 MAPK kinase, which is in turn activated by two MAPK kinase kinases, Wis4 or Win1. Pmk1 is a MAPK that regulates cell Integrity and which, with Calcineurin Phosphatase, antagonizes Chloride homeostasis. Pek1 is a MAPKK for Pmk1 MAPK. Pek1, in its unphosphorylated form, acts as a potent negative regulator of Pmk1 MAPK signaling. Mkh1, an upstream MAPKK kinase (MAPKKK), converts Pek1 from being an inhibitor to an activator. Thus Pek1 has a dual stimulatory and inhibitory function, which depends on its phosphorylation state. This switch-like mechanism could contribute to the all-or-none physiological response mediated by the MAPK signaling pathway.

The win1/wis4->wis1->sty1 SAPK pathway is one of the major players in general stress adaptation in fission yeast. Thus, deletion of the components of the SAPK pathway in *S. pombe* causes hypersensitivity to various stress agents during growth. Strains carrying a deletion of *sty1* and its upstream activator *wis1* are extremely sensitive to heat shock and elevated temperatures, salt stress, DNA damaging agents like bleomycin or UV, low pH or hydroxyurea and lose viability rapidly in the stationary phase (Kato et al., 1996; Sanso et al., 2011; Zuin et al., 2010). Sty1 regulates the expression of the core stress response genes in fission yeast. Upon stress-activated phosphorylation, *sty1* is translocated from the cytoplasm into nucleolus and activates the *atf1* transcriptional factor (homologue of mammalian ATF-2) (Gaits et al., 1998) that subsequently induces an expression of the core stress response genes (Wilkinson et al., 1996). Deletion of *atf1* is associated with many, but not all, phenotypes linked to *sty1*Δ (loss of viability in the stationary phase, sensitivity to sorbitol, decreased mating efficiency and several others) (Shiozaki and Russell, 1996). During quiescence entry, *atf1*Δ maintains viability and morphology similar to the wild-type, indicating that the core stress response genes are not directly involved in the phenotype observed in *sty1* and *wis1* mutants upon quiescence entry (Sajiki et al., 2009). Like in fission yeast, the Hog1 MAPK in *S. cerevisiae* is implicated in stress response, but the budding yeast SAPK pathway is restricted to respond to osmotic stress (Schüller et al., 1994). The fact that Hog1 is responsible only for one particular type of stress can be explained by the presence of the 5 different MAP kinase pathways, each of them being specialized for a given type of stress (reviewed in (Brewster and Gustin, 2014)). Human cells contain four p38 MAP kinase homologues of *sty1*: p38-α, -β, -γ, -δ characterized by the presence of the conservative Thr-Gly-Tyr (TGY) phosphorylation motif in the activation domain. All isoforms of p38 kinases are widely expressed in vivo, but their expression pattern varies with the tissues. Only p38-α is ubiquitously expressed, while expression of other isoforms is more tissue-specific (Jiang et al., 1997; Mertens et al., 1996). Identically to in fission yeast, p38 can be activated by diverse forms of stress (Banuett, 1998).

The SAPK pathway controls multiple functions in the cell beside stress response. Sty1 controls cell cycle progression at various stages and cell cycle arrest upon stress. Sty1Δ cells have a mitotic delay, do not enter quiescence and show decreased mating efficiency (Sajiki et al., 2009). Sty1 function is essential for G_2/M transition and *sty1*Δ-*cdc25*-22 (M phase inducer) double mutant is synthetically lethal (Shiozaki and Russell, 1995). Sty1-dependent quiescence entry is mediated by the inhibition of *srk1* (MAPK-activated serine-threonine protein kinase)

(Smith, 2002). The cyclin-dependent kinase inhibitor Rum1 is phosphorylated by Sty1 in vivo and in vitro and links stress response with cell cycle (Matsuoka et al., 2002). Similar to Sty1 in fission yeast, the budding yeast homologue Hog1 modulates a transient arrest in cell cycle progression at several phases to enable cells to adapt before progressing through essential cell cycle transitions (Clotet et al., 2006; Escoté et al., 2011). Similarly, p38 in mammalian controls cell cycle arrest at the G_2/M checkpoint in response to double strand breaks (Bulavin et al., 2002). Activation of p38 can also contribute to the induction of a G_1/S checkpoint in response to osmotic stress and ROS.

Activation of the *sty1* stress-response pathway under nutrient-limiting conditions extends CLS. Thus, during the transition to the stationary phase in glucose-limiting conditions, Sty1 triggers a transcriptional stress program (Zuin et al., 2010).

The MAPK mkh1->pek1->pmk1 pathway has been discovered as a cell wall integrity pathway by the fact that *pmk1*Δ and *mkh1*Δ loose viability upon treatment with β-glucanase (Sengar et al., 1997; Toda et al., 1996). Similar to the SAPK pathway, the impact of the MAPK pathway on cellular homeostasis is multifunctional. The MAPK pathway is implicated in cytogenesis, morphogenesis, cell wall remodeling, ionic homeostasis and stress response. Activation of the last component of this pathway, the Pmk1 MAPK, has been reported in response to a variety of osmotic conditions, cell wall damage, oxidative stress and glucose deprivation (Barba et al., 2008).

Components of the MAPK pathway have an impact on CLS. Accordingly, the MAPKK *pek1*Δ was detected among the long-lived strains in the pool of strains sequenced after several months of quiescence (Sideri et al., 2014). Several truncating mutations in the *mkh1*, *pek1* and *pmk1* genes have been reported after long-term quiescence (Gangloff et al., 2017). These data indicate that the function of the cell wall integrity pathway is not essential for the quiescence entry, but its disruption may contribute to survival during prolonged periods of starvation. By contrast, the *mkk1* mutant, the orthologue of the *pek1* kinase in budding yeast, is short-lived (Fabrizio et al. 2010), suggesting different adaptations to ecological niches among species. Deletion of the components of the cell wall integrity pathway in budding yeast results in rapid death upon nitrogen starvation, suggesting that in two yeast species the adaptation to starvation conditions is different (Krause and Gray, 2002).

The stress response pathway is essential for quiescence entry, maintenance and exit. Genetic screens of Yanagida's pioneering work using temperature sensitive mutants that lose viability upon entry into quiescence have identified *wis1* and *sty1*. In budding yeast, deletion of *wis1* and *sty1* homologues – *pbs2* and *hog1* – do not affect viability in stationary phase-induced quiescence. However, *pbs2*Δ and *hog1*Δ result in a delay of quiescence exit after four days of quiescence (but not after 2), suggesting a possible role in quiescence maintenance (Escoté et al., 2011; Toda et al., 1996).

Dysregulation of both ERK and p38 MAP kinase pathways in humans is associated with multiple diseases: primary cancer progression (Dhillon et al., 2007) and neurodegenerative disorders (Colucci-D'Amato et al., 2003; Corrêa and Eales, 2012).

The primary role of the p38 kinases has been classified as tumor suppression, based on their ability to negatively regulate proliferation and induce differentiation of several cell types. (Bulavin and Fornace, 2004).

Recent findings have suggested that the proliferation/quiescence decision in human cancers is under the control of a balanced activity of the two kinase pathways defined by ERK1/2 and p38 (Sosa et al., 2011). A low ERK and high p38 activity was observed in nearly 90% of the dormant cell lines, including prostate, breast, melanoma, ovarian and fibroblastoma cell lines. Activation of the p38 pathway has been associated with dormant tumor cells in multiple solid tumors as well, including HNSCC, (Bragado et al., 2013), breast and prostate (Kobayashi et al., 2011). Inhibition of p38 results in reduced proliferation but also in the inhibition of cell death and maintenance in an undifferentiated state (Soeda et al., 2017).

Among the possible mechanisms, it has been proposed that the initial activity of the MEK-ERK pathway under RAS modulation is inhibited by a classical negative feedback loop, implicating several possible regulators like the dual specificity MAPK phosphatases (namely MKPs or DUSPs) (Courtois-Cox et al., 2006; Kidger and Keyse, 2016). The inhibition mechanism by dual specificity MAPK phosphatases is universally found in all eukaryotic organisms. It is a subtype of protein kinases performing both positive and negative regulation of the MAP kinase pathways. They control the crosstalk between different signaling pathways and their dysregulation leads to multiple diseases (Caunt and Keyse, 2012). The activated form of the MAP kinase acquires an affinity for the MAP phosphatase and their association causes a conformation change that activates the phosphatase. The MAP kinase phosphatase, in turn,

catalyzes the dephosphorylation of the activated MAP kinase that inactivates it (Kondoh and Nishida, 2007).

1.4 Genome Stability in Dividing Versus Quiescent Cells

A genome is a highly dynamic structure that is exposed to different agents (replication or transcription machinery, cell metabolites) that can damage DNA, cause lesions and distort the functional information. Little information exists on how cells cope with DNA damage in quiescence. DNA damage can be repaired in quiescence, during the first round of replication upon exit from quiescence or upon replication during proliferation. DNA repair mechanisms and pathways may be different from those used during growth. DNA damage in quiescent cells can originate from exogenous or endogenous sources. Exogenous sources include chemical agents, physical agents like radiation or biological agents like viruses. DNA lesions from endogenous sources include stochastic perturbations due to the physical-chemical nature of the DNA molecule (tautomerization, apirymidation), chemical modification as a result of the interaction with cellular metabolites (oxidation, alkylation etc.), errors in repair processes (incorporation of the incorrect nucleotide) (Lombard et al., 2005). Endogenous causes of DNA damage are the major threat to reduce CLS (Gensler and Bernstein, 1981) (Figure 10).

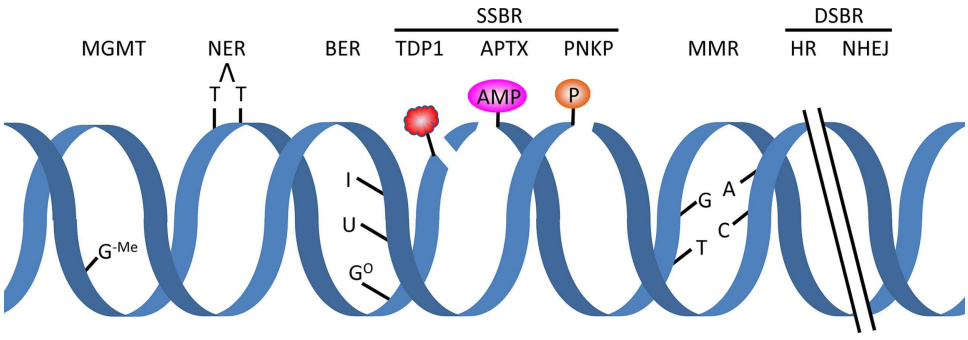

Figure 10: DNA damage and repair response. DNA repair pathways (top) and examples of corresponding DNA damage (bottom). From (Iyama and Wilson, 2013)

DNA repair pathways (top) and examples of corresponding DNA damage (bottom). The detailed molecular mechanisms for the repair responses are provided in text. APTX, aprataxin; BER, base excision repair; DSBR, DNA double strand break repair; HR, homologous recombination; MGMT, O^6-methylguanine-DNA methyltransferase; MMR, mismatch repair; NER, nucleotide excision repair; NHEJ, nonhomologous end joining; PNKP, polynucleotide kinase 3'-phosphatase; SSBR, DNA single strand break repair; SSBs, DNA single strand breaks; TC-NER, transcription-coupled NER; TDP1, tyrosyl-DNA phosphodiesterase 1; G-Me, O^6-Methylguanine; T^T, thymine dimer; I, inosine; U, uracil; G^o, 8-oxoguanine.

Three major processes involved in genome stability are different between proliferation and quiescence: replication, checkpoints and activation of cell cycle specific DNA-repair pathways. While cycling, cells pass several checkpoints, including the DNA damage checkpoints at the G_1/S and G_2/M boundaries. The DNA damage checkpoint network, composed of sensors, signal transducers and effectors, coordinates DNA damage repair processes with cell cycle progression to preserve the integrity of the cell. In the presence of damage, the cell cycle progression is blocked and the corresponding DNA repair pathways are activated. The first demonstration that quiescent cells repair DNA damage differently was established in Yanagida's laboratory using *S. pombe* (Mochida and Yanagida, 2006). Quiescent cells are more sensitive to ultraviolet (2-fold compared to growing cells) and γ-rays (20% of the quiescent population is viable compared to almost 100% in proliferation after a moderate treatment) that produce thymine dimer crosslinks and double-strand breaks, respectively. It was shown that quiescent cells do repair the damage, but distinctively from vegetative cells. The response to DNA damage in *S. pombe* quiescent cells does neither involve the activation of the checkpoint kinases Chk1 nor genes involved in HR-DSBR like Crb2. The repair mode in quiescent cells is different from the proliferative one; *S. pombe* removes thymidine dimers faster but repairs double-strand breaks slower (24 hours compared to 8 hours in growing cells), involving the non-homologous end-joining (NHEJ) repair pathway rather than homologous recombination (HR). The authors have left it an open question as to whether the response to DNA damage in G_0 cells is identical to G_1 in its mechanistic aspects. (Arcangioli and Ben Hassine, 2009) has demonstrated that checkpoint kinases are implicated in programed cell death in response to the accumulation of unrepaired damage (in particular, unrepaired SSB produced in the absence of topoisomerase I).

Replication itself serves as a source of mistakes both under physiological and under stress conditions, and is believed to be necessary to transform DNA lesions into mutations (Ganai and Johansson, 2016). When a replication fork meets a damaged region, cell recruits a DNA repair machinery to fix the damage (Branzei and Foiani, 2005). Despite several early reports on stationary-phase mutations in bacteria (Grigg and Stuckey, 1966; Ryan, 1955), it has been adopted that fixation of the mutations somehow requires DNA synthesis, either by full genome replication during cycling or by repair synthesis, like during transcription-coupled DNA repair (reviewed in (Hanawalt, 2008) or transposon mutagenesis. By contrast, in quiescent cells, the only source of DNA synthesis is that coupled with DNA repair.

There are 5 canonical DNA repair pathways identified both in prokaryotes and eukaryotes: mismatch repair (MMR), base excision repair (BER), nucleotide excision repair (NER), homologous recombination (HR), non-homologous end-joining (NHEJ). All are found in fission yeast (Lehmann, 1996). Some the DNA repair pathways are restricted to a specific stage of the cell cycle. Homology-directed repair (HDR) is functional only in S or G_2 phase of the haploid cell cycle, when a second copy of the information is available. Other pathways may also exhibit a different mode of activity depending on the cell stage (Schroering et al., 2007) (Table 2).

Table 2: Functional capacity of the different DNA repair pathways in dividing/non-dividing cells and their connection to inherited cancer/neurological disorders. (modified from (Iyama and Wilson, 2013))

Repair Pathway	Sub-pathway	Dividing cells	Non-dividing cells	Disease associated in	
		Capacity of DNA repair		Cancer	Neurological diseases
NER	TC-NER	++	+	NO	YES
	GG-NER	++	+	YES	YES
BER		+	+	YES	NO
SSBR	TDP1	++	+	NO	YES
	APTX	++	+	NO	YES
	PNKP	++	+	NO	YES
MMR		++	+/-	YES	NO
DSBR	HR	++	+/-	YES	YES
	NHEJ	+	++	YES	YES

The proliferation-coupled mutation rate has become a general way to evaluate the mutation rate in an organism by providing the number of nucleotides modified per generation. For instance, Farlow has determined the mutation rate during growth in *S. pombe* as $2.00 \pm 0.1 \times 10^{-10}$ per nucleotide per generation (1 mutation per genome every 400 generations) by sequencing the genome of 96 colonies after 1716 generations (Farlow et al., 2015). Similar data were obtained

from budding yeast with a mutation rate of $1.67x10^{-10}$ per generation per nucleotide (Zhu et al., 2014). In fission yeast, the accumulation of mutations in quiescence is linear and the average frequency is $6.8x10^{-3}$ mutations per day (Gangloff et al., 2017). The replication-dependent mutations acquired during growth define a spectrum quite similar among species, with the domination of Single Nucleotide Variants (SNVs) over Insertions/ Deletions (Indels) and Structural Variants (SVs).

Very little information exists on how quiescent cells convert DNA lesions into mutations. Quiescent cells accumulate DNA lesions that are either repaired in quiescence or upon exit from quiescence during first round of DNA replication. (Beerman et al., 2014) have demonstrated that, at least in quiescent hematopoietic stem cells, DNA damage accumulates with time (during ageing) and is repaired upon entry into the cell cycle during replication and, probably some of the incorrectly repaired lesions can result in the fixation of the mutation. Similarly, dormant bacterial endospores remain metabolically inactive, and thus do not repair DNA in resting stage. However, endospores usually contain at least some of the DNA repair enzymes that cells could use during the process of germination to repair DNA lesions, and DNA repair mutants show a lower level of survivors during germination (Munakata and Ikeda, 1968; Munakata and Rupert, 1975; Setlow and Setlow, 1996). Single cell sequencing of 161 single neurons from 15 young adults and old humans (from 4 months to 82 years of age) has first demonstrated that post-replicative cells not only accumulate DNA damage with time in form of lesions but also convert at least some of the lesions in mutations (Lodato et al., 2018).

1.5 Objectives

Mutations that arise in the absence of replication in non-dividing cells may undergo a selection process during quiescence leading to their enrichment in the population. The stress-response MAP kinases cover a broad range of functions in eukaryotic cells, including differentiation, quiescence maintenance, response to exogenous stimuli, starvation, stress etc. The genetics of quiescence is largely unknown and mutations in these genes may provide a selective advantage in quiescence.

During my Ph.D., I used a fission yeast quiescence model to investigate the role of "adaptative" mutations in the MAP kinase pathway.

1. "*Adaptive mutations":* The first objective of my Ph.D. was to confirm that mutations in the S/MAP kinase pathways arise during quiescence;

2. *The selection process:* The second objective of my Ph.D. was to identify the type of selection process that affects the fitness of S/MAP kinase mutants in quiescence;

3. *The mechanism of selection:* Finally, the last objective of my Ph.D. was to propose a model that describes the selection process that is affected by mutations in S/MAP kinase pathway in quiescence.

MATERIALS AND METHODS

2 MATERIALS AND METHODS

The progress in Next-Generation Sequencing (NGS) technologies allows to measure directly the rate and spectrum of mutations genome-wide. For my thesis, I used several NGS techniques to investigate the genetics of quiescence.

2.1 Schizosaccharomyce pombe long-term quiescence

To minimize the unavoidable bias introduced by stochastic mutation events induced by DNA replication during growth, the number of cell divisions was limited to that necessary to produce the number of cells required for the subsequent experiments. The protocol for long-term quiescence is described below.

The wild-type haploid prototrophic Msmt0 strain (PB1623) was used for all experiments. Starting from a glycerol stock at -80 °C, cells were grown on a plate containing Edinburg minimum medium (EMM) (Mitchison and Creanor, 1971) for approximately 60 hours (2.5 days) at 32 °C to form individual colonies. As soon as colonies reach approximately 5 x 10^6 cells (22 to 23 generations or 1.2 mm in diameter), they are transferred into 10 ml of EMM to start a liquid culture. The number of cells was measured with a Beckman Counter (Z-series). At a density of 10^6 cells/ml, the cells are immediately centrifuged at 3000 g, washed in minimum medium without nitrogen (EMM-N) and finally suspended in 10 ml of EMM-N. The medium was not changed during the experiment, but the glucose concentration was set to 4% to maintain a sufficient amount of energy. To compensate for the water lost by evaporation during the incubation, the cultures were weighed every week and their volume was readjusted with water. The viability of the cultures was regularly monitored by plating out cells at an appropriate dilution onto rich medium (YES) and counting the colony forming units (CFU%).

2.1.1 Screening for a phenotype after long-term quiescence

To determine the presence of a phenotype, 200 colonies were picked randomly after 3 months of quiescence and tested for their sensitivity to a range of temperatures (18 °C, 25 °C, 32 °C, 37 °C), to chemical agents (2 M sorbitol, 4 mM and 8 mM hydroxyurea, 10% and 0.15% SDS, 15 µg/ml Thiabendazole) and to high concentrations of salts (0.8 M KCl, 0.15 M $Ca(NO_3)_2$, 0.2 M and 0.3 M $CaCl_2$) that do not affect the growth of wild-type cells. Drop assays starting with 10^4 cells per drop with 5-fold serial dilutions were spotted onto YES plates containing a selective agent and grown for 3 days to form colonies (Figure 11).

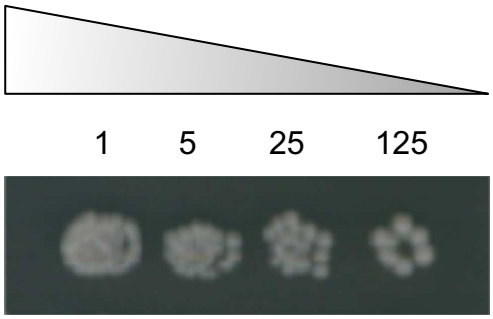

Figure 11: Spot assay for phenotypic test.

10 µl of 1/5 serial dilutions starting at 10^5 cells per ml were spotted onto YES plates and incubated at 32 °C for 3 days.

2.2 Whole genome sequencing

2.2.1 DNA preparation and sequencing

10 ml of the stationary phase culture was used to prepare genomic DNA for Whole Genome Sequencing. Cells were centrifuged for 3 minutes at 3000 rpm. The supernatant was discarded and the pellet re-suspended in TENS buffer (Tris pH 8 0.1 M, EDTA pH 8 0.1 mM, 0.2 M NaCl, 1% SDS). 300 µl of the solution were transferred to a 2 ml Eppendorf tube containing 800 µl of glass beads 0.5 mm size (Glass Beads: Sigma G8772). The samples were installed on a Vibrax Vortex (IKA) for 10 minutes with at 1500 rpm to lyse the cells. The cell lysate was treated twice with a mix of Phenol-Chloroform-Isoamyl alcohol (24/24/1) followed by centrifugation for 10 minutes at 13 000 g prior to the precipitation step. To precipitate the DNA, 2.5 volumes of the 100% ice-cold ethanol and 1/10 volume of 3M Sodium Acetate were added and the samples were rested for 10 min at -80 °C prior to the centrifugation. Precipitated DNA was washed once with the 70% ice-cold ethanol at 13 000 rpm for 10 minutes. Finally, the DNA was dissolved in Tris-EDTA buffer and incubated at 37 °C overnight with RNase (Thermo Fisher Scientific) at a final concentration of 20 µg/ml. To eliminate the residual ribonucleotides, the extracted DNA was precipitated and washed twice with 70% ethanol and dissolved in TE buffer. The quality and quantity of the resulting DNA determined with a Nanodrop. Library construction and sequencing were performed by Illumina HiSeq 2500 paired-end sequencing technology following the manufacturer's instructions.

2.2.2 Data analysis and variant calling

The quality of the produced paired-end reads was evaluated by analyzing the Phred quality score of the raw reads (a probability of an incorrect base call at the given position) with the FastQC software (v.0.10.1) (Arcangioli2006). FastQC imports fasta files and analyze main statistical properties of a high-throughput sequencing data. Further, the reads were preprocessed using fqCleanER software (v.5.01). The preprocessing step includes the trimming of short and aberrant reads with AlienTrimmer (Criscuolo and Brisse, 2013), correcting sequencing mistakes with Musket (Liu et al., 2013), and merging the overlapping reads using Flash (Magoč, 2011). The remaining reads were aligned to the *S. pombe* ASM294v2.23 reference genome with Burrows-Wheeler Aligner (v.0.7.5a.) (Li and Durbin, 2009) applying BWA-MEM algorithm developed for long sequencing reads (from 70 bp to 1 Mbp). SAMtools (v.0.1.19) was used to convert the aligned reads (.sam files) into binary format (.bam files), sort and index.

At this stage resulting sequencing data with the potential mutations in a form of the sorted and indexed .bam files could be visualized by IGV browser (Robinson et al., 2011). Prior to the raw variant calling the quality score recalibration and indel realignment were performed with Genome Analysis Toolkit (GATK (v.2.7–2) (McKenna et al., 2010). In addition, processing step includes marking and elimination of the duplicates with Picard-tools (v.1.96) (Li et al., 2009). SNPs and Indels variant calling and filtration were accomplished with standard filtering parameters according to GATK Best Practices recommendations. Finally, the automated annotation was performed using snpEff (v.3.5) (Cingolani et al., 2014). The programming steps are described in detail in the code section 1.

Code section 1: Whole genome sequencing analysis

```
# Modules used in this chapter

SLURM cluster

Module load

fqCleanER.sh/5.01: # read preprocessing

        -AlienTrimmer/0.4.0

        -khmer/1.3
```

-**musket**/1.1

-**FLASH**/1.2.11

bwa/0.7.5a # read alignment

picard-tools/1.94 # read preprocessing

samtools/0.1.19 # read preprocessing

GenomeAnalysisTK/2.7-2 # variant calling

snpEff/3.5 # variant annotation

 # reads quality control

fastqc $f > $f.fastqc

 # reads preprocessing

fqCleanER.sh -l $f1.fq -2 $f2.fq -l 80 -q 30 -s TRCM > $f_preprocessed.fq

-**s** **TRCM** – set of the programs used for read pre-processing:

#**T**rimming and discarding short reads with **AlienTrimmer** with parameters -**l** **80** discarding the reads with a read **l**ength below **80**, -**q** **30** trim the tails of the reads if the Phred **q**uality drops below **30** (probability of the incorrect base is < 0,1%). These parameters were chosen based on analyses performed previously for sequencing fission yeast genomes after long-term quiescence (Gangloff et al., 2017);

Reducing overrepresented reads with **khmer** software package (by default 100, ruled by parameter **c**, not specified);

Correcting sequencing mistakes with **Musket**, correction is made based on the number of threads (by default 1, ruled by parameter **t**, not specified);

Merging overlapping paired-ended reads with **Flash**

 # aligning reads to the reference genome

bwa mem -M genome.fa $f.fq > $f.fq.sam

mem - an algorithm to align 70 bp – 1 Mbp sequences by seeding alignments with maximal exact matches (MEM) and then extending seeds with the affine gap Smith-Waterman algorithm (SW)

-M – parameter for compatibility with picard-tools

 # Sorting and indexing the .bam files

samtools view -bS -q 30 $f.fq.sam -o $f.fq.sam.bam

view an algorithm to convert high-throughput data within different file formats

-q skip all the alignments with mapping quality below 30

-bS – parameters that determine the types of the input and output files for data analysis: input is in .sam format and output is in .bam format

-o – output file in .bam format

samtools sort $f.fq.sam.bam -o $f_sorted.fq.sam.bam

sort an algorithm to sort by the alignments by leftmost coordinates

-o – output file in .bam format

BuildBamIndex I=$f.fq.sam.bam > $f.bai

BuildBamIndex – an algorithm from picard-tools to index a .bam file. Indexing .bam file provide a rapid access to the aligned sequences. As an output program creates a companion .bai file based on the .bam input;

I – input file in .bam format

 # marking duplicate reads with picard-tools

MarkDuplicates I=$f.fq.sam.bam O=$f_marked.fq.sam.bam M=$f.txt

I – input (in .bam format) ;

O – output (in .bam format);

M – .txt file with marked duplicates

 # Indel realignment to improve indel calling

GenomeAnalysisTK -T IndelRealigner -R genome.fa –I $f.fq.sam.bam -o $f_realigned.fq.sam.bam

-T – parameter to define the algorithm to be used in an analysis from the proposed in GATK. IndelRealigner; IndelRealigner – algorithm to realign indels to improve indel calling;

-R – reference genome (ASM294v2.23);

-I – input file (in .bam format);

#-o – output file (in .bam format)

 # filtering raw variants

GenomeAnalysisTK -T UnifiedGenotyper -R genome.fa -I $f.fq.sam.bam -ploidy 1 -glm BOTH -stand_call_conf 10 -stand_emit_conf 5 -o $f.fq.sam.bam.vcf

-T – parameter to define the algorithm to be used in an analysis from the proposed in GATK. UnifiedGenotyper – algorithm call raw variants;

-R reference genome (ASM294v2.23);

-I – input file to be analyzed;

-ploidy – setting the ploidy of the analyzing genome (haploid for *S. pombe*);

-stand_call_conf – minimum confidence threshold (phred-scaled, based on the QUAL score) to filtered;

--stand_emit_conf – a minimum confidence threshold (phred-scaled, based on the QUAL score) of the variant included into analysis;

-glm general linear model – genotype likelihood model, calling BOTH indels and SNVs,
-o – output file (in .vcf format);

#filtering the SNVs variants

GenomeAnalysisTK -T VariantFiltration -R genome.fa -o $f.fq.sam.bam.vcf --variant $f --filterExpression 'QD < 2.0 || FS > 60.0 || MQ < 40.0' --filterName "snp_filter"

#**QD** (QualByDepth) – a variant confidence (a **QUAL**ity score) divided by the allele depth (**AD**) of a variant.

QUAL – Phred-scaled quality score for the assertion made in **ALT**ernative alleles

AD – **A**llele **D**epth, a number of reads that support each of the reported alleles

#**FS** (FisherStrand) – Phred-scaled p-value using Fisher's Exact Test to detect strand bias (the variation being seen on only the forward or only the reverse strand) in the reads. More bias is indicative of false positive calls.

#**MQ** (RMSMappingQuality) – A Root Mean Square of the mapping quality of the reads. An equivalent to the mean of the mapping qualities of the variant plus the standard deviation of the mapping qualities

 # filtering the indel variants

GenomeAnalysisTK -T VariantFiltration -R genome.fa -o $f.fq.sam.bam.vcf --variant $f --filterExpression 'QD < 2.0 || FS > 200.0 || ReadPosRankSum < -20.0' --filterName "indel_filter"

#**QD** and **FS** are identical parameters that have been defined for SNV calling

 # ReadPosRankSum – Mann-Whitney-Wilcoxon Rank Sum Test for site position within reads (position supporting reference vs position within reads supporting alternative)

```
# variant annotation

snpEff -c snpEff.config -v -o gatk genome.genome $f.vcf > $f_annotation
GenomeAnalysisTK -T VariantAnnotator -R genome.fa -A SnpEff --variant $f.vcf –
snpEffFile $snpeffannotation -o $f_annotated.vcf

# -c specifies config file, a file containing a database for annotation

# -v –verbose (detailed) mode
```

In a first approximation, unique mutations called through the pipeline were defined as those that have arisen during quiescence, while those that are present in multiple copies occurred by replication (i.e. during growth). However, we cannot rule out that identical mutations in quiescence result from either division during quiescence or mutation hotspots.

2.3 Backcross of the strains with the wild-type

To verify if the phenotype is associated with a single mutation, the phenotypic candidates were crossed with the original wild-type PB1653 strain of the opposite mating type (PΔ17) and dissected. A drop containing an equimolar mixture of the wild-type and the mutant cells was placed on a SPAS mating medium plate and incubated for 2 days at 25 °C to form spores. On the third day, a drop of the cell suspension was placed on a YES plate in the morning and incubated at 32 °C during several hours to liberate the spores from the asci. In the afternoon, 12 tetrads per strain were dissected using a Singer dissection microscope manipulator (MSM 400). After 3 days of growth, the phenotype of the spores was examined by testing their sensitivity to selective agents as it was described previously either directly by replica plating or by making a drop assay. If the phenotype is linked to a single mutation, the colony growth during the phenotypic test will exhibit a 2:2 segregation in every tetrad. As a final verification, the presence of a mutation was tested directly by PCR amplification and Sanger sequencing the candidates (the primers used to verify the mutations are listed in Table 3).

Table 3: List of primers used to verify the mutations after long-term quiescence

Strain name	Mutation to verify	Phenotype associated	Forward primer	Forward primer sequence 5' > 3'	Reverse primer	Reverse primer sequence 5' > 3'
29R	*win1*-394+13 bp	37 °C	OL645	CTGTTTCCCGTTTTGGGTT	OL646	ACGCTTGGGCTTTTCTGG
6P	*sty1*-G74C	37 °C	OL690	TGTTCCCAGAAGCTCCGT	OL692	ACCTCCTTACCACAACTTAACC
8R	*sty1*-C197A	37 °C	OL690	TGTTCCCAGAAGCTCCGT	OL692	ACCTCCTTACCACAACTTAACC
15R	*pek1*-T969A	0.2M $CaCl_2$	OL608	ACCGGTTTCCATTCCCTC	OL609	CCTGGGAAGTTTGGTGTAGT
34R	*pmk1*-153A	0.2M $CaCl_2$	OL617	TTTTTCCACATCCCTTTTGCC	OL618	CGCGTAACATACCAACTCT
19R	*pmc1*-G1246T	0.2M $CaCl_2$ and 10% SDS	OL629	AACGGCGACGACTAACAAA	OL630	CCGTGGGTGGTGTGAATGA
2P	*pmc1*-2906-C	0.2M $CaCl_2$ and 10% SDS	OL589	GGAGTAGGAGGGTCAGTGGCAA	OL588	CTTGCACGCTCATCTCCT
10R	*pmc1*-2920-9 bp	0.2M $CaCl_2$ and 10% SDS	OL589	GGAGTAGGAGGGTCAGTGGCAA	OL588	CTTGCACGCTCATCTCCT
3P	*sgf73*-890+T	4 mM HU and 18°C	OL846	AGAGGCTAGCAAGAAGAAGAA	OL847	GGCGGGCACTAAAAGGAA
21R	*tif452*-G251T	37 °C	OL632	ACGACCACCGCATCTTTT	OL633	GCCCATTTCCCACCATTCA
9P	*win1*-1086-G	37 °C	OL947	CCAGAAAAGCCCAAGCGT	OL946	GTTAATTCGTTGCTCTCATCCC
10P	*qcr6*-325+7 bp	18 µg/ml TBZ resistance	OL648	CGCCCTGCTCTACCTTCTTT	OL649	CAGCTTTCACCCCGATTT
11P	*SPCC14G10.04*-A1T	37 °C	OL651	AGCGAGTTTCTGTTCCATTT	OL652	GCCCTACCTTTTCATTTCCTT

2.4 Targeted resequencing of 9 genes of interest

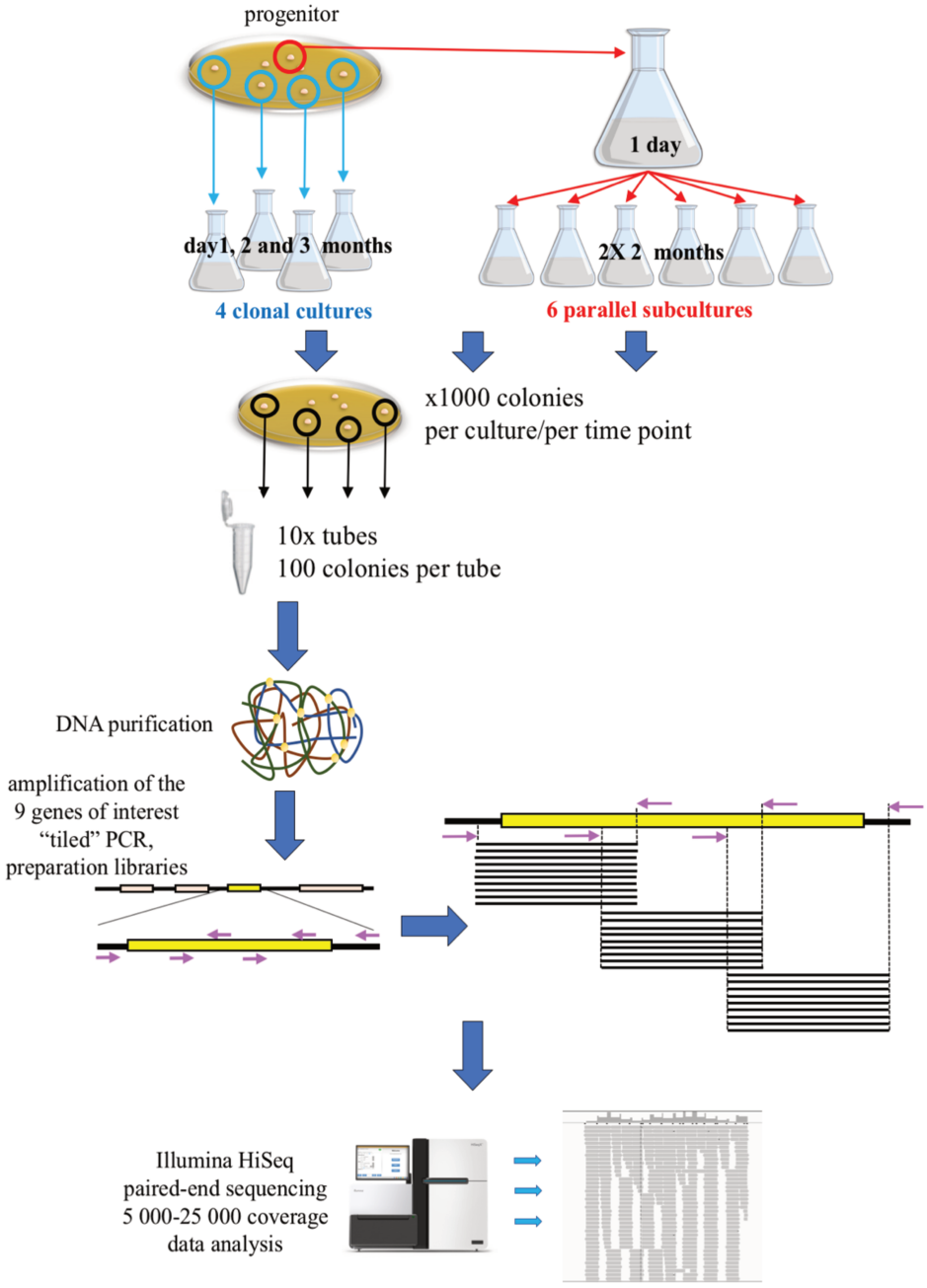

Figure 12: The experimental design for targeted resequencing.

Schematic of the different steps described below.

To investigate if the mutations in the MAP kinase pathway genes (*mkh1, pek1, pmk1, win1, wis1, sty1, pmc1, sgf73*) that were detected in individual cells through whole genome sequencing provide a selective advantage in quiescence, the dynamics of these mutations at the population level were studied. In this experimental design, I re-sequenced with a coverage

greater than 10,000 the 9 genes previously identified in a pool of 1000 surviving colonies taken from independent quiescent cultures at different time points. The proportion of the variants among the reads reflects the distribution of the mutations in the population: If a mutation has appeared in the culture and forms a colony on the plate, this mutated locus will represent 1/1000 of the collected DNA. Hence, a 10,000 coverage will produce 10 reads on average containing this particular mutation. The details of the experiment are described below.

2.4.1 Sample preparation: Colony picking

Aliquots of the cultures after 1 day, 2 months and 3 months of quiescence were taken and frozen in 20% glycerol prior to plating to reduce the proportion of diploid cells that were previously shown to accumulate in the long-term quiescence experiment. The survivors were plated on YES plates and grown for 3 days at 32 °C to form the colonies. The 1,000 picked colonies were dispatched into 10 Eppendorf tubes containing 100 µl of water each and 100 colonies per tube. After long-term quiescence, *S. pombe* forms colonies of different sizes. Therefore, to collect a similar number of cells for each colony, the colonies were picked in three waves; the biggest ones in the morning, the second wave in the evening, and finally the last ones in the morning the following day. Each colony contained approximately $5x10^6$ cells. The pool of colonies that were picked together were stored at -80 °C in 20% glycerol.

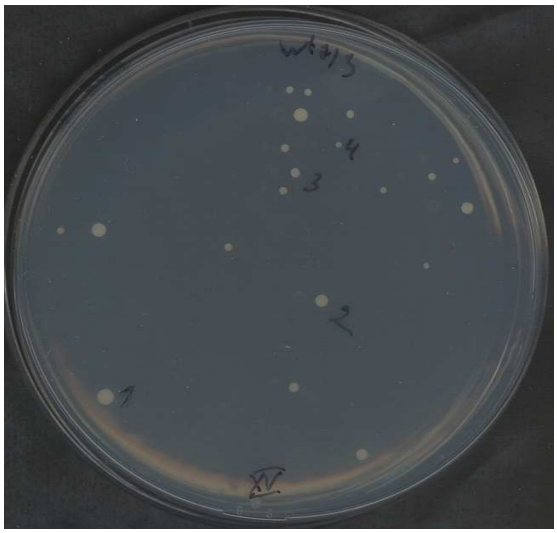

Figure 13: The size of the colonies formed after 3 months of quiescence.

The colony size by number: **1.** 2.8 x 10^7 cells, **2.** 1.1 x 10^7, **3.** 2.8 x 10^6, **4**. 9.6 x 10^5

2.4.2 DNA extraction, quantification and normalization

From each pool of colonies, approximately 2.5x10^7 cells were used for DNA extraction (20 µl from the stock of each tube). DNA was extracted using a standard phenol-chloroform protocol, quantified on agarose gels and normalized for PCR reactions. The DNA purification mix contains 180 µl of solution A (2% Triton X-100, 10% SDS, 5M NaCl, 1M Tris pH 8.0, 0.5M EDTA pH 8.0), 200 µl of glass beads, 200 µl of phenol-chloroform mix. To break the cells, samples were placed on a Vibrax for 20 minutes, then centrifuged at 13 000 rpm for 5 minutes to separate the 2 phases. The next steps are identical to the protocol mentioned in previous chapter. The final precipitation inside each Eppendorf tube was diluted in 50 µl of TE buffer. 2 µl from each sample of the final solution was used to verify the quality of the DNA extraction on agarose gels (mixed with 2 µl of water and 1 µl of 6x LB buffer). (Figure 14 and Figure 15.) To normalize the DNA for PCR reaction, DNA concentration was assessed on agarose gels by staining DNA with Ethidium Bromide. The concentration of DNA was measured by comparison with known concentrations of serial dilutions of a phage lambda molecular marker, digested with HindIII (Promega). The fluorescence was activated by long UV light and images were taken and processed with Image Lab software (Bio-Rad). The amount of DNA (in copies), based on the DNA mass (in ng) measured by relative fluorescence was determined with an online calculator https://cels.uri.edu/gsc/cndna.html via the formula:

Equation 1: The number of copies of a template

$$N = \frac{m \times N_A}{l \times 10^9 \times 650}$$

where N – a number of copies, m – mass of the measured DNA (in ng), N_A – Avogadro constant (6.022×10^{23}), l – length of the analyzed DNA in base pairs, 650 – an average molecular mass of a base pair (in Daltons) 10^9- number to convert into nanograms.

The mass of purified DNA corresponds to the expected number of cells it was extracted from. For instance, 10.4 ng from 2 µl corresponds to 260 ng in the final volume of 50 µl and 10^7 cells. This calculation is important to retain enough genetic material for the PCR reactions (see chapter below). DNA was normalized, adjusted to the minimum concentration and pooled.

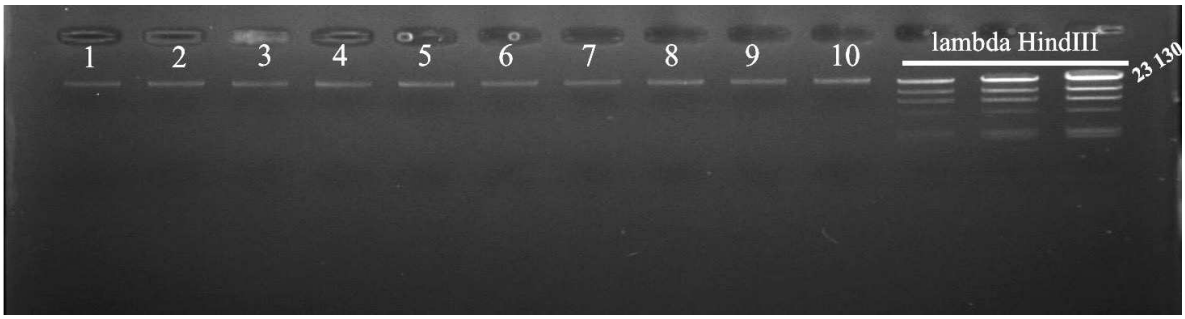

Figure 14: Example of DNA after extraction.

0.7% agarose gel after a 20 min migration at 5 Volts/cm in TAE 1X buffer. DNA was stained with Ethidium Bromide.

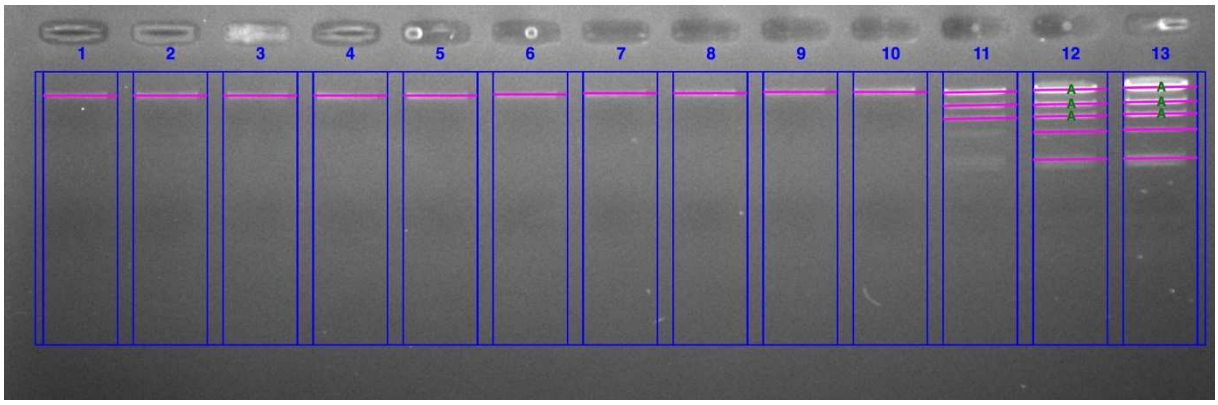

Figure 15: Quantification of DNA on agarose gels.

Relative comparison of the fluorescence of known concentrations of a marker DNA (λ/HindIII) was performed with Image Lab software (Bio-Rad).

The relevant normalized quantity of genomic DNA from each of the 10 tubes was collected into a single tube, and precipitated with ethanol in order to increase the concentration of DNA as described before. The precipitated DNA was dissolved in 50 µl of TE buffer.

2.4.3 PCR of the genes of interest

To cover the 9 genes of interest (*win1*, *wis1*, *sty1*, *mkh1*, *pek1*, *pmk1*, *sgf73*, *pmc1*, *tif452*), 64 overlapping primer pairs were designed for 64 independent PCR reactions to generate fragments of an average size of 420 base pairs. (Table 5). The PCR reactions were performed using the Q5 Hot-Start high-fidelity polymerase delivered as a 2x Master mix (New England Biolabs) (Table 4). This polymerase creates few mistakes in the reaction (Potapov and Ong, 2017). With a fidelity rate of 5.3×10^{-7} substitutions per nucleotide per doubling, it is expected to have 99.8 % of mutation-free copies after 25 cycles of amplification. The calculation was

made with the PCR Fidelity Estimator (v.1.0.2) (http://biosoft-ipcms.fr/files/code.php). Each PCR reaction is initiated with 1.25 µl of DNA (30 ng of DNA template). Thereby, each genome from the pool of colonies is present at least in 5000 copies. The final volume is 50 µl. The quantity of products from each PCR amplification was estimated on agarose gels and adjusted to a similar concentration by quantification of the fluorescence with ImageLab software as described previously for genomic DNA. 2 µl from each PCR reaction mix was used for quantification on agarose gels.

Table 4: Conditions of PCR reactions for targeted resequencing

	time	t° C
1st cycle	00:30	98
denaturation	00:10	98
annealing	00:15	51
hybridization	00:15	72
last cycle	01:00	72
storage		8
number of cycles	25	

Table 5: Primers used in targeted resequencing experiments

Gene targeted	Forward primer	Primer Sequence 5' > 3'	Reverse primer	Primer Sequence 5' > 3'
win1	OL1073	TAGTTGCATTGACTTCGCT	OL1074	TGGCCTTCTGTGATTTTCTT
win1	OL1075	CATCGTCGCTCTTTGACT	OL1076	CTGTGCATATAATCGTCTTCCT
win1	OL1077	CTTCTTCCTCTTCCATTCC	OL1078	CGAGTCCTCCTCATCATAA
win1	OL1079	CTTCTCTAAGCATTCGTC	OL1080	TAGCACATCAACCATACC
win1	OL1081	GTGGATGGAAATATGGTGT	OL1082	TGGTCCGTTTGAAATTTGAG
win1	OL1083	GGTTGGTAATGAGGAAATGG	OL1084	TTGTTGAATGATATGGACGG
win1	OL1085	CGTCTTCTTTCTTTTCCGT	OL1086	ATATTTCACCAACCAGCG

win1	OL1087	CCACATCGAACACGGATT	OL1088	CGCATATGGAGGTACACTTT
win1	OL1089	CGAACATGAAGGAGCATAC	OL1090	CACATCAAGCAATGACAAAG
win1	OL1091	CTCACTTGTTGATTCTGC	OL1092	CCACACATTTTCCAACCT
win1	OL1093	CAGTTGGGTTGGATTCAT	OL1094	CCTGTTCTCCTTTGTCGT
win1	OL1095	AAAGTAATAGAAGGGACCGA	OL1096	CCTCAATTCTACCGTAAC
win1	OL1097	GAAGTGCATCGTGAAAAAG	OL1098	AATATCCATAGCACCAACC
win1	OL1099	GCAGCATCTAGACCAAAA	OL1100	TTCGACTACGGATGAGTT
win1	OL1101	CGTTGTTTTGTTTCTGATCCC	OL1102	TCTCTTCCTAGCGCCGTA
wis1	OL1509	AACAGAGCAGGCAATTAGA	OL1510	ACATGGCTCCTGAAAGAA
wis1	OL1511	GATAAGCTCCTAAAGCCA	OL1512	TGGTGCCTTTTTTGTGGA
wis1	OL1513	ACTCCTTCGTCTTTGATACC	OL1514	CTAAACATTCCTCCCACCC
wis1	OL1515	GAAAATGTGGAAAAAGGGG	OL1516	ACAGGAGAAATTGAAGGC
wis1	OL1517	TCCGGCATTGATTTTGATCT	OL1518	CTTCTCCAAATAATCAACCC
sty1	OL1041	CATAACATACCCCGAGAACA	OL1042	CCGAGACCACGTTAACCA
sty1	OL1043	ATTACTTCCATAGGCGGC	OL1044	ACTACTTACATCGCGACC
sty1	OL1045	TGGGTTTCAGATCACGGT	OL1046	CCTTTGGCCTCGTTTGTT
sty1	OL1047	AACAGCGACATTCATTCCA	OL1048	ACATACCTCCTTACCACAAC
mkh1	OL1329	CGAGGAAACGCTAAGTAA	OL1330	GCAAACCTGTCCATGCAA
mkh1	OL1331	TTCCAACACTACACATCC	OL1332	TAGTGCAATATCTGGGTTTC
mkh1	OL1333	AATTCCGCAAACATCGAC	OL1334	AAATACGACATAACGCGAG
mkh1	OL1335	TACAATCCTAGAGCCCCAAA	OL1336	TCGCCTAAAACTCCTGAA
mkh1	OL1337	CCCAGTTACCAGAATTGA	OL1338	CCGGACATAACGAAGCTA
mkh1	OL1339	GCTTCCACACTTTCCTTT	OL1340	GACGTTTTCGAGGGTTTG
mkh1	OL1341	GCCATTTCTCCTTTAGCAC	OL1342	GGCGGGGCTCAATACATA

mkh1	OL1343	CACTATCCATACCCGATTCT	OL1344	CAAATTCGAACCCATTCCA
mkh1	OL1345	TACCCACTCACCTTGATCC	OL1346	CTCTGGTTTCCGCTCTTC
mkh1	OL1347	CTTTTGAGGGACGAATTTTG	OL1348	GTTCTGGGTATATGGCTG
pek1	OL1049	GGTTGTTTGTTTGCGAGG	OL1050	TATCCCGGCTCTCCTTTC
pek1	OL1051	TGGTGTTTTCTAGCGAGT	OL1052	TTTGTATATCGCGTCGAG
pek1	OL1053	GGAATATTGCGGAGCAGG	OL1054	AGGTAAAAGGGGAGGTGG
pek1	OL1055	GGTTTAACATTGATGGAGG	OL1056	AACAAGCGAACTGGAAGA
pek1	OL1057	AGAGTTCCTTCGTCAAGT	OL1058	AAGCTAGCAAGGCGTAAA
pmk1	OL1059	TTTTTCCACATCCCTTTTGCC	OL1060	GAAAGAACATCGCCGGAC
pmk1	OL1061	GAGAGAGATAAAACTGCTGA	OL1062	GTGTCGAATGGGTGGAAG
pmk1	OL1063	TGCATTTACGATCTCGAC	OL1064	ATTTCTACTCACGAACCTCA
pmk1	OL1065	TGGTTTTATGACGGAGTATG	OL1066	TTCCTCGGTGTTCCTTCT
pmk1	OL1067	ACAGGAGTATGTTCGAAG	OL1068	TCTCCTCTTCATCTTCTCTT
pmk1	OL1069	CTCATCCAACAAACCCAAC	OL1070	GCAAACCTGTCCATGCAA
pmk1	OL1201	CTTGCATTTACGATCTCGAC	OL1202	TAGTGCAATATCTGGGTTTC
pmc1	OL1293	GGCGATTTCCAACGAGAA	OL1294	GAACCCACATCTCCCAAC
pmc1	OL1295	GAGTTGTTGAGTAGGTGG	OL1296	CGGAGATTGGATAACAAG
pmc1	OL1297	GCACCTCCGAAAAAAACAA	OL1298	TCGACTGACCAAAGCTCT
pmc1	OL1299	TCTCAGGTTTCCTCTTTAACAC	OL1300	TTGCACGCTCATCTCCTT
pmc1	OL1301	CTTTTTTTAGTGCAGGCG	OL1302	TCCCAAAGATATTCCCACCA
pmc1	OL1303	GTCAAACACACGATAGCAT	OL1304	ACTTCGGGACTTAACTCT
pmc1	OL1305	CCTTGGGGTGTCAGAATTA	OL1306	AGAACAAGGGTCAAGAGT
pmc1	OL1307	AGCAAAAGCCAAAGCCAA	OL1308	GAAAGAACATCGCCGGAC
pmc1	OL1309	AATTAACACCGACAGCAG	OL1310	GTGTCGAATGGGTGGAAG

pmc1	OL1311	CAGTCATTCACACCACCCA	OL1312	ATTTCTACTCACGAACCTCA
pmc1	OL1313	CTCATCTGCAATTTATCGGC	OL1314	TTCCTCGGTGTTCCTTCT
pmc1	OL1315	CCACTTCGAGAGCTATTT	OL1316	TCTCCTCTTCATCTTCTCTT
sgf73	OL1451	AAAGTCGAAAATGCGTGG	OL1452	TGTTTTGCTTGCAGCTTGT
sgf73	OL1453	TTCTTTTGCAGTTTCGAGG	OL1454	TAAATCGACAGCTAAGGG
sgf73	OL1455	TTCTTTTCATGATTCCCAG	OL1456	AAACTCGGTTCTTATCAA
tif452	OL1175	AACCCAATTACGACCACC	OL1174	CCCCAAAACTCTTCCACT
tif452	OL1177	AAAAACACACCCCCTTCA	OL1176	CACCAGTAACTTCTTTCCCA
tif452	OL1173	ACTGCTGTGATATCGACT	OL1178	TCGTAAATGAACACCCCT

2.4.4 PCR products purification.

At least 500 ng is required to generate a library to be sequenced by NGS. From each PCR reaction mix, 10µl of the normalized PCR reactions (approximately 100-200 ng of PCR products) was used for PCR purification (6.4 – 12.8 mg of DNA). For PCR product purification, QIAGEN PCR purification kit was used. For each 64 PCR samples, 7 silica spin columns were used to purify PCR products. 9 PCR reactions per silica spin column were pooled to purify the DNA. PCR purification was carried out according to the manufacturer's recommendations. Finally, for NGS, the quality and quantity of the purified samples were determined by Nanodrop.

2.4.5 Library construction and sequencing.

The library preparation and sequencing of the PCR products from 4 independent cultures were carried out by the sequencing platform at the Institut Pasteur. The libraries were prepared using NEXTflex PCR-Free DNA Library Prep Kit with the standard Illumina adapters. MiSeq system (Illumina) was used to generate pair-end reads of 300 nt in size. The coverage in this sequencing experiment ranged from the 8 to 75,850 with an average of 12,500. The 14 libraries of the duplicate of six subcultures and a control of day1 were prepared using Illumina TrueSeq DNA PCR-Free Prep Kit on the Illumina HiSeq 2500 system. The coverage in this experiment ranged from 5 to 150 079 with an average of 53 000. The sequencing was performed by Novogene

Bioinformatics Technology Company LTD.

2.4.6 Data analysis.

Prior to process the data, the quality of the sequenced reads was verified by FastQC software (v.0.10.1.). fqCleaner (v.5.01) was used to clean and preprocess the raw reads. Reads preprocessing includes removing the oligo alien sequences, trimming short and aberrant reads with AlienTrimmer (Criscuolo and Brisse, 2013), correcting sequencing mistakes with Musket (Liu et al., 2013), and merging the overlapped reads using Flash (Magoč, 2011). Removing overrepresented reads and marking duplicate reads are not applicable for targeted resequencing analysis. Since in this sequencing experiment we used the overlapping PCR fragments, the low-quality bases that are present at the beginning or at the end of the Illumina read ends are corrected by the high-quality bases of neighboring overlapping reads. The clean paired-end reads were aligned to the *Schizosaccharomyces pombe* reference genome ASM294v2.23 using BWA-MEM software (v.0.7.5a) (Li and Durbin, 2009) applying BWA-MEM algorithm developed for long sequencing reads (from 70 bp to 1 Mbp). SAMtools (v.1.9) was used to convert the aligned reads (.sam files) into binary format (.bam files), sort and index. At this stage, the sequencing data can be visualized with the IGV browser (Robinson et al., 2011). The .bam files were converted into the .mpileup format using SAMtools software to generate an input file for VarScan. VarScan was used to extract the second most frequent variant and sequencing properties for each potential variant (Koboldt et al., 2009). The subsequent analysis was performed using custom R scripts.

Code section 2: Targeted resequencing analysis

```
#Modules used in this charter

SLURM cluster

Module load

FastQC/0.10.1

fqCleanER.sh/5.01:

        -AlienTrimmer/0.4.0

        -musket/1.1
```

-**FLASH**/1.2.11

bwa/0.7.5a

samtools/1.9

varscan/2.3.6

R/3.5.1:

package(**ggplot2**)

package(**gsubfn**)

package(**trackViewer**)

SLURM cluster

#reads quality control

fastqc $f > $f.fastq

#reads preprocessing

fqCleanER.sh -1 $f1.fq -2 $f2.fq -a primer_list.fa -l 50 -s TCM > $f_preprocessed.fq

-s TCM - – set of the programs used for read pre-processing as it was mentioned for

#Trimming and discarding short reads with **AlienTrimmer** with parameters **- l 80 - a** primer_list.fa: discarding the reads with a read **l**ength below **50**, **-a** removing the sequencing of the primers used during PCR amplification step from .fasta file primer_list.fa.

#alignment reads to the reference

bwa mem -M genome.fa $f_preprocessed.fq > $f_.fq.sam

```
#Sorting and indexing the .bam files
samtools view -bS -q 30 $f.sam > $f.sam.bam
samtools sort $f.bam -o $sorted_f.bam
BuildBamIndex I=$f.bam > $f.bam.bai
```

```
#Creating .mpileup file
samtools mpileup -d 100000 -ABQ0 -f genome.fa -L gene.bed $f.sgl.sam.bam. -o
$f.sgl.sam.bam.mpileup

# mpileup – multi-way pileup

# d – maximum per –BAM depth

# A – count anomalous read pairs

# B disable BAQ computation

# Q skip bases with baseQ/BAQ smaller than INT

# 0 – output base positions on reads

# f – faidx indexed reference sequence file

# L – only output alignments overlapping the input .bed file

# o – output file in .mpileup format

#Variant calling

VarScan mpileup2cns $f.sgl.sam.bam.mpileup > $f.sam.bam.mpileup.txt

# mpileup2cns – algorithm to call consensus and variants from an .mpileup file

# As an output VarScan mpileup2cns generates Tab-delimited with the following columns:

Chrom    chromosome name

Position  position (1-based)

Ref      reference allele at this position
```

Cons	consensus genotype of the sample */(var) indicates heterozygous
Reads1	reads supporting reference allele
Reads2	reads supporting variant allele
VarFreq	frequency of variant allele by read count
Strands1	strands on which reference allele was observed
Strands2	strands on which alternative allele was observed
Qual1	average base quality of reference-supporting read bases
Qual2	average base quality of variant-supporting read bases
Pvalue	Significance of variant read count vs. expected baseline error
MapQual1	Average map quality of ref reads (only useful if in pileup)
MapQual2	Average map quality of var reads (only useful if in pileup)
Reads1Plus	Number of reference-supporting reads on + strand
Reads1Minus	Number of reference-supporting reads on – strand
Reads2Plus	Number of variant-supporting reads on + strand
Reads2Minus	Number of variant-supporting reads on – strand
VarAllele	Most frequent non-reference allele observed

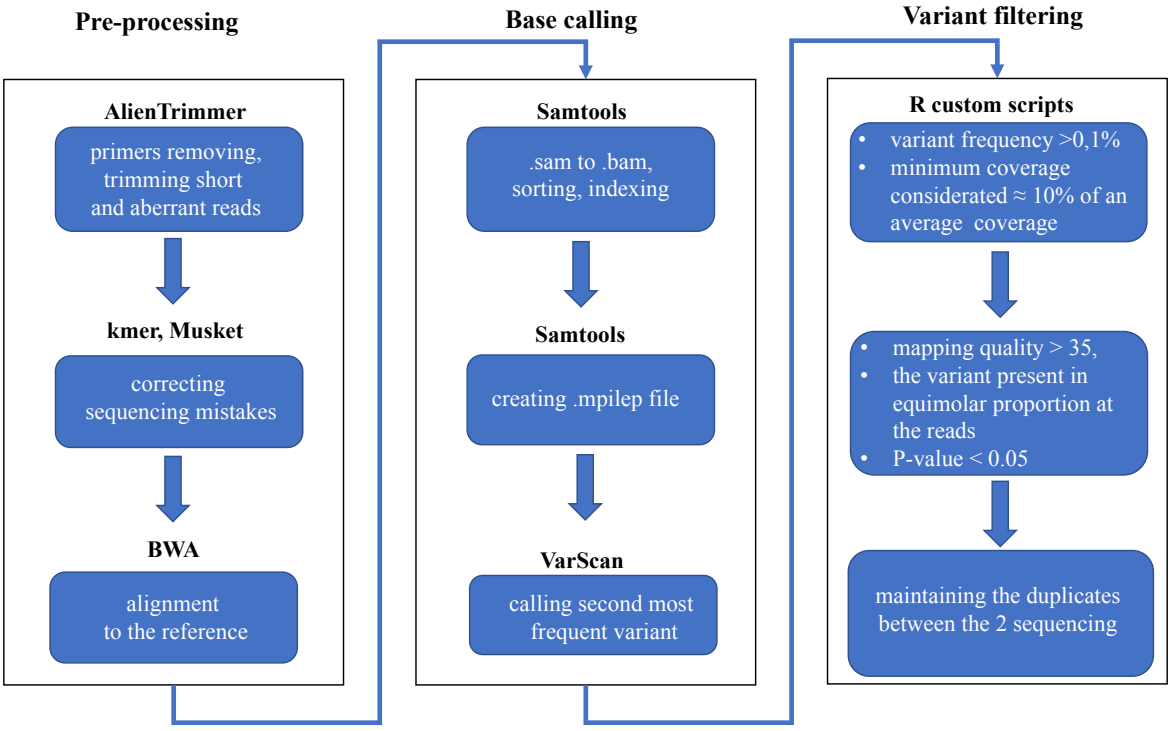

Figure 16: bioinformatics pipeline for the analysis of data from targeted resequencing experiments.

Pre-processing and Base calling steps were performed according to standard procedures, whereas Variant filtering was acchieved through custom filters described below.

2.4.7 Variant calling

We used the mpileup2cns algorithm from VarScan (Koboldt et al., 2009). to extract the second most frequent variant present in the dataset at a given position. Typically, detection threshold limits the variants called by VarScan at a 1% frequency (Koboldt et al., 2009). The algorithm calculates p-values based on the p-value calculated from Fisher's exact test for the distribution of the observed reads versus expected non-variants. To improve the calling efficiency, we applied several additional filters. First, only the variants covered over a 1,000 time in the first experiment and 5,000 time in the second one that are present at frequency above 0.08% were kept (a little above the frequency 1 for 1000) (Code section 2 Targeted resequencing analysis). Second, I considered as a true positive variant those that have a base quality (Phred score) that is at most 7% lower than that of the reference (base quality filter). In the second sequencing experiment, the samples were sequenced twice, and only the variants that were present in both sequencing datasets were considered as true positive variants.

The main parameters to consider called variant as potential mutations are 1) base quality of the called variant and 2) proportion of the variant called from the forward (+) and the reverse (-) direction of a paired-end read should be approximately equivalent to that of the reference allele (filter_reads_proportion_indels) and (filter_reads_proportion_SNVs). This protocol allowed us to extract all the possible SNVs and indels except the small indels (insertion of deletion of 1 nucleotide) at homopolymeric runs of nucleotides at a variant frequency below 0.5%. As a sequencing control, 2 mutants (*win1*-394+13 bp at proportion 1% and *sty1*-G197T at proportion 0.1 %) were added to a control sequencing. Histograms of variant frequencies were drawn with the ggplot2 package (R). The mutation type for SNVs based on their effect on the function of the protein was verified with genome browser CLC Genomics Workbench 6 (https://www.qiagenbioinformatics.com/).

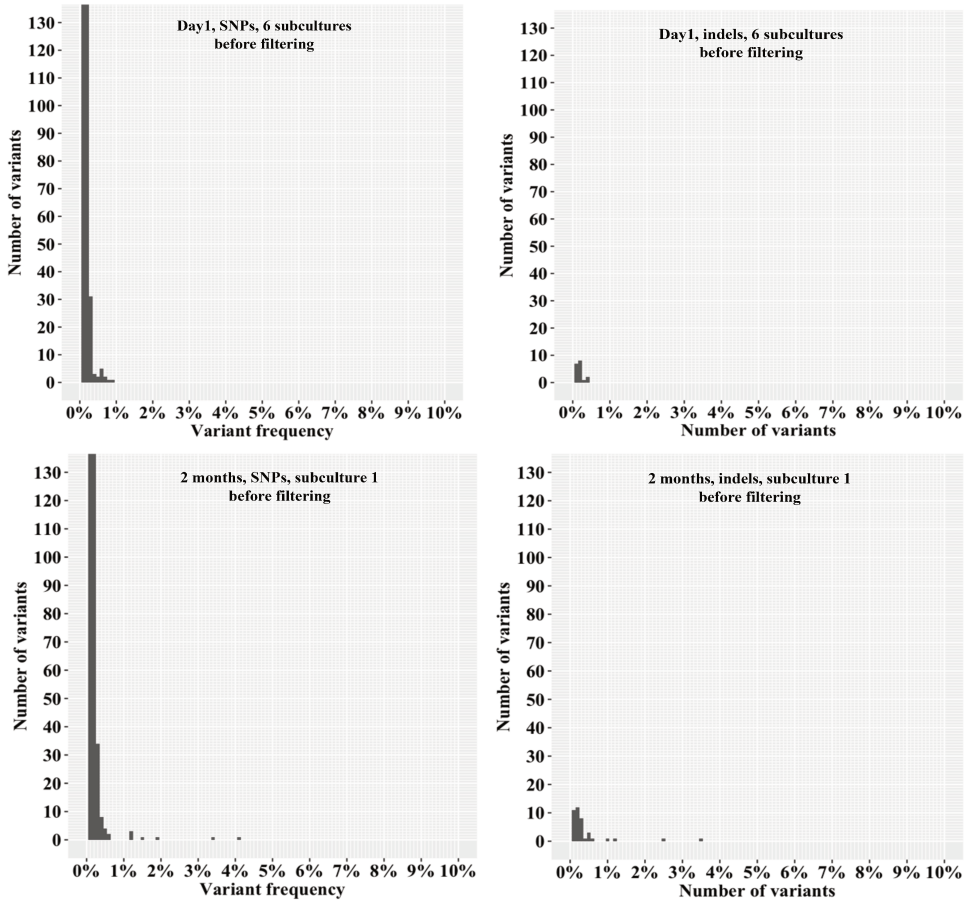

Figure 17: Distribution of raw variants prior to applying filters.

The frequency of the variant is given as a function of the number of variants. SNVs (left) and indels (right) before splitting the culture at day 1 (top). Subculture 1 at 2 months of quiescence (bottom) before filtering. The variants present outside the main distribution are likely to be true positives variants.

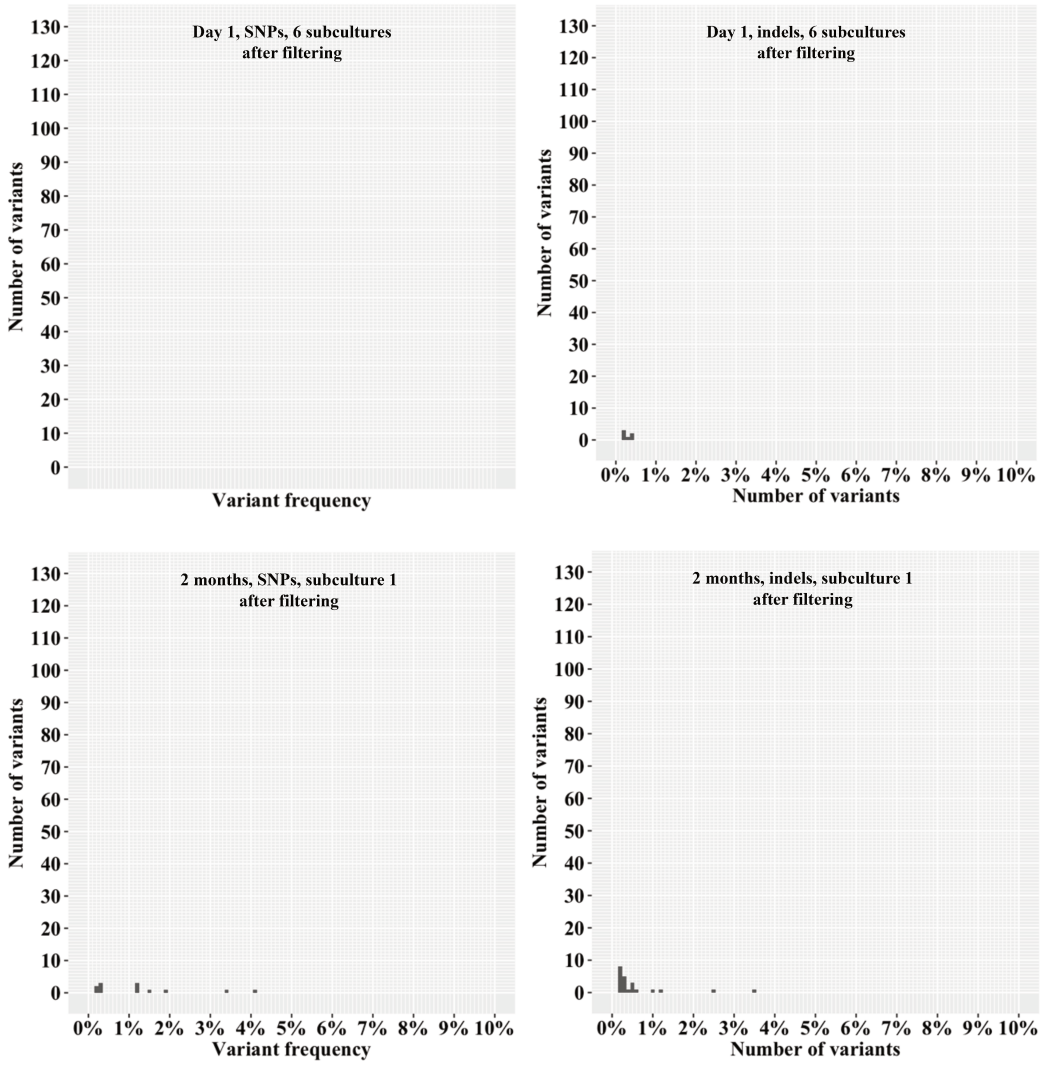

Figure 18: Distribution of raw variants after filtering.

The frequency of the variant is given as a function of the number of variants. SNVs (left) and indels (right) before splitting the culture at day 1 (top). Subculture 1 at 2 months of quiescence (bottom) after filtering. The variants present outside the main distribution are likely to be true positives variants.

Code section 3: Custom scripts to filtrate the variants from targeted resequencing experiment

```
#load the libraries
library(ggplot2) # visualization the data
library(grid) #a rewrite of the graphics layout capabilities
library(gridExtra) #arranging multiple plots on one page
library(plyr) #data manipulation
library(dplyr) # data manipulation
```

```
library(gsubfn) #text manipulation
library(Cairo) #graphics manipulation during saving into output file

########################################
# Variant filtering
########################################

##-----------------------------------------------
# subsetting the variants according to experimental design
##-----------------------------------------------

# keep the variants that present at frequency > 0.1%
subset (x, VarFreq > 0.0008)

# keep the variants that comes from coverage > 5000 reads/nucleotide
subset (x, Reads1 + Reads2 > 1000) # subsetting the variants that are called from the regions with coverage at least 1000 reads (1st sequencing experiment, the average coverage is 12500 )
subset (x, Reads1 + Reads2 > 5000)# subsetting the variants that are called from the regions with coverage at least 5000 reads (1st sequencing experiment, the average coverage is 53000 )

##-----------------------------------------------
# filters used in this analysis
##-----------------------------------------------

#subsetting the variants based on P-values that are calculated using a Fisher's Exact Test on the read counts supporting reference and variant alleles.
subset(x, Pvalue < 0.05)

#subsetting the variants based on the base quality of the alternative variant compared to the reference one
base_quality <- function(x){
  x <- subset(x, ((abs(x$Qual1 - x$Qual2) < 0.07*((x$Qual1 + x$Qual2/2))) == TRUE))
  return(x)
```

```
}

#This function subset the SNVs that are present in equimolar proportions on both reads
filter_reads_proportion_SNVs <- function(x) {
  tmp <- subset(x, mutation_type == "SNVs")
  tmp1 <- subset(x, mutation_type != "SNVS")
  tmp2<- subset(tmp,
(tmp$Reads1Plus/tmp$Reads2Plus)/(tmp$Reads1Minus/tmp$Reads2Minus) <1.2 &
(tmp$Reads1Plus/tmp$Reads2Plus)/(tmp$Reads1Minus/tmp$Reads2Minus)>0.8)
  x <- rbind(tmp1, tmp2)
  return(x)
}

#This function subset the indels that are present in equimolar proportions on both reads
filter_reads_proportion_indels <- function(x) {
  tmp <- subset(x, mutation_type != "SNVs")
  tmp1 <- subset(x, mutation_type == "SNVS")
  tmp2<- subset(tmp,
(tmp$Reads1Plus/tmp$Reads2Plus)/(tmp$Reads1Minus/tmp$Reads2Minus) <1.2 &
(tmp$Reads1Plus/tmp$Reads2Plus)/(tmp$Reads1Minus/tmp$Reads2Minus)>0.8)
  x <- rbind(tmp1, tmp2)
  return(x)
}

#sorting and subsetting duplicated variants between 2 dataset within 1 sample
duplo <- function(x){
  tmp <- ddply(x, .(Position), nrow) #indexing duplicates and not duplicates between two
sequencing samples by Position
  tmp2 <- merge(tmp, x, by=c("Position")) # adding indexes to dataframes
  tmp3 <- tmp2[!(!duplicated(tmp2[, 1:2], fromLast=T) & !duplicated(tmp2[, 1:2])),] #keeping
the duplicates
  x <- subset(tmp3, Sample!=tmp3$Sample[1]) # keeping duplicates from one subsample
```

```
  return(x)
}



#plotting the histogram of the  raw variants
plot_histogram <- function(x) ggplot(data = x, aes(VarFreq)) +
  list(
    geom_histogram(binwidth = 0.001, show.legend = T),
    coord_cartesian(xlim = c(0, 0.1), ylim=c(0,130)),
    scale_x_continuous(labels = percent, breaks = seq(0, 0.1, 0.01), minor_breaks = seq(0, 0.1,
0.001), name = "Variant frequency"),
    scale_y_continuous(breaks = seq(0, 200, 10), minor_breaks = seq(0, 200, 1), name =
"Number of variants"),
    theme(axis.title=element_text(family = "Times New Roman", face="bold",
size=14,color="black"), axis.text=element_text(family = "Times New Roman", face="bold",
size=14,color="black")) ,
    NULL
  )
```

2.1.6.4 Annotation and visualizations of the mutations

The filtered variants were sorted by mutation type and prepared for annotation (SNV, Indel, Deletion or Complex) by their effect on the protein sequence. The mutations were plotted with Lolliplot mutation distribution graphics tool from the Bioconductor R package named trackViewer (Ou et al., 2019) (Code section 4).

Code section 4: Annotation and visualization of the mutations

```
# creating the coordinates on the gene sequence

prokin <- c(60, 899) #protein kinase domain
ATP <- c(78, 105) #ATP-binding region
TXY_1 <- c(513, 521) #short sequence motif – TXY
TXY_2 <- c(528, 536) #short sequence motif – TXY
```

```
block_names <- c("cDNA", "protein kinase domain", "ATP-binding region", "short sequence motif - TXY", "short sequence motif - TXY") #assign the names for domains

tmp <- subset(dataframe, gene == "sty1")

sty <- as.vector(tmp$cDNA) #mutation positions on cDNA in sty1 gene

seq_names <- tmp$annotation_lolliplot #assigning the names of the lolliplot

sty.gr <- GRanges("chr1", IRanges(sty, width=1, names=paste0(seq_names))) #align mutations from the vector to the provided coordinates

sty_features <- GRanges("chr1", IRanges(c(1, 60, 78, 147, 528), #start coordinates for (domains)

                                        width= c(1050, 893, 27, 8, 8), # length for features (domains)

                                        names=paste0(block_names))) # create place for domain names

#Control the labels

sty.gr.rot <- sty.gr

sty.gr.rot$label.parameter.rot <- 60

#saving the plot into a .pdf file

cairo_pdf(file = "lolliplot_sty1.pdf", width = max(xaxis)/100/2.54, height =15/2.54, pointsize = 9, family = 'Times New Roman', bg = "white", fallback_resolution=70)

lolliplot(sty.gr.rot, sty_features, legend=legend, xaxis=xaxis, ylab = NULL, yaxis=FALSE, cex=.9) #plot the grap

dev.off()
```

2.4.8 Validation of the called mutations.

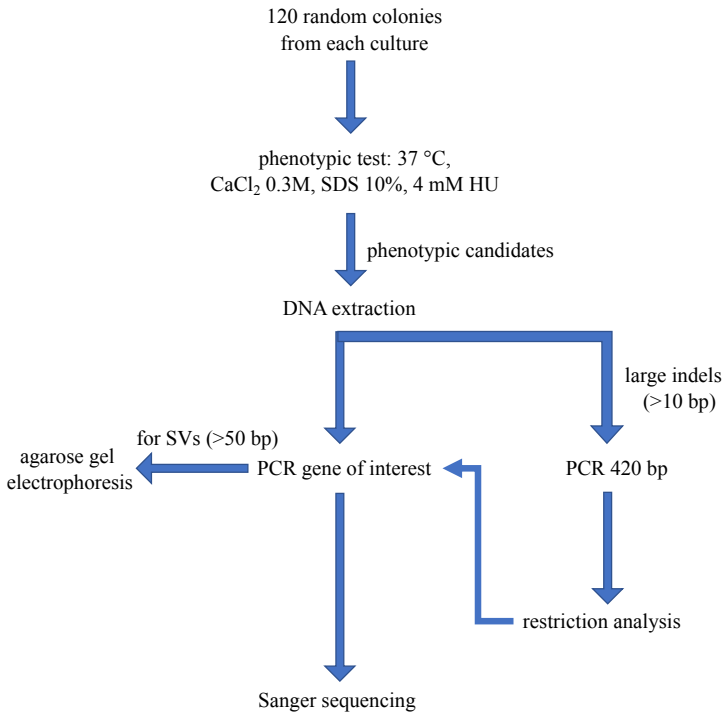

Figure 19: Global strategy for validating the mutations called from targeted sequencing.

To verify the presence of the mutations in the pool of colonies, a phenotypic test in the form of a drop assay was performed, as described previously, on 120 randomly isolated colonies (12 from each tube of 100 colonies mix) from samples of culture 1 at 3 months, of culture 2 at 2 months and 3 months, and of culture 3 at 3 months. The colonies exhibiting a phenotype were amplified with the primers used previously for targeted resequencing. The presence of large indels (>10 bp) was tested by restriction analysis with the Sau3AI, HaeIII and MseI enzymes and separation of cut fragments in polyacrylamide gel. The presence of small indels and SNVs was verified by Sanger sequencing.

2.5 Co-culture of the mutants and the wild-type.

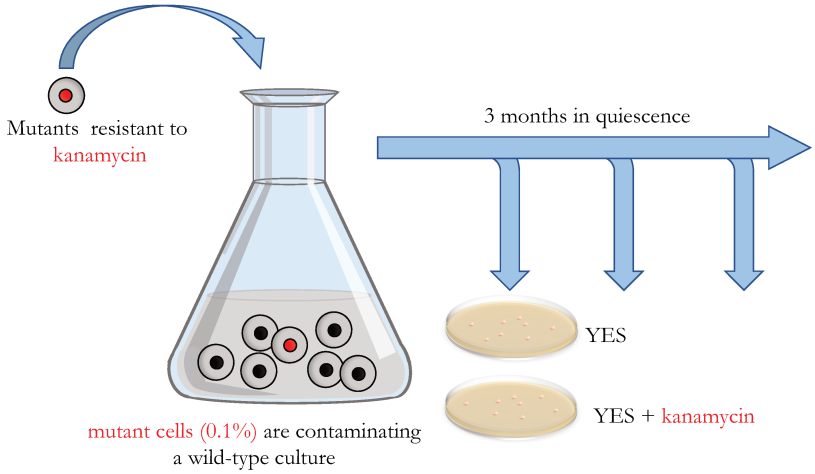

Figure 20: Experimental design for growing mutants with wild-type.

Various proportions of mutants were introduced into a wild-type culture. Both wild-type and mutants were transferred independently into quiescence and mixed at day 1. The proportion of mutants was followed for 3 months by determining the proportion of kanamycin resistant colonies among the CFUs.

To analyze when mutations appear in quiescence, experiments where the wild-type culture is contaminated with a mutant (*pmc1*-3089+18 bp, *mkh1*-2938-10 bp, *sty1*-C74G, *sty1*-G197T, *win1*-394+13 bp, *sgf73*-896+T) were performed at day1 of quiescence. The strains were marked with a kanamycin resistance cassette at the chromosome locus chr2 SPBC1A8.02. The evolution of the proportion of wild-type and mutant was monitored for up to 3 months by plating twice per week an aliquot of each culture both on YES plates and YES plates containing kanamycin.

2.6 Doubling time for the mutants and wild-type.

To calculate the doubling time, the strains were grown up to the stationary phase and 1 µl of the stationary culture was inoculated into 100 µl of YES or EMM into 96 well microplates. The measurements were taken automatically every 10 seconds by a TECAN sunrise for 24 hours. All measurements were made in triplicate. The generation time was calculated by the formula:

Equation 2: Doubling time

$$DT = \frac{ln2}{r}, where\ r\ (growth\ rate) = \ln(\frac{OD2}{OD1})/(T2 - T1)$$

2.7 Exit from quiescence with low traces of glutamate

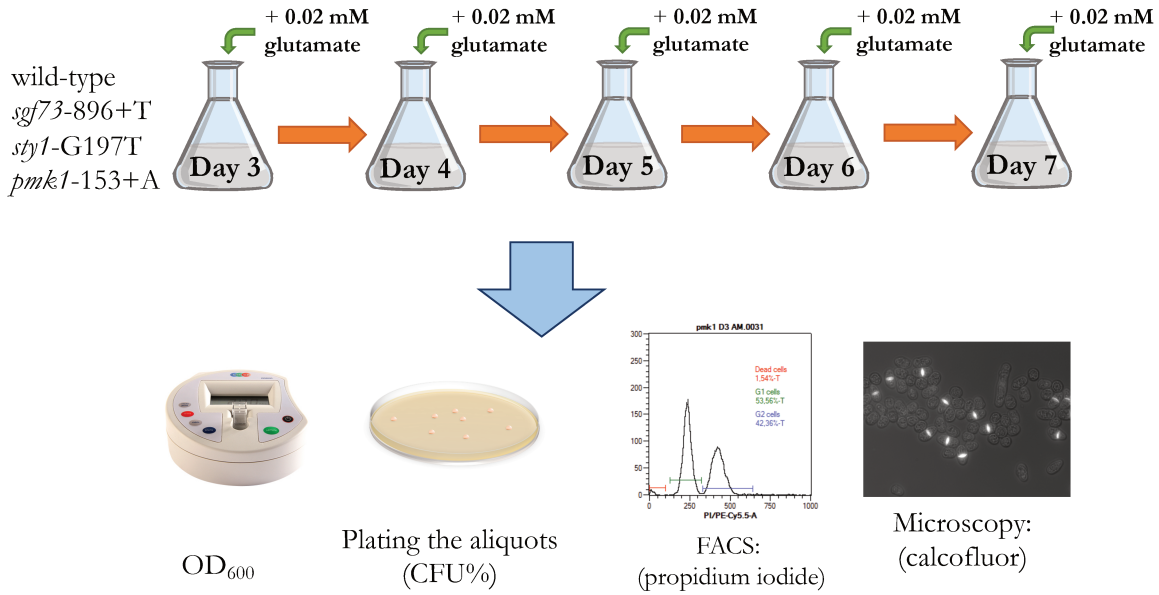

Figure 21: Experimental design of the exit from quiescence with traces of glutamate.

Glutamate was added twice a day starting at day 3. Growth, CFUs FACS and microscopy were performed every day until day 7 of quiescence.

Wild-type and mutants were grown as individual cultures and passed into quiescence as described before. At day 1 of quiescence, 0.02 mM of glutamic acid (0.05% of the standard concentration) was added to the culture twice per day during the 8 days of the experiment. Immediately after the addition, an aliquot of the culture was taken and fixed with 70% ethanol for further analysis by flow cytometry and fluorescent microscopy. The viability of the culture was followed by plating aliquots on YES plates every day. Cell growth was monitored by OD_{600}.

2.7.1 Flow Cytometry Analysis

DNA content and cell cycle stages were monitored by FACS. The proportion of 1C and 2C DNA-containing population was analyzed to capture S-phase cells. Dying cells that no longer contain DNA are not stained with the dye. For FACS analysis, the samples were prepared as follows: 1 ml of quiescent cells were fixed with 70% ethanol, washed twice with Sodium Citrate 50 mM, sonicated at medium strength for 20 seconds, and treated with RNase at 37 °C overnight. The following day, the cells were stained with propidium iodide (4 µg/ml) and 10^4 cells were used for FACS analysis (MACSQuant).

2.7.2 Fluorescence microscopy

An aliquot of the 100 µl ethanol-fixed cells were centrifuged at 3,000 g and rehydrated. 20 µl of the solution was fixed at 55 °C. To follow septum formation and nuclei, 10 µl of mounting solution (1 µg/ml DAPI, 1 mg/ml p-phenylenediamine, 200 µl Calcofluor White, 40% glycerol) were used to stain the cells. Images were taken with a Zeiss microscope (UV light and detection through a blue filter).

2.8 Measurement of the activity of the S/MAP kinase pathways in quiescence

Quiescent cultures of wild-type, *sty1*-C74G, *sty1*-G197T, *win1*-1086-G, and *win1*-393+13 bp at day 1 were exposed for two hours to a range of temperatures (32 °C, 44 °C, 46 °C, 48 °C) and to a spectrum of concentrations of hydroxyurea (0 mM – 1 mM – 2 mM – 4 mM – 6 mM – 8 mM). After two hours of treatment, aliquots of the cells were plated on YES medium, and viability was measured by counting the colony forming units.

2.9 Screening for the effect of chemicals during exit from quiescence

The effect of chemicals was tested during the slow exit from quiescence. Exit was initiated by the addition of traces of glutamate as described previously. In parallel to glutamate addition, various drugs affecting cell cycle progression and ROS balance were added every day twice per day to cultures of wild-type, *sgf73*-896+T, *sty1*-C197T, *mkh1*-640+A, *pmk1*-153+A. The list of drugs is described in (Table 6). Cell viability, microscopy and flow cytometry was performed as described above.

Table 6: Chemicals used in this experiment.

Chemical	Cellular effect	Concentration used
Vitamin B_6	Antioxidant	100 µM
Rapamycin	TOR inhibitor	20 µM
Hydroxyurea	S-phase inhibitor	6 mM
Menadione	ROS inductor	4 µM
Methotrexate	inhibits dihydrofolate reductase	80 µM
5-fluorouracile	thymidine synthase inhibitor	80 µM

RESULTS

“Mutations in the S/MAPK pathways increase the fitness in quiescence”

Makarenko R.[1,2], Denis C.[1] , Francesconi[1] S. , Gangloff S.[1] and Arcangioli B. [1]

4 RESULTS

4.1 Article

Abstract

The genetics of quiescence is incipient compared to the genetics of growth, yet both states generate spontaneous mutations and genetic diversity that fuel evolution. After prolonged quiescence, mutations in the stress/mitogen-activated protein kinase (S/MAPK) pathways that by far exceed those expected by chance were isolated among the survivors. These highly conserved pathways transduce extracellular signals and stress to coordinate cell division. Targeted resequencing and competition experiments indicate that mutations in these genes arise in the first month of quiescence, expand clonally during the second month at the expense of the parental population and provide a selective advantage for quiescence exit. Thus, mutations in the general stress response in eukaryotes provides a gain of fitness similar to that of the Growth Advantage in Stationary Phase (GASP) described in bacteria. Our work highlights the cooperation in a heterogenous cell population, a common feature observed in cancer and infectious diseases.

Introduction

In nature, cells alternate between periods of growth and quiescence depending on the fluctuating environmental conditions and physiological requirements [1]. The transition between these states is interpreted by the cell as an environmental/physiological stress which requires a quick response for cell survival. Therefore, the cells have evolved mechanisms to cope with the perpetual fluctuation between states through optimized epigenetics and genetics [2] involving the RNA interference machinery [3] and specific telomere repair mechanism[4].The major source of spontaneous mutations arising during the growth of an organism is generated by errors during DNA replication and repair. However, during quiescence, DNA mutations result from the absence or faulty repair of physical and chemical lesions [5]. As a consequence, any experimental or natural condition that changes the relative contribution of DNA repair processes will affect the rate and spectrum of mutations, as was shown for the *chronos* mutational force [6]. During growth, spontaneous mutations accumulate as a function of cell divisions [7] or DNA replication [8]. Genome-wide sequencing approaches have shown that, during growth, the mutation rate is relatively low, in

the range of 2.10^{-10} mutation per nucleotide and per generation in fission yeast [9,10]. Extensive work in many species has shown a similar mutation spectrum where single nucleotide variants (SNVs) are more frequent than insertions and deletions (indels) during growth. In quiescence, we recently found that mutations accumulate linearly as a function of time, with a range of 10^{-10} mutation per nucleotide per day, with SNVs and indels accumulating at the same pace and deletions dominating insertions [6]. Thus, the quiescence system fulfills the experimental conditions to select for mutations and identify genes and functions required to improve the life span in the absence of cell divisions. In eukaryotes, the TOR (target of rapamycin) and the S/MAPKs (stress or mitogen-activated protein kinases) signaling pathways are required for sensing and responding to internal and external stimuli and various environmental stress [11]. This fast response involves a cascade of kinases that controls basic biological processes including cell cycle, transcription, translation and metabolism [12,13]. In humans, abnormal expression of p38 and ERK, members of the S/MAPK pathways, plays a role in tumorigenesis and differentiation of various cell types [14-17]. In fission yeast, the S/MAPK pathway has also been described [18]. The SAPK module is composed of the MAPKKKs Win1 and Wis4, the MAPKK Wis1 and MAPK Sty1/Spc1. Early work [2] has identified the Sty1 and Wis1 as essential genes to rapidly arrest the cell cycle in G1 and to enter in quiescence [19,20]. The MAPK module, required for cytokinesis and cell wall integrity, is composed of Mkh1 (MAPKKK), Pek1 (MAPKK) and Pmk1 (MAPK) [21-23]. Although it was reported that Pmk1 participates in the Sty1 activation of the downstream effector Atf1 [24-28], the crosstalk between the SAPK and MAPK modules is not fully understood. In mammalian cells, serum starvation induces quiescence [29]; similarly, nitrogen starvation is commonly used in fission yeast to study quiescence entry and maintenance [30]. In this condition, the TOR pathway sets off with the SAPK pathway two rapid cell divisions with no cell growth to arrest the cells in G1 before entering quiescence [11,31,32]. The role of the S/MAPK pathways when cells return to growth is less well understood. The SAPK module is required to properly enter and survive in quiescence [11], conditional mutants will be required to study quiescence exit. In this work, we identified mutants that survived three months of quiescence. We tested the survivors for their sensitivity to drugs affecting a wide range of biological functions and found stress sensitive clones in a proportion that greatly exceeds that expected by chance. Whole genome sequencing of these clones identified many mutations in genes of the S/MAPK pathways. Next, we evaluated the frequency and chronology of appearance of these mutations and found that the same pathways

were reproducibly mutated in independent experiments. Our work indicates that deprivation of nitrogen provides a selective advantage to S/MAPK mutants arising in a quiescent population to sustain prolonged survival.

Results

Accumulation of stress sensitive mutants in a quiescent population

A culture of a haploid prototrophic strain in minimum medium (EMM) was transferred to EMM without nitrogen (EMM-N) at 10^6 cells/ml and kept quiescent for three months without changing the medium (see Materials and Methods) [6,30]. The viability curve (Fig 1A) shows three phases; during the first three weeks, the viability is maintained (phase I), followed by a rapid decline (phase II), before slowly getting stabilized around 1% (phase III). On the contrary, when the medium is refreshed every other week [6], phase III is not observed (Fig 41A). After two months, the presence of phase III in the unrefreshed culture indicates a gain in fitness of the cells in the surviving population. To determine the extent of the fitness, we routinely monitored the sensitivity of the survivors to conditions affecting a broad range of cellular functions, including temperature and various chemical agents (see Materials and Methods). After three months, 30 clones out of 152 (20%) exhibit a strong sensitivity to various agents. This high proportion of phenotypic variants is not observed when the medium is replenished every other week [6]. To determine whether the condition-sensitive phenotype is linked to a single locus, we picked four such strains isolated after three months of quiescence and crossed them with the isogenic strain of the opposite mating type and found a 2 to 2 meiotic segregation of the sensitivity indicating that a single locus is responsible for the phenotype in each of the four strains, indicating that quiescence promotes genetic diversity. To identify the mutations that accumulate after three months of quiescence, we sequenced the genome of 36 survivors picked randomly, as well as of 12 strains selected for their sensitivity to damaging agents. The DNA was paired-end sequenced with an average coverage greater than 50 x allowing the efficient calling of SNVs, insertions and deletions (indels) (Materials and Methods). We found 36 mutations in the genome of the 36 clones picked randomly and 21 mutations in the genome of the 12 clones that exhibited a sensitivity phenotype. 8 out of 12

strains with a phenotype contain a single mutation suggesting that this mutation is responsible for the phenotype (Fig 1B). Importantly, some of the genes uncovered in the 12 strains were also found mutated in the 36 strains picked randomly (Table S1). We found unique mutations in genes belonging to the Sty1 and Pmk1 S/MAPK modules, mutations in the Pmc1 vacuolar calcium transporter, and in the eIF4E/CAP-binding factor Tif452 (Table 1). Two mutations adding an A to a stretch of As were found in both Sgf73 coding for a subunit of the SAGA transcriptional complex and in Mkh1, a member of the MAPK pathway for which two unique mutations were also detected. Because we cannot ascertain that the mutations in the homopolymers are unique, we included them in our analysis. However, if these mutations are not unique, they must either have appeared prior to G0 entry, have arisen and divided during quiescence, or be hotspot mutations (Table 1 and Table S1). Thus, many of the mutated genes found after 3 months of quiescence play a role in the general stress response pathways suggesting a rapid and powerful genetic selection, while Pmc1, Tif452 and Sgf73 are known downstream targets of TOR or S/MAPK signaling [33-37] (Fig 1C). Other mutations, including *cut1*, *gap1*, *papb* and *pfl4* were also identified, but were not further studied in this work (Table S1).

Targeted sequencing from quiescent cultures

To assess when and how the mutations arise in our cultures, we focused on the 9 genes (Table 1) related to the S/MAPK pathways by targeted sequencing. We grew three independent 10 ml cultures with the minimum number of cell divisions (< 30) required to generate 10^7 quiescent cells (cultures 1-3) and isolated 1,000 colonies after 1, 60 and 90 days of quiescence from each culture (Fig 2A). We also included 1,000 colonies at each time point from the frozen culture that generated the 48 strains that were sequenced (thereafter called culture 0). We designed primers (Table S2) covering the 9 genes of interest of Table 1 to generate tiled fragments of about 420 bp in length. Equimolar amounts of PCR products were Illumina sequenced with a coverage of 12,000 per nucleotide and per culture. Mutations in 8 targeted genes (*wis1* was not included in this first round) were detected in the four cultures after two and three months, and account for 17.7% to 64.7% of the surviving cell population. Between two and three months, the distribution of alleles in each culture is fluctuating. For example, in culture 2 the *sgf73*-896+T allele represents 9.6% of the population at 2 months of quiescence

and reaches 43.5% a month later at the expense of *mkh1*-640+A, suggesting clonal interference within the population (Figure 2BC). Conversely, in culture 3 the proportion of *win1* alleles remains stable (14.5% vs 13.7%) over the same time frame. Surprisingly, the *mkh1*-640+A allele was found in the four cultures (Fig 2BC). The mutations *sgf73*-896+T and *mkh1*-640+A are located in stretches of 8 As and 7 As, respectively. The *win1*-1273+17 bp and *win1*-394+13 bp mutations are a direct-repeat duplication of 17 and 13 bp, respectively (Fig S1). To evaluate our calling procedure, we went back to the pools of 100 colonies (Materials and Methods) from the 3 months-old cultures and plated out 120 cells per pool that were subsequently scored for their sensitivity to temperature, calcium, HU and SDS (Table S3). The DNA of the sensitive colonies was prepared and used to amplify the relevant target genes. Sanger sequencing of the fragments confirmed the presence of several mutations in the various pools (alleles in red in Fig 2 and Table S4). Taken together, these data indicate that genes in the S/MAPK pathways previously identified in culture 0 were found mutated again independently in the 3 cultures, sometimes with the same allele that defines a hotspot. The more frequent alleles (*mkh1*-640+A or *sgf73*-896+T) can be explained by an early occurrence of a hotspot mutation followed by proliferation. However, the presence of 11 alleles of *win*1 representing 14.5% of the mutations found in culture 3 at 2 months is more complicated to explain and raises the question of when and how these mutations came up. We found a high proportion of indels (Fig 2E) supporting the view that many mutations are generated during quiescence.

Mutations occur in quiescent subcultures

We reasoned that the mutations arising during growth will be maintained in similar proportions after two months of quiescence. Thus, if a culture is divided on day 1 of G0 into subcultures, it should be possible to distinguish preexisting mutations that will be present in subcultures from mutations that have occurred independently during quiescence. To address this issue, we grew a culture from a single colony that was transferred to EMM-N for 1 day prior to be dispatched into 6 subcultures of 10 ml each (Fig 2A). In this experiment, we pooled colonies from each subculture after two months of quiescence (Material and Methods). Next, the 9 genes including *wis1* were PCR amplified in duplicate from each pool and were individually Illumina sequenced with a coverage of 53,000 per nucleotide and per culture

(Materials and Methods). Hence, the sensitivity of our calling procedure in this experiment has been enhanced by limiting fluctuation by collecting the cells at two months, discarding false positives that are present only in one PCR set and increasing the coverage. The proportion of mutations in the targeted genes in the subcultures is ranging from 19.5% to 50.9% (Fig 2D). The most frequent alleles are *sty1*-C545T and *sty1*-A553T and are restricted to subcultures 5 and 2, respectively. Several mutations found in the previous experiments (*mkh1*-640+A*, win1*-1273+17 bp and *win1*-394+13 bp) were found again in some but not all subcultures. The multiple occurrence of mutations in the *win1* gene is observed again in subculture 6 and to a lower extent in subcultures 3, 4 and 5. The relative abundance of *win1* alleles in those subcultures is not conserved (Fig 2D and Table S4). Because most of the mutations in the subcultures are not the same and because their abundance is different when they are, our data strongly support the model in which mutations arise and proliferate during quiescence. In the 4 cultures and 6 subcultures analyzed, we identified 199 mutations, including 4 complex ones (Fig 2 and S1), in the targeted genes with a large proportion of indels. When the spectrum of mutations in each gene is analyzed, different distributions of variant types are observed, highlighted for example by many indels in *win1* and almost none in *sty1* (Fig 2E), indicating that quiescence exercises selection.

A gain of fitness of S/MAPK mutants is revealed in quiescent co-cultures

To determine how our mutants achieve a better fitness in quiescence, we first analyzed the viability of several mutants in the S/MAPK modules during long-term quiescence. The survival profile of *mkh1*-2929 -10 bp and *sgf73*-896 +T mutant strains is similar to the parental wild-type strain while that of *win1*-394 +13 bp*, sty1*-C74G and *sty1*-G197T die rapidly before getting stabilized around 1% (Fig 3A), suggesting that the advantage may only manifest itself in cooperation in a heterogenous cellular population [38]. To test this idea, we set up competition experiments with cultures containing the wild-type and one of the mutant strains, as previously performed in bacteria to define the growth advantage in stationary phase (GASP) phenotype [39]. To follow the two populations in the co-cultures, we introduced the kanamycin marker in a neutral location of the genome in both the wild-type and the mutant strains by genetic crosses (see Materials and Methods). We set up after one day of quiescence

co-cultures of 50 ml (2.10^8 cells) containing 99.9% wild-type and 0.1% kanamycin marked strains. The proportion of the two strains was determined by plating the cells onto rich medium ± kanamycin periodically during quiescence incubation (Fig 3B). The proportion of the wild-type marked strain is constant in the co-culture, validating that the kanamycin reporter does not affect the population survival during quiescence (Fig 3B). In the co-culture conditions, the *win1*-394 +13 bp*, sty1*-C74G, *sty1*-G197T, *mkh1*-2929 -10 bp and *sgf73*-896 +T marked mutant strains reveal a gain in fitness (Fig 3B). During the initial 20-30 days, the mutants die with kinetics similar to the single cultures (Fig 3AB). Subsequently, the mutants start to proliferate exponentially with a generation time of one division every three days and start outcompeting the wild-type at two months of quiescence (Fig 3B). The strains mutated in the SAPK pathway (*win1* and *sty1)* maintain their population size until the end of the experiment. The simplest hypothesis to account for this result is that the progressive death of the cells (mainly the wild-type) generates a residual release of nitrogen that primarily benefits the mutant cells. This hypothesis implies that the time frame of appearance of a mutation impacts on the expression of the adaptive phenotype; too early, the mutant will die, and too late the mutant will be outcompeted by mutants that came up earlier. This view is supported by the behavior of the individual cultures shown in Fig 3A, where the liberated nitrogen during phases I and II is not sufficient to induce the division of the entire mutant population.

The S/MAPK pathway is active during quiescence

The above competition experiment demonstrates that the S/MAPK pathways are functional during quiescence. It was previously shown that upon nitrogen starvation *sty1*Δ or *wis1*Δ cells remain elongated, contain enlarged nuclei with a 2C DNA content, indicating a poor quiescence entry [2]. We took advantage of the *sty1*-C74G *and sty1*-G197T alleles to analyze quiescence entry. Our mutant strains are exhibiting a better entry into quiescence than the deletion (although slower than wild-type) (Fig S2), consistent with only a partial loss of function of the two *sty1* alleles as suggested by the absence of disruptive mutations (Fig S1). The viability of the strains is not affected during the 24 hours of the time course. Since *sty1*Δ and *win1*Δ mutants are sensitive to temperature and H2O2 [19,40-42] while *pmk1*Δ and *mkh1*Δ are sensitive to caspofungin [43,44] during growth, we determined the sensitivity of our alleles. The results indicate that, like the deletions, our alleles are sensitive to their

cognate treatment (Fig S3ABE). Next, we tested the sensitivity of these alleles in quiescence. The *mkh1* and *pmk1* alleles showed no sensitivity to caspofungin in G0, while the *sty1* and *win1* alleles are sensitive to both temperature and H2O2 (Fig S3CD). These results indicate that the SAPK pathway is required to cope with stress during quiescence but that hampering its function provides a gain of fitness during quiescence and/or exit from quiescence.

Scavenging promotes quiescence exit of the S/MAPK mutants

Since the S/MAPK pathways are active in quiescence and their impediment provides a gain in fitness prompted us to investigate a scavenging behavior. We established by FACS analysis the minimal concentration of glutamate necessary to engage the first S phase to be 0.03 mM and that to complete one replication round to be in between 0.09 and 0.12 mM in the wild-type strain, a concentration 1,000-fold lower than in growing conditions (Fig S4). Thus, to mimic slow nitrogen release during an extensive quiescence period, we provided traces of glutamate (at a starting concentration of 0.02 mM) to 3-day-old quiescent cultures twice a day for several days (Fig 4, see Materials and Methods). The size (OD600), viability, DNA content by FACS and calcofluor staining of wild-type and the 3 most downstream players of the S/MAPK pathways (*sgf73*-896 +T*, sty1*-G197T and *pmk1*-869+A strains - Fig synopsis) were followed for at least six days (Fig 4). All the strains increase their cell size with time, but with no cell division (Fig 4A). While the mutants remain viable, the wild-type cells progressively lose viability (Fig 4B). The analysis of the DNA content by FACS (Fig 4C) indicates that the wild-type cells engage DNA replication that is followed by the appearance of a new propidium negative peak indicative of nuclear DNA degradation and stain positive for calcofluor (Fig 4CD). These cells also fail to enter mitosis efficiently, as evidenced by the low presence of binucleated of septated cells. The same analysis showed that the *sgf73* and *pmk1* mutants engage DNA replication, mitosis and septation, whereas the *sty1* mutant is delayed, and no septation was observed over the 7-day time course (Fig 4CD). We also noticed that only a fraction of both *sgf73* and *pmk1* mutant cells is responsive to nitrogen and engages DNA replication and septation, suggesting a phenotypic diversity in the populations (Fig 4). When the concentration of glutamate is brought up to 0.2 mM in a single step in a 3-day-old quiescent culture, all the strains exit quiescence, replicate their DNA and remain

viable (Fig S5). This experiment supports the idea that the slow and progressive release of nitrogen by the dying cells promotes the further killing of the wild-type cells, thus allowing the mutant population to proliferate and ultimately take over the co-culture. Thus, the scavenging behavior also provides a mechanistic explanation for the competitive fitness of the mutants in the S/MAPK pathways in the presence of wild-type cells during extended periods of quiescence.

Discussion

Using laboratory evolution experiments, we found mutants related to the S/MAPK response pathway that survive better a long-term quiescence. These mutations are far more frequent than anticipated in a neutral model of random occurrence, and their isolation in quiescence becomes predictable. The number, distribution, proportion and *chronos* mutational signature of the mutants [6] described in this work strongly suggests that the mutations arise during quiescence and not during the proliferating phase. Our approach is not exhaustive since it is built only on the mutants identified in the 48 sequenced strains (culture 0). However, additional mutants were found and not further studied here (i.e., *cut1*, *gap1, papb* and *pfl4* in Table S1). Thus, this work extends the identification in fission yeast of genes important to sustain and exit quiescence [2,45]. Other systematic screens searching for mutants that survive longer in limiting nutrient conditions or that are resistant to TORC1 inhibition that mimics nitrogen starvation have been performed in yeast [46,47]. In fission yeast, most mutants that have been identified encode proteins associated with membranes and autophagy functions, among which the *pek1* mutant (MAPK module) is the only gene shared with this work [6,47]. In budding yeast, high throughput screening identified *HOG1*, *SSK2* (SAPK pathway) and *SGF73* in glucose- and sulfate-limited conditions, respectively [48]. Here, the genetic variants spontaneously arising during two-three months of quiescence exhibit their pleiotropic effects that cause differential survival, offering a model system to study adaptive evolution by selection in a predefined but naturally evolving environment [49]. Numerous studies have revealed the important roles of the S/MAPK modules during differentiation, senescence and cell death of normal and stressed or aging tissues [50]. In fission yeast, the Wis1 and Sty1 activities of the SAPK module are required to properly enter and survive in quiescence [11], to undergo mating and meiosis and to coordinate cell cycle progression and

stress responses [2,32,51-55]. Because their function is essential to enter quiescence, their involvement in quiescence exit could not be addressed with null alleles. All the mutations in the *sty1* and *wis1* genes identified in our work generate partial loss of function because they are able to enter quiescence but are sensitive to stress compared to wild-type (Fig S3), allowing to study the role of the SAPK pathway in quiescence exit. In agreement, the genes in the SAPK pathway accumulate mostly SNVs and few indels located at the very end of the genes that most likely only generate a partial loss of function (Fig S1). Despite the chronos signature, *sty1* has a large excess of SNVs, indicative of positive selection. Therefore, we cannot formally rule out that mutations in *sty1* have arisen during the proliferation phase. Homopolymers (2 hotspots in *mkh1* and *sgf73*) only expand. Intriguingly, we found invalidating indels in *win1* that acts upstream of *wis1* in the kinase cascade. Although we did not recover mutations in *wis4* encoding another SAPKKK that is phosphorylating Wis1 [56,57], our result can be rationalized if we assume that the lost phosphorylation activity of Win1 is achieved by that of Wis4. On the other hand, mutations in the genes of the MAPK module accumulate indels and destructive SNVs that likely result in loss of function (Fig S1). This suggests that better quiescence survival and exit can occur in the absence of the MAPK pathway but requires to maintain some SAPK function, and that the two kinase cascades are playing different functions during nitrogen starvation or exit. Among the mutants that we have not characterized further, we isolated downstream targets of the S/MAPK signaling pathways. eIF4E /tif452 binds the mRNA 5'-CAP structure to form the translational initiation complex and is a downstream target of both TOR and S/MAPK signaling [58]. Interestingly, in activated lymphocytes, p38α (Sty1) deficiency causes hyperproliferation, correlating with a decrease in eIf4E activity [59]. Pmc1 is the vacuole Ca++ pump that allows keeping the cytosolic concentration of Ca++ low. The *pmc1* mutant strain is sensitive to a high concentration of calcium that activates calcineurin and inhibits cell growth [60]. The calcineurin and S/MAPK crosstalk is intricate and not fully understood [22,61]. Sgf73 is a subunit of the deubiquitinating module of the transcriptional SAGA complex that has been connected to the environmental transcriptional response induced by Tor and S/MAPK signaling [34,62-64]. Recently, it was shown that Sgf73 and Sir2 activate the transcription of ribosomal protein genes [65,66], a prerequisite for rapid proliferation. The distinct phenotypic response following the addition of sub-limiting quantities of glutamate during quiescence (Fig 4) provides information concerning the role of the S/MAPK during quiescence exit. In wild-type cells, quiescence exit is accompanied by nuclear DNA degradation that occurs between

the first round of DNA replication and mitosis (Fig 4C), suggesting that S-phase entry under conditions of suboptimal nitrogen concentration is an event triggering nuclear DNA degradation and cell-death program as previously proposed [67]. The mutations in the S/MAPK modules or in *sgf73* protect cells from dying by at least by two different pathways. The mutation in *sty1* protects the cells by delaying the G1/S transition, until the glutamate concentration reaches 0.2 mM, allowing a complete round of DNA replication (Fig S5). A similar G1/S transition delay was observed in budding yeast when the *sty1*-related kinase Hog1 is repressed, correlating with a low level of G1- CDK [68,69]. Similar to Hog1, we speculate that the *sty1* mutant is affected in inducing the degradation of the CDK inhibitor Rum1 required to activate the CDK and trigger an entry into the S phase [70]. In mice, the absence of p38α delays the initiation of hematopoietic stem and progenitor cells proliferation through an altered level of nucleotides [71], a metabolic defect also reported in fission yeast [72]. The Sty1 function is twofold: on the one hand it protects proliferating and quiescent cells from stress, accelerates quiescence entry but, on the other hand, it promotes cell death at quiescence exit when the amounts of nitrogen are not sufficient to sustain both cell growth and full DNA replication. The mutations in the Pmk1 MAPK module and the Sgf73 SAGA transcriptional complex protect the cells from death upon quiescence exit under insufficient nitrogen likely because they limit the number of mutant cells that engage DNA replication, cell growth and septation (Fig 4. C, D). Such a condition could arise if a heterogenous cell population is generated in which only a small fraction of the cells is scavenging nitrogen allowing full genome duplication and cellular growth. However, the molecular mechanism underlying this phenotypic heterogeneity in the mutant population remains elusive. We propose a scenario in which the wild-type cells are using the glutamate for both DNA replication and cell growth (Fig 4A, C). Under limiting glutamate and considering that cellular growth is exhausting most of the nitrogen, DNA replication cannot be completed, resulting in cell death. This interpretation is consistent with the three-step survival curve observed for the quiescent wild-type cells (Fig 1A). During the first three weeks, the viability is retained before rapidly decreasing to finally poise again. Second, the competitive advantage of the mutants requires the slow death of a large portion of the culture to provide enough nitrogen to sustain their slow growth. Since RNA and protein synthesis is scarce during quiescence, the mutations that occur exhibit a prolonged phenotypic lag that provides a larger window to generate advantageous phenotypic and genetic diversity [73,74]. Because the gain of fitness of the mutants in quiescence is accompanied by a decrease in their stress resistance,

this gain is circumscribed and might not be preserved in a natural and changing environment. However, about half of the mutations were found in homonucleotide runs and near low complexity sequences known to be prone to reversion during DNA replication. Finally, the nine mutants isolated here are not sterile and can therefore be efficiently removed by sexual reproduction with beneficial effects for the population as a whole [75]. Our results are reminiscent of the GASP phenotype described in bacteria [73,74]. In bacteria, long-term stationary phase is associated with induction of stress response genes and alternative metabolic pathways, followed by a type of programed cell death and selection of survivors with GASP mutations. This phenotype appears reproducibly in stationary phase and results mainly from mutations reducing the activity of the sigma S transcription factor (RpoS), the general starvation/stress-response transcriptional regulator [76]. The universally conserved activity of the S/MAPK modules in eucaryotes is different from that of RpoS, but achieves a similar biological function: adjusting the cellular response to the changing environmental conditions [75]. Furthermore, mutations in these broadly pleiotropic functions occur in quiescence in fission yeast and in stationary phase in bacteria to improve fitness. However, hyperactivation of RpoS or S/MAPK induces a persistent arrest in bacteria [77] and oncogene-induced senescence in mammalian cells [78,79], both providing resistance to antibiotics and antitumor agents, respectively [80]. In addition, RpoS reorganizes the DNA repair pathways participating in stress-induced mutagenesis [80-82](Fig 5), a notion that is also emerging in eucaryotes [83]. As a consequence, RpoS and S/MAPK are functional analogs. We are still far from understanding the importance of the genetics of quiescence in the evolutionary process, but we uncovered a novel and shared fundamental aspect pertaining prokaryotic and eukaryotic non-replicative genetics.

Materials and methods

Long-term quiescence experiment

For quiescence experiments, we used an unswitchable M-smt0 haploid prototrophic wild-type strain (PB1623, Table S6). Cells were grown in minimal medium (EMM, [84]) containing 5 g/l of glutamate up to a cell density below 10^7 cells/ml and shifted to minimal medium without nitrogen (EMM-N) containing 4% glucose at a starting concentration of 10^6 cells/ml.

We did not refresh the medium for the entire length of the experiment but compensated for the water lost by evaporation during the incubation by weighing the culture every week. After three months, the glucose concentration was still above 2%. We monitored the viability in quiescence for 3 months by plating aliquots of the cultures on YES plates at various time points. All the strains used in this study are listed in Table S6.

Phenotype screening

200 colonies were picked randomly at various times in quiescence and tested for their sensitivity to a range of temperatures, to chemicals agents (2 M sorbitol, 4 mM hydroxyurea, 0.01% SDS, 15 µg/ml Thiabendazole) and to a high concentration of salts (0.8 M KCl, 0.15 M Ca(NO3)2, 0.2 M and 0.3 M CaCl2) that do not affect the growth of wild-type cells. Drop assays starting with 10^4 cells per drop with 5-fold serial dilutions were spotted onto YES plates containing a selective agent and incubated for 3 to 4 days.

Colony picking and DNA extraction

Aliquots of the cultures after 1 day, 2 months, and 3 months of quiescence were frozen in 20% glycerol. Survivors were plated onto YES plates and grown for 3 days at 32 °C to form colonies. 1,000 colonies were picked from each culture at every timepoint and dispatched into 10 Eppendorf tubes containing each 100 µl of water and 100 colonies per tube. To collect a similar number of cells for each colony, colonies of a similar size were taken (~5.10^6 cells). The pools of 100 colonies were stored at -80 °C in 20% glycerol. From each pool, approximately $2.5x10^7$ cells were used for standard DNA extraction. The various amounts were normalized and used to prime all the PCR fragments. Each individual PCR product was purified after separation on agarose gels and quantified. Barcoded adapter primers were added to generate the libraries.

Targeted resequencing

After 1 day and 2 months of quiescence cells were plated on YES medium and grown for 3 days to form colonies. 1000 colonies of similar size from each culture and timepoint were

picked randomly and pooled as previously described. DNA from 10^8 cells was purified and treated as previously described before being used in PCR reactions. To cover the genes of interest, primer-pairs were designed to generate overlapping PCR fragments of an average size of 420 base pairs (Suppl. Appendix Table S2?). PCR reactions were performed with the Q5 high-fidelity polymerase Master Mix (New England Biolabs) according to the manufacturer's recommendations. Each PCR reaction was performed in duplicate to generate two independent batches making it possible to exclude some variants due to errors occurring during the amplification process. The amount of each PCR product was estimated on agarose gels and adjusted to the lowest concentration. Next, equal volumes of normalized PCR products from each sample were pooled and purified using the QIAGEN PCR purification kit following manufacturer's recommendations.

Whole genome sequencing and analysis

Library construction was performed using Illumina TrueSeq DNA PCR-Free Prep Kit following the manufacturer's instructions. Paired-end sequencing was achieved with either Illumina HiSeq 2500 (250 nucleotide-long reads at Novogene Bioinformatics Technology Company LTD) or an Illumina MiSeq System (300 nucleotide-long reads at the Pasteur Institute) technology following the manufacturer's instructions. The preprocessing step was performed with fqCleanER (v.5.01) which includes the trimming of short and aberrant reads with AlienTrimmer [85], correcting sequencing mistakes with Musket [86], and merging the overlapping reads using Flash [87]. The remaining reads were aligned to the *S. pombe* ASM294v2.23 reference genome with Burrows-Wheeler Aligner (v.0.7.5a.) [88]. The resulting reads were sorted and indexed with Samtools (v.0.1.19) and duplicated reads were marked with Picard tools (v.1.96). Indel realignment, removing the duplicates, variant filtering and calling was performed according to the GATK best practices using GATK version 2.7–2 [89]. The output .vcf file was annotated using snpEff (v.3.5) {Cingolani:2012cz}. In the targeted resequencing experiments, the aligned reads were sorted and indexed, further processed with Samtools (v.1.3) and converted to the .mpileup format. We used VarScan [90]to call the variants. According to the experimental design that we have developed, we only consider variants from the positions covered at least 5,000 times exhibiting an allele frequency above 0.1%. To distinguish mutations from sequencing errors,

we have applied several filters. First, based on the comparison of the distribution of the reference and alternative variants on the reads, VarScan calculates a p-value based on the Fisher's exact test. Second, we discarded the variants with a base quality below 35 and exhibiting more than a 7% difference in quality with the reference allele. Third, we retained the alleles for which mutations are present in equimolar proportions on the paired reads (within a 20% range). In addition, in the 6 subcultures experiment in which two independent PCR reactions were performed and sequenced, we have considered as true positive variants only those that were found in both batches. Using this approach, we are able to detect both SNPs and indels present at a 0.1% frequency, and short indels (± 1 nucleotide) at frequency of 0.5%.

Co-cultures

Mutants and wild-type cells were grown separately in EMM prior to transferring to EMM-N, as described before. At day 1 of quiescence, the wild-type culture was contaminated with the mutant at 0.1%. The kanamycin resistance cassette was inserted at the chromosomal locus chr2SPBC31A8.02 to mark the mutants, making them readily identifiable. The proportion of kanamycin resistant colonies was monitored during quiescence by plating aliquots of the co-culture on YES plates and YES plates supplemented with kanamycin twice per week during the three months of the experiment.

Exit from quiescence with glutamate

Glutamate was added to the quiescent cultures twice a day in the morning and in the evening. The concentration of glutamate added starts at 20 µM the first day to reach 200 µM five days later and is therefore 10,000 to 1,000-fold lower than that used for growth. Cell size was monitored by OD600, cell number by Beckman Coulter and viability by plating onto YES plates. DNA content was determined on ethanol fixed cells using Fluorescent Activated Cell Sorting with a Miltenyi Biotech MACSQuant. For microscopy, cells were stained with a DAPI-Calcofluor solution (2 µg/ml DAPI, 1 mg/ml p-phenylenediamine, 2 µg/ml Calcofluor White) to visualize the nuclei and the septum formation with a Zeiss Axioplan 2 Imaging M.

Acknowledgments

RM was supported by the Pasteur – Paris University (PPU) International PhD Program (CdV) and La Ligue Nationale contre le Cancer. This work was supported by the CNRS, the Institut Pasteur and the ANR-13-BSV8-0018 grant.

References

1. Koch AL. The Adaptive Responses of Escherichia coli to a Feast and Famine Existence. Advances in Microbial Physiology Volume 6. Elsevier; 1971. pp. 147–217. doi:10.1016/S0065-2911(08)60069-7 465

2. Sajiki K, Hatanaka M, Nakamura T, Takeda K, Shimanuki M, Yoshida T, et al. Genetic control of cellular quiescence in *S. pombe*. Journal of Cell Science. 2009;122: 467 1418–1429. doi:10.1242/jcs.046466

3. Roche B, Arcangioli B, Martienssen RA. RNA interference is essential for cellular quiescence. Science. 2016;354. doi:10.1126/science.aah5

4. Maestroni L, Audry J, Matmati S, Arcangioli B, Géli V, Coulon S. Eroded telomeres are rearranged in quiescent fission yeast cells through duplications of subtelomeric equences. Nat Commun. Nature Publishing Group; 2017;8: 1684. 473 doi:10.1038/s41467-017-01894-6

5. Gangloff S, Arcangioli B. DNA repair and mutations during quiescence in yeast. FEMS Yeast Res. 2017;17. doi:10.1093/femsyr/fox002

6. Gangloff S, Arcangioli B. Quiescence unveils a novel mutational force in fission yeast. 477 Elife. 2017;6: 149. doi:10.7554/eLife.27469

7. Luria SE, Delbrück M. Mutations of Bacteria from Virus Sensitivity to Virus Resistance. Genetics. Genetics Society of America; 1943;28: 491–511.

8. Lea DE, Coulson CA. The distribution of the numbers of mutants in bacterial populations. J Genet. 1949;49: 264–285.

9. Lynch M. Rate, molecular spectrum, and consequences of human mutation. Proc Natl 483

476 Acad Sci USA. National Acad Sciences; 2010;107: 961–968. doi:10.1073/pnas.0912629107

477 10. Drake JW, Charlesworth B, Charlesworth D, Crow JF. Rates of spontaneous mutation.
478 486 Genetics. Genetics Society of America; 1998;148: 1667–1686.

479 11. Yanagida M, Ikai N, Shimanuki M, Sajiki K. Nutrient limitations alter cell division
480 control and chromosome segregation through growth-related kinases and phosphatases.
481 2011;366: 3508–3520. doi:10.1098/rstb.2011.0124

482 12. Sajiki K, Pluskal T, Shimanuki M, Yanagida M. Metabolomic analysis of fission yeast
483 491 at the onset of nitrogen starvation. Metabolites. 2013;3: 1118–1129.
484 doi:10.3390/metabo3041118

485 13. Marguerat S, Schmidt A, Codlin S, Chen W, Aebersold R, Bähler J. Quantitative analysis
486 of fission yeast transcriptomes and proteomes in proliferating and quiescent cells. Cell.
487 2012;151: 671–683. doi:10.1016/j.cell.2012.09.019

488 14. Pandey V, Bhaskara VK, Babu PP. Implications of mitogen-activated protein kinase 497
489 signaling in glioma. J Neurosci Res. Wiley-Blackwell; 2016;94: 114–127.
490 doi:10.1002/jnr.23687

491 15. Igea A, Nebreda AR. The Stress Kinase p38α as a Target for Cancer Therapy. Cancer 500
492 Res. American Association for Cancer Research; 2015;75: 3997–4002. doi:10.1158/0008-
493 5472.CAN-15-0173

494 16. Dankner M, Rose AAN, Rajkumar S, Siegel PM, Watson IR. Classifying BRAF
495 alterations in cancer: new rational therapeutic strategies for actionable mutations. Oncogene.
496 Nature Publishing Group; 2018;37: 3183–3199. doi:10.1038/s41388-018-0171-x

497 17. Segalés J, Perdiguero E, Muñoz-Cánoves P. Regulation of Muscle Stem Cell Functions: A
498 Focus on the p38 MAPK Signaling Pathway. Front Cell Dev Biol. Frontiers; 2016;4: 91.
499 doi:10.3389/fcell.2016.00091

500 18. Pérez P, Cansado J. Cell Integrity Signaling and Response to Stress in Fission Yeast. Curr
501 Protein Pept Sci. 2010;11: 680–692.

19. Millar JB, Buck V, Wilkinson MG. Pyp1 and Pyp2 PTPases dephosphorylate an osmosensing MAP kinase controlling cell size at division in fission yeast. Genes Dev. 1995;9: 2117–2130.

20. Shiozaki K, Russell P. Cell-cycle control linked to extracellular environment by MAP kinase pathway in fission yeast. Nature. 1995;378: 739–743. doi:10.1038/378739a0

21. Toda T, Dhut S, Superti-Furga G, Gotoh Y, Nishida E, Sugiura R, et al. The fission yeast *pmk1*+ gene encodes a novel mitogen-activated protein kinase homolog which regulates cell integrity and functions coordinately with the protein kinase C pathway. Mol Cell Biol. American Society for Microbiology (ASM); 1996;16: 6752–6764.

22. Sugiura R, Toda T, Dhut S, Shuntoh H, Kuno T. The MAPK kinase Pek1 acts as a phosphorylation-dependent molecular switch. Nature. Nature Publishing Group; 1999;399: 479–483. doi:10.1038/20951

23. Madrid M, Soto T, Khong HK, Franco A, Vicente J, Pérez P, et al. Stress-induced response, localization, and regulation of the Pmk1 cell integrity pathway in *Schizosaccharomyces pombe*. J Biol Chem. American Society for Biochemistry and Molecular Biology; 2006;281: 2033–2043. doi:10.1074/jbc.M506467200

24. Chen DR, Toone WM, Mata J, Lyne R, Burns G, Kivinen K, et al. Global transcriptional responses of fission yeast to environmental stress. Botstein D, editor. 2003;14: 214–229. doi:10.1091/mbc.E02-08-0499

25. Zhou X, Ma Y, Kato T, Kuno T. A Measurable Activation of the bZIP Transcription Factor Atf1 in a Fission Yeast Strain Devoid of Stress-activated and Cell Integrity Mitogen-activated Protein Kinase (MAPK) Activities. J Biol Chem. American Society for Biochemistry and Molecular Biology; 2012;287: 23434–23439. doi:10.1074/jbc.C111.338715

26. Vázquez B, Soto T, del Dedo JE, Franco A, Vicente J, Hidalgo E, et al. Distinct biological activity of threonine monophosphorylated MAPK isoforms during the stress response in fission yeast. Cell Signal. 2015;27: 2534–2542. 538 doi:10.1016/j.cellsig.2015.09.017

27. Madrid M, Vazquez-Marin B, Franco A, Soto T, Vicente-Soler J, Gacto M, et al. Multiple crosstalk between TOR and the cell integrity MAPK signaling pathway in fission yeast. Sci

530 Rep. Nature Publishing Group; 2016;6. doi:10.1038/srep37515

531 28. Schutt KL, Moseley JB. Transient activation of fission yeast AMPK is required for cell
532 proliferation during osmotic stress. J Lew D, editor. 2017;28: 1804–1814.
533 doi:10.1091/mbc.E17-04-0235

534 29. Zetterberg A, Larsson O. Kinetic analysis of regulatory events in G1 leading to
535 proliferation or quiescence of Swiss 3T3 cells. Proc Natl Acad Sci USA. National Academy
536 of Sciences; 1985;82: 5365–5369.

537 30. Tanaka K, Yanagida M. A nitrogen starvation-induced dormant G0 state in fission yeast:
538 the establishment from uncommitted G1 state and its delay for return to proliferation. Journal
539 of Cell Science. 1996;109 (Pt 6): 1347–1357.

540 31. Young PG, Fantes PA. *Schizosaccharomyces pombe* Mutants Affected in Their Division
541 Response to Starvation. Journal of Cell Science. 1987;88: 295–304.

542 32. Petersen J, Nurse P. TOR signalling regulates mitotic commitment through the stress
543 MAP kinase pathway and the Polo and Cdc2 kinases. Nat Cell Biol. 2007;9: 1263–1272.
544 doi:10.1038/ncb1646

545 33. Ishiguro J, Shibahara K, Ueda Y, Nakamura K. Fission yeast TOR signaling is essential
546 for the down-regulation of a hyperactivated stress-response MAP kinase under salt stress. Mol
547 Genet Genomics. Springer-Verlag; 2013;288: 63–75. doi:10.1007/s00438-012-0731-7 560

548 34. Hickman MJ, Spatt D, Winston F. The Hog1 Mitogen-Activated Protein Kinase Mediates
549 a Hypoxic Response in *Saccharomyces cerevisiae*. Genetics. Genetics; 2011;188: 325–U164.
550 doi:10.1534/genetics.111.128322 563

551 35. Ptushkina M, Malys N, McCarthy J. eIF4E isoform 2 in *Schizosaccharomyces pombe* is a
552 novel stress-response factor. EMBO Press; 2004;5: 311–316. doi:10.1038/sj.embor.7400088

553 36. Waskiewicz AJ, Flynn A, Proud CG, Cooper JA. Mitogen-activated protein kinases
554 activate the serine/threonine kinases Mnk1 and Mnk2. EMBO J. EMBO Press; 1997;16:
555 1909–1920. doi:10.1093/emboj/16.8.1909

556 37. Sanso M, Vargas-Perez I, Quintales L, Antequera F, Ayté J, Hidalgo E. Gcn5 facilitates
557 Pol II progression, rather than recruitment to nucleosome-depleted stress promoters, in
558 *Schizosaccharomyces pombe*. Nucleic Acids Res. 2011;39: 6369–6379.
559 doi:10.1093/nar/gkr255

560 38. Tabassum DP, Polyak K. Tumorigenesis: it takes a village. Nat Rev Cancer. Nature
561 Publishing Group; 2015;15: 473–483. doi:10.1038/nrc3971

562 39. Zambrano MM, Siegele DA, Almirón M, Tormo A, Kolter R. Microbial competition:
563 *Escherichia coli* mutants that take over stationary phase cultures. Science. 1993;259: 1757–
564 1760.

565 40. Rodríguez-Gabriel MA, Russell P. Distinct signaling pathways respond to arsenite and
566 reactive oxygen species in *Schizosaccharomyces pombe*. Eukaryotic Cell. American Society
567 for Microbiology Journals; 2005;4: 1396–1402. doi:10.1128/EC.4.8.1396-1402.2005

568 41. Degols G, Shiozaki K, Russell P. Activation and regulation of the Spc1 stress-activated
569 protein kinase in *Schizosaccharomyces pombe*. Mol Cell Biol. American Society for
570 Microbiology (ASM); 1996;16: 2870–2877.

571 42. Shieh JC, Wilkinson MG, Buck V, Morgan BA, Makino K, Millar JB. The Mcs4 response
572 regulator coordinately controls the stress-activated Wak1-Wis1-Sty1 MAP kinase pathway
573 and fission yeast cell cycle. Genes Dev. 1997;11: 1008–1022.

574 43. Villar-Tajadura MA, Coll PM, Madrid M, Cansado J, Santos B, Pérez P. Rga2 is a Rho2
575 GAP that regulates morphogenesis and cell integrity in *S. pombe*. Mol Microbiol. John Wiley
576 & Sons, Ltd (10.1111); 2008;70: 867–881. doi:10.1111/j.1365- 591 2958.2008.06447.x

577 44. Sánchez-Mir L, Soto T, Franco A, Madrid M, Viana RA, Vicente J, et al. Rho1 GTPase
578 and PKC ortholog Pck1 are upstream activators of the cell integrity MAPK pathway in fission
579 yeast. Arkowitz RA, editor. PLoS ONE. Public Library of Science; 2014;9: e88020.
580 doi:10.1371/journal.pone.0088020

581 45. Sajiki K, Tahara Y, Uehara L, Sasaki T, Pluskal T, Yanagida M. Genetic regulation of
582 mitotic competence in G0 quiescent cells. Sci Adv. American Association for the
583 Advancement of Science; 2018;4: eaat5685. doi:10.1126/sciadv.aat5685

584 46. Rallis C, López-Maury L, Georgescu T, Pancaldi V, Bähler J. Systematic screen for
585 mutants resistant to TORC1 inhibition in fission yeast reveals genes involved in cellular
586 ageing and growth. Biol Open. The Company of Biologists Ltd; 2014;3: 161–171.
587 doi:10.1242/bio.20147245

588 47. Sideri T, Rallis C, Bitton DA, Lages BM, Suo F, Rodríguez-López M, et al. Parallel
589 profiling of fission yeast deletion mutants for proliferation and for lifespan during long-term
590 quiescence. G3 (Bethesda). G3: Genes, Genomes, Genetics; 2014;5: 145–155.
591 doi:10.1534/g3.114.014415

592 48. Payen C, Sunshine AB, Ong GT, Pogachar JL, Zhao W, Dunham MJ. High-Throughput
593 Identification of Adaptive Mutations in Experimentally Evolved Yeast Populations. PLoS
594 Genet. 2016;12: e1006339. doi:10.1371/journal.pgen.1006339

595 49. Kram KE, Geiger C, Ismail WM, Lee H, Tang H, Foster PL, et al. Adaptation of
596 *Escherichia coli* to Long-Term Serial Passage in Complex Medium: Evidence of Parallel
597 Evolution. Hallam SJ, editor. mSystems. American Society for Microbiology Journals;
598 2017;2: e00192–16. doi:10.1128/mSystems.00192-16

599 50. Milanovic M, Yu Y, Schmitt CA. The Senescence-Stemness Alliance - A Cancer-
600 Hijacked Regeneration Principle. Trends Cell Biol. 2018;28: 1049–1061.
601 doi:10.1016/j.tcb.2018.09.001

602 51. Kato T, Okazaki K, Murakami H, Stettler S, Fantes PA, Okayama H. Stress signal,
603 mediated by a HOG1-like MAP kinase, controls sexual development in fission yeast. FEBS
604 Lett. Wiley-Blackwell; 1996;378: 207–212. doi:10.1016/0014-5793(95)01442-X

605 52. Zuin A, Carmona M, Morales-Ivorra I, Gabrielli N, Ayté J, Hidalgo E. Lifespan extension
606 by calorie restriction relies on the Sty1 MAP kinase stress pathway. EMBO J. 2010;29: 981–
607 991. doi:10.1038/emboj.2009.407

608 53. Duch A, Felipe-Abrio I, Barroso S, Yaakov G, García-Rubio M, Aguilera A, et al.
609 Coordinated control of replication and transcription by a SAPK protects genomic integrity.
610 Nature. Nature Publishing Group; 2013;493: 116–119. 626 doi:10.1038/nature11675

611 54. Fletcher J, Griffiths L, Caspari T. Nutrient Limitation Inactivates Mrc1-to-Cds1

612 Checkpoint Signalling in *Schizosaccharomyces pombe*. Cells. Multidisciplinary Digital
613 Publishing Institute; 2018;7. doi:10.3390/cells7020015

614 55. Daga RR, Bolaños P, Moreno S. Regulated mRNA stability of the Cdk inhibitor Rum1
615 links nutrient status to cell cycle progression. Curr Biol. 2003;13: 2015–2024.

616 56. Samejima I, Mackie S, Fantes PA. Multiple modes of activation of the stress- responsive
617 MAP kinase pathway in fission yeast. EMBO J. EMBO Press; 1997;16: 6162–6170.
618 doi:10.1093/emboj/16.20.6162

619 57. Morigasaki S, Ikner A, Tatebe H, Shiozaki K. Response regulator-mediated MAPKKK
620 heteromer promotes stress signaling to the Spc1 MAPK in fission yeast. Lew DJ, editor. Mol
621 Biol Cell. 2013;24: 1083–1092. doi:10.1091/mbc.E12-10-0727

622 58. Batool A, Aashaq S, Andrabi KI. Reappraisal to the study of 4E-BP1 as an mTOR
623 substrate - A normative critique. Eur J Cell Biol. 2017;96: 325–336.
624 doi:10.1016/j.ejcb.2017.03.013

625 59. Salvador-Bernaldez M, Mateus SB, Barrantes IDB, Arthur SC, Martinez-A C, Nebreda
626 AR, et al. p38 alpha regulates cytokine-induced IFN gamma secretion via the Mnk1/eIF4E
627 pathway in Th1 cells. Immunol Cell Biol. Wiley-Blackwell; 2017;95: 814–823.
628 doi:10.1038/icb.2017.51

629 60. Cunningham KW, Fink GR. Calcineurin-dependent growth control in *Saccharomyces*
630 *cerevisiae* mutants lacking PMC1, a homolog of plasma membrane Ca2+ ATPases. J Cell
631 Biol. The Rockefeller University Press; 1994;124: 351–363.

632 61. Kojima K, Bahn YS, Heitman J. Calcineurin, Mpk1 and Hog1 MAPK pathways
633 independently control fludioxonil antifungal sensitivity in *Cryptococcus neoformans*.
634 Microbiology (Reading, Engl). 2006;152: 591–604. doi:10.1099/mic.0.28571-0

635 62. Laboucarie T, Detilleux D, Rodriguez-Mias RA, Faux C, Romeo Y, Franz-Wachtel M, et
636 al. TORC1 and TORC2 converge to regulate the SAGA co-activator in response to nutrient
637 availability. EMBO Rep. EMBO Press; 2017;18: 2197–2218. doi:10.15252/embr.201744942

638 63. Morgan MT, Haj-Yahya M, Ringel AE, Bandi P, Brik A, Wolberger C. Structural basis

639 for histone H2B deubiquitination by the SAGA DUB module. Science. American

640 Association for the Advancement of Science; 2016;351: 725–728.
641 doi:10.1126/science.aac5681 659

642 64. Deng X, Zhou H, Zhang G, Wang W, Mao L, Zhou X, et al. Sgf73, a subunit of SAGA
643 complex, is required for the assembly of RITS complex in fission yeast. Sci Rep. Nature
644 Publishing Group; 2015;5: 14707. doi:10.1038/srep14707

645 65. McCormick MA, Mason AG, Guyenet SJ, Dang W, Garza RM, Ting MK, et al. The SAGA
646 Histone Deubiquitinase Module Controls Yeast Replicative Lifespan via Sir2 Interaction. Cell
647 Rep. 2014;8: 476–485. doi:10.1016/j.celrep.2014.06.037

648 66. Mason AG, Garza RM, McCormick MA, Patel B, Kennedy BK, Pillus L, et al. The
649 replicative lifespan-extending deletion of SGF73 results in altered ribosomal gene expression
650 in yeast. Aging Cell. Wiley/Blackwell (10.1111); 2017;16: 785–796. doi:10.1111/acel.12611
651 669

652 67. Arcangioli B, Ben Hassine S. Unrepaired oxidative DNA damage induces an ATR/ATM
653 apoptotic-like response in quiescent fission yeast. Cell Cycle. 2009;8: 2326–2331.
654 doi:10.4161/cc.8.15.9147

655 68. Mendenhall MD, Hodge AE. Regulation of Cdc28 cyclin-dependent protein kinase
656 activity during the cell cycle of the yeast *Saccharomyces cerevisiae*. Microbiol Mol Biol Rev.
657 1998;62: 1191–1243.

658 69. Escoté X, Miranda M, Rodríguez-Porrata B, Mas A, Cordero R, Posas F, et al. The stress-
659 activated protein kinase Hog1 develops a critical role after resting state. Mol Microbiol. John
660 Wiley & Sons, Ltd; 2011;80: 423–435. doi:10.1111/j.1365- 2958.2011.07585.x

661 70. Matsuoka K, Kiyokawa N, Taguchi T, Matsui J, Suzuki T, Mimori K, et al. Rum1, an
662 inhibitor of cyclin-dependent kinase in fission yeast, is negatively regulated by mitogen-
663 activated protein kinase-mediated phosphorylation at Ser and Thr residues. Eur J Biochem.
664 2002;269: 3511–3521.

665 71. Karigane D, Kobayashi H, Morikawa T, Ootomo Y, Sakai M, Nagamatsu G, et al. p38α

Activates Purine Metabolism to Initiate Hematopoietic Stem/Progenitor Cell Cycling in Response to Stress. Cell Stem Cell. 2016;19: 192–204. doi:10.1016/j.stem.2016.05.013

72. Sajiki K, Tahara Y, Villar-Briones A, Pluskal T, Teruya T, Mori A, et al. Genetic defects in SAPK signalling, chromatin regulation, vesicle transport and CoA-related lipid metabolism are rescued by rapamycin in fission yeast. Open Biol. Royal Society Journals; 2018;8: 170261. doi:10.1098/rsob.170261 691

73. Zinser ER, Kolter R. *Escherichia coli* evolution during stationary phase. Res Microbiol. 2004;155: 328–336. doi:10.1016/j.resmic.2004.01.014

74. Finkel SE. Long-term survival during stationary phase: evolution and the GASP phenotype. Nat Rev Microbiol. Nature Publishing Group; 2006;4: 113–120. doi:10.1038/nrmicro1340

75. Ram Y, Hadany L. Stress-induced mutagenesis and complex adaptation. Proc Biol Sci. The Royal Society; 2014;281: –20141025. doi:10.1098/rspb.2014.1025

76. Battesti A, Majdalani N, Gottesman S. The RpoS-Mediated General Stress Response in *Escherichia coli*. Annu Rev Microbiol. 2011;65: 189–213. doi:10.1146/annurev-micro-090110-102946

77. Harms A, Maisonneuve E, Gerdes K. Mechanisms of bacterial persistence during stress and antibiotic exposure. Science. 2016;354: aaf4268. doi:10.1126/science.aaf4268

78. Serrano M, Lin AW, McCurrach ME, Beach D, Lowe SW. Oncogenic ras provokes premature cell senescence associated with accumulation of p53 and p16INK4a. Cell. 1997;88: 593–602.

79. Liu X-L, Ding J, Meng L-H. Oncogene-induced senescence: a double edged sword in cancer. Acta Pharmacol Sin. Nature Publishing Group; 2018;39: 1553–1558. doi:10.1038/aps.2017.198

80. Fitzgerald DM, Hastings PJ, Rosenberg SM. Stress-Induced Mutagenesis: Implications in Cancer and Drug Resistance. Annu Rev Cancer Biol. 2017;1: 119–140. doi:10.1146/annurev-cancerbio-050216-121919

693 81. Bjedov I, Tenaillon O, Gérard B, Souza V, Denamur E, Radman M, et al. Stress-induced
694 mutagenesis in bacteria. Science. American Association for the Advancement of Science;
695 2003;300: 1404–1409. doi:10.1126/science.1082240

696 82. Foster PL. Stress-induced mutagenesis in bacteria. Crit Rev Biochem Mol Biol. 2007;42:
697 373–397. doi:10.1080/10409230701648494

698 83. Canovas B, Igea A, Sartori AA, Gomis RR, Paull TT, Isoda M, et al. Targeting p38 alpha
699 Increases DNA Damage, Chromosome Instability, and the Anti-tumoral Response to Taxanes
700 in Breast Cancer Cells. Cancer Cell. 2018;33: 1094–.doi:10.1016/j.ccell.2018.04.010 721

701 84. Moreno S, Klar A, Nurse P. Molecular genetic analysis of fission yeast
702 *Schizosaccharomyces pombe*. Meth Enzymol. 1991;194: 795–823.

703 85. AlienTrimmer: a tool to quickly and accurately trim off multiple short contaminant
704 sequences from high-throughput sequencing reads. Genomics. 2013;102: 500–506.
705 doi:10.1016/j.ygeno.2013.07.011

706 86. Liu Y, Schröder J, Schmidt B. Musket: a multistage k-mer spectrum-based error corrector
707 for Illumina sequence data. Bioinformatics. 2013;29: 308–315.
708 doi:10.1093/bioinformatics/bts690

709 87. Magoč T. FLASH: fast length adjustment of short reads to improve genome assemblies.
710 Bioinformatics. 2011;27: 2957–2963. doi:10.1093/bioinformatics/btr507

711 88. Li H, Durbin R. Fast and accurate short read alignment with Burrows-Wheeler transform.
712 Bioinformatics. Oxford University Press; 2009;25: 1754–1760.
713 doi:10.1093/bioinformatics/btp324

714 89. McKenna A, Hanna M, Banks E, Sivachenko A, Cibulskis K, Kernytsky A, et al. The
715 Genome Analysis Toolkit: A MapReduce framework for analyzing next-generation DNA
716 sequencing data. Genome Res. Cold Spring Harbor Lab; 2010;20: 1297–1303.
717 doi:10.1101/gr.107524.110 738

718 90. Koboldt DC, Chen K, Wylie T, Larson DE, McLellan MD, Mardis ER, et al. VarScan:
719 variant detection in massively parallel sequencing of individual and pooled samples.

720 Bioinformatics. 2009;25: 2283–2285. doi:10.1093/bioinformatics/btp373

721

Figure 1

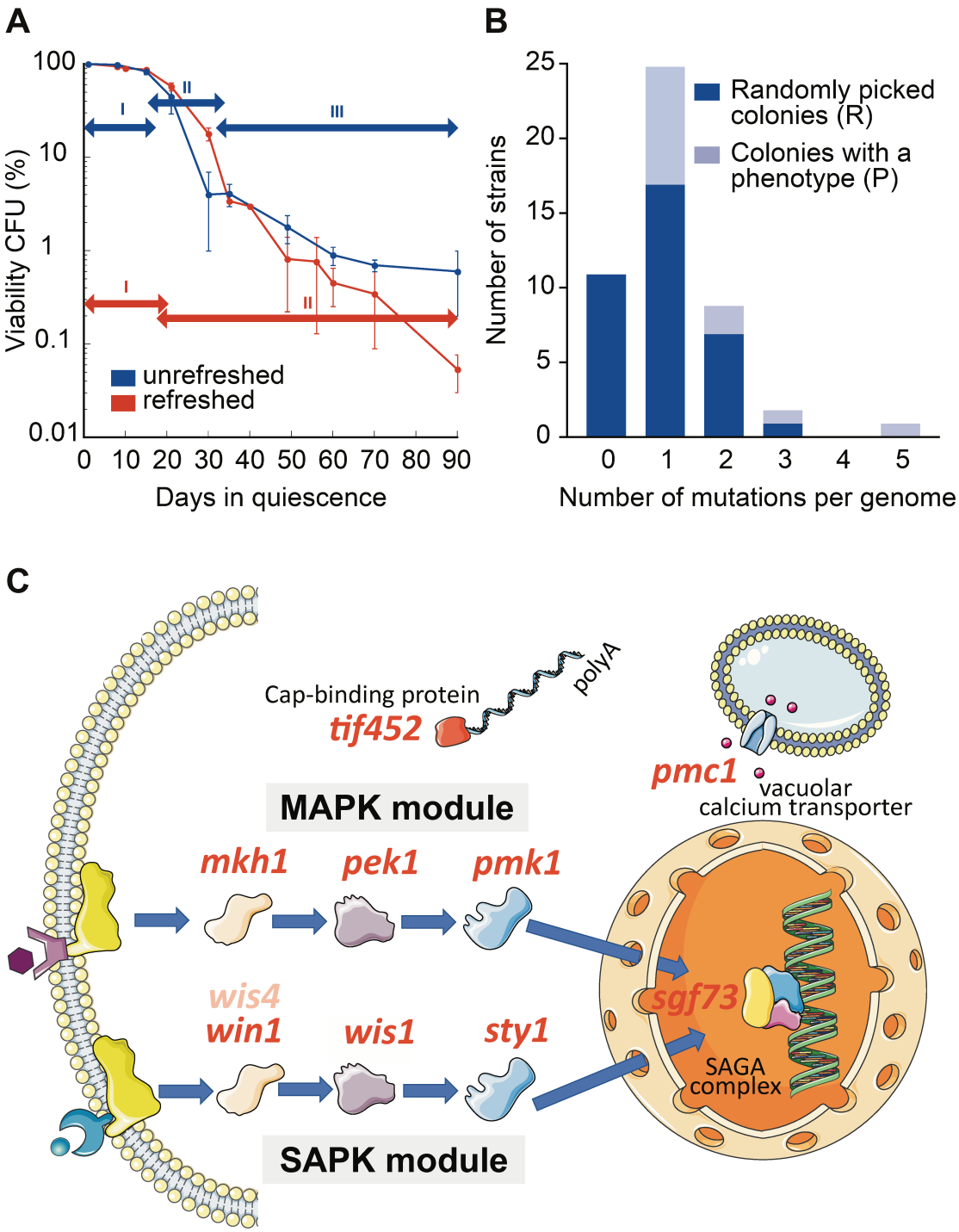
A
100
10
1
0.1
0.01
Viability CFU (%)
I
II
III
I
II
unrefreshed
refreshed
0 10 20 30 40 50 60 70 80 90
Days in quiescence
B
25
20
15
10
5
0
Number of strains
Randomly picked colonies (R)
Colonies with a phenotype (P)
0 1 2 3 4 5
Number of mutations per genome
C
Cap-binding protein
tif452
polyA
pmc1
vacuolar calcium transporter
MAPK module
mkh1
pek1
pmk1
wis4
win1
wis1
sty1
sgf73
SAGA complex
SAPK module

Figure 2

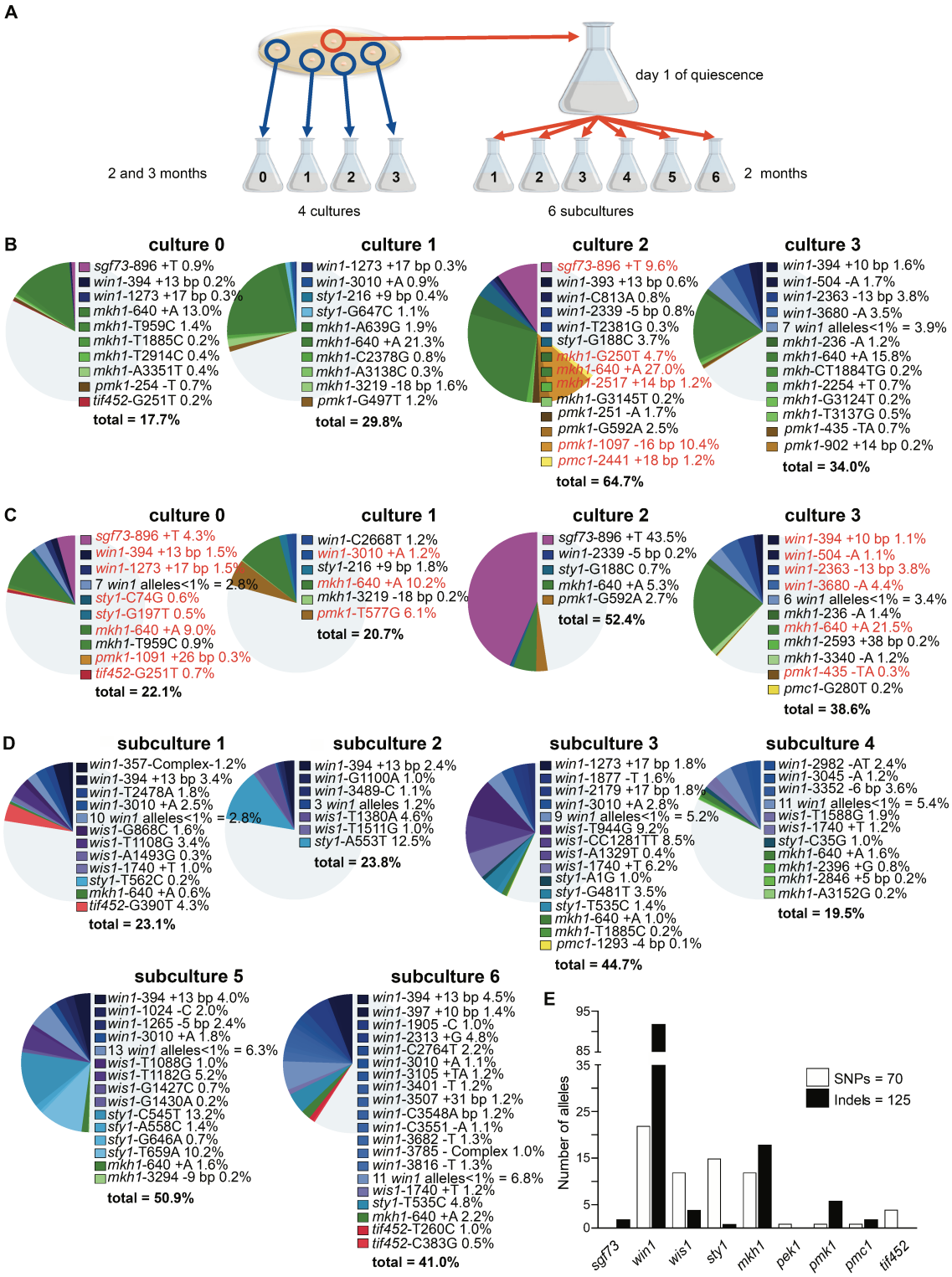
A
day 1 of quiescence
2 and 3 months
0
1
2
3
4 cultures
1
2
3
4
5
6
2 months
6 subcultures
B
culture 0
sgf73-896 +T 0.9%
win1-394 +13 bp 0.2%
win1-1273 +17 bp 0.3%
mkh1-640 +A 13.0%
mkh1-T959C 1.4%
mkh1-T1885C 0.2%
mkh1-T2914C 0.4%
mkh1-A3351T 0.4%
pmk1-254 -T 0.7%
tif452-G251T 0.2%
total = 17.7%
culture 1
win1-1273 +17 bp 0.3%
win1-3010 +A 0.9%
sty1-216 +9 bp 0.4%
sty1-G647C 1.1%
mkh1-A639G 1.9%
mkh1-640 +A 21.3%
mkh1-C2378G 0.8%
mkh1-A3138C 0.3%
mkh1-3219 -18 bp 1.6%
pmk1-G497T 1.2%
total = 29.8%
culture 2
sgf73-896 +T 9.6%
win1-393 +13 bp 0.6%
win1-C813A 0.8%
win1-2339 -5 bp 0.8%
win1-T2381G 0.3%
sty1-G188C 3.7%
mkh1-G250T 4.7%
mkh1-640 +A 27.0%
mkh1-2517 +14 bp 1.2%
mkh1-G3145T 0.2%
pmk1-251 -A 1.7%
pmk1-G592A 2.5%
pmk1-1097 -16 bp 10.4%
pmc1-2441 +18 bp 1.2%
total = 64.7%
culture 3
win1-394 +10 bp 1.6%
win1-504 -A 1.7%
win1-2363 -13 bp 3.8%
win1-3680 -A 3.5%
7 win1 alleles<1% = 3.9%
mkh1-236 -A 1.2%
mkh1-640 +A 15.8%
mkh-CT1884TG 0.2%
mkh1-2254 +T 0.7%
mkh1-G3124T 0.2%
mkh1-T3137G 0.5%
pmk1-435 -TA 0.7%
pmk1-902 +14 bp 0.2%
total = 34.0%
C
culture 0
sgf73-896 +T 4.3%
win1-394 +13 bp 1.5%
win1-1273 +17 bp 1.5%
7 win1 alleles<1% = 2.8%
sty1-C74G 0.6%
sty1-G197T 0.5%
mkh1-640 +A 9.0%
mkh1-T959C 0.9%
pmk1-1091 +26 bp 0.3%
tif452-G251T 0.7%
total = 22.1%
culture 1
win1-C2668T 1.2%
win1-3010 +A 1.2%
sty1-216 +9 bp 1.8%
mkh1-640 +A 10.2%
mkh1-3219 -18 bp 0.2%
pmk1-T577G 6.1%
total = 20.7%
culture 2
sgf73-896 +T 43.5%
win1-2339 -5 bp 0.2%
sty1-G188C 0.7%
mkh1-640 +A 5.3%
pmk1-G592A 2.7%
total = 52.4%
culture 3
win1-394 +10 bp 1.1%
win1-504 -A 1.1%
win1-2363 -13 bp 3.8%
win1-3680 -A 4.4%
6 win1 alleles<1% = 3.4%
mkh1-236 -A 1.4%
mkh1-640 +A 21.5%
mkh1-2593 +38 bp 0.2%
mkh1-3340 -A 1.2%
pmk1-435 -TA 0.3%
pmc1-G280T 0.2%
total = 38.6%
D
subculture 1
win1-357-Complex-1.2%
win1-394 +13 bp 3.4%
win1-T2478A 1.8%
win1-3010 +A 2.5%
10 win1 alleles<1% = 2.8%
wis1-G868C 1.6%
wis1-T1108G 3.4%
wis1-A1493G 0.3%
wis1-1740 +T 1.0%
sty1-T562C 0.2%
mkh1-640 +A 0.6%
tif452-G390T 4.3%
total = 23.1%
subculture 2
win1-394 +13 bp 2.4%
win1-G1100A 1.0%
win1-3489-C 1.1%
3 win1 alleles 1.2%
wis1-T1380A 4.6%
wis1-T1511G 1.0%
sty1-A553T 12.5%
total = 23.8%
subculture 3
win1-1273 +17 bp 1.8%
win1-1877 -T 1.6%
win1-2179 +17 bp 1.8%
win1-3010 +A 2.8%
9 win1 alleles<1% = 5.2%
wis1-T944G 9.2%
wis1-CC1281TT 8.5%
wis1-A1329T 0.4%
wis1-1740 +T 6.2%
sty1-A1G 1.0%
sty1-G481T 3.5%
sty1-T535C 1.4%
mkh1-640 +A 1.0%
mkh1-T1885C 0.2%
pmc1-1293 -4 bp 0.1%
total = 44.7%
subculture 4
win1-2982 -AT 2.4%
win1-3045 -A 1.2%
win1-3352 -6 bp 3.6%
11 win1 alleles<1% = 5.4%
wis1-T1588G 1.9%
wis1-1740 +T 1.2%
sty1-C35G 1.0%
mkh1-640 +A 1.6%
mkh1-2396 +G 0.8%
mkh1-2846 +5 bp 0.2%
mkh1-A3152G 0.2%
total = 19.5%
subculture 5
win1-394 +13 bp 4.0%
win1-1024 -C 2.0%
win1-1265 -5 bp 2.4%
win1-3010 +A 1.8%
13 win1 alleles<1% = 6.3%
wis1-T1088G 1.0%
wis1-T1182G 5.2%
wis1-G1427C 0.7%
wis1-G1430A 0.2%
sty1-C545T 13.2%
sty1-A558C 1.4%
sty1-G646A 0.7%
sty1-T659A 10.2%
mkh1-640 +A 1.6%
mkh1-3294 -9 bp 0.2%
total = 50.9%
subculture 6
win1-394 +13 bp 4.5%
win1-397 +10 bp 1.4%
win1-1905 -C 1.0%
win1-2313 +G 4.8%
win1-C2764T 2.2%
win1-3010 +A 1.1%
win1-3105 +TA 1.2%
win1-3401 -T 1.2%
win1-3507 +31 bp 1.2%
win1-C3548A bp 1.2%
win1-C3551 -A 1.1%
win1-3682 -T 1.3%
win1-3785 - Complex 1.0%
win1-3816 -T 1.3%
11 win1 alleles<1% = 6.8%
wis1-1740 +T 1.2%
sty1-T535C 4.8%
mkh1-640 +A 2.2%
tif452-T260C 1.0%
tif452-C383G 0.5%
total = 41.0%
E
Number of alleles
95
85
35
25
15
5
0
SNPs = 70
Indels = 125
sgf73
win1
wis1
sty1
mkh1
pek1
pmk1
pmc1
tif452

Figure 3

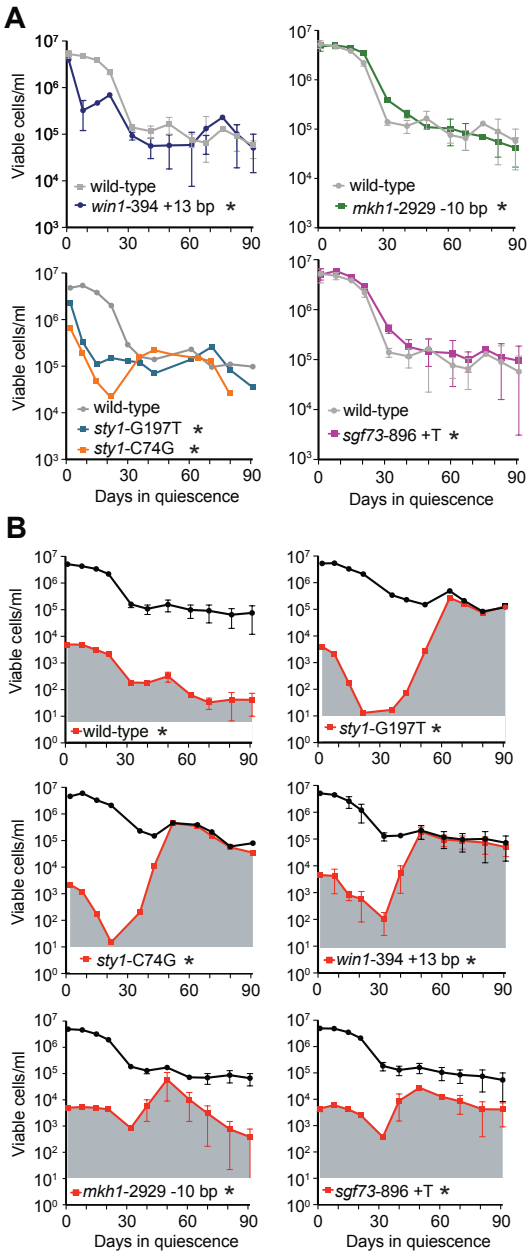
A
Viable cells/ml
wild-type
win1-394 +13 bp *
mkh1-2929 -10 bp *
sty1-G197T *
sty1-C74G *
sgf73-896 +T *
Days in quiescence
B
wild-type *
sty1-G197T *
sty1-C74G *
win1-394 +13 bp *
mkh1-2929 -10 bp *
sgf73-896 +T *

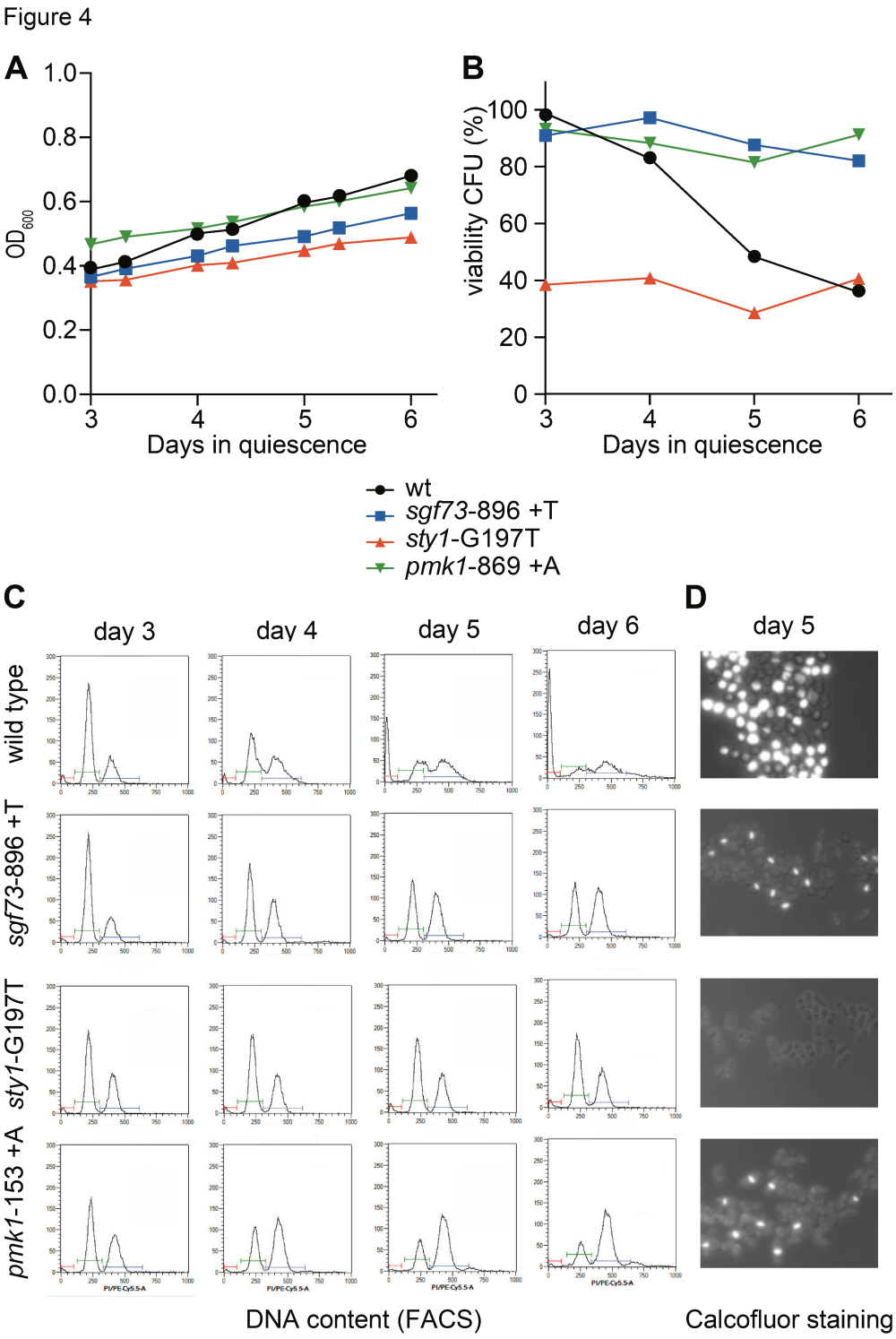
Figure 4
A
B
OD600
viability CFU (%)
Days in quiescence
Days in quiescence
wt
sgf73-896 +T
sty1-G197T
pmk1-869 +A
C
D
day 3
day 4
day 5
day 6
day 5
wild type
sgf73-896 +T
sty1-G197T
pmk1-153 +A
DNA content (FACS)
Calcofluor staining

Figure 5

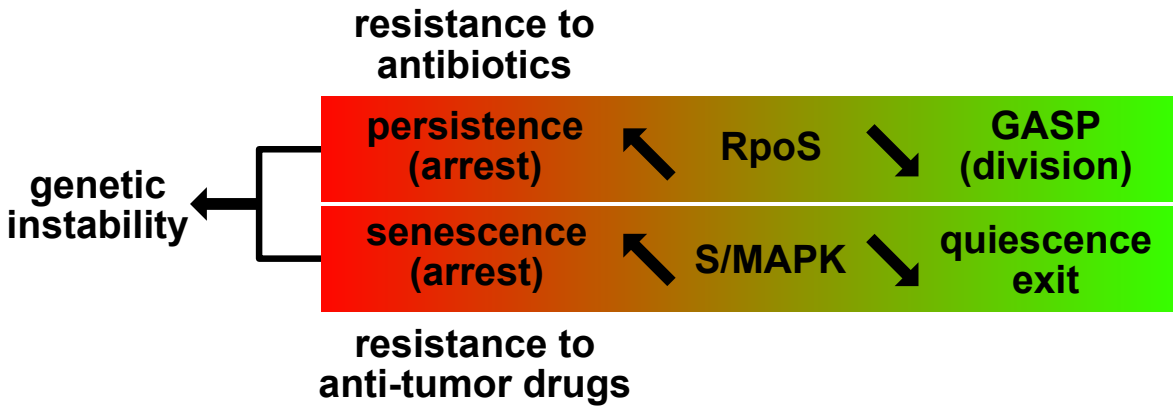
resistance to
antibiotics
persistence
(arrest)
RpoS
GASP
(division)
genetic
instability
senescence
(arrest)
S/MAPK
quiescence
exit
resistance to
anti-tumor drugs

Figure S1

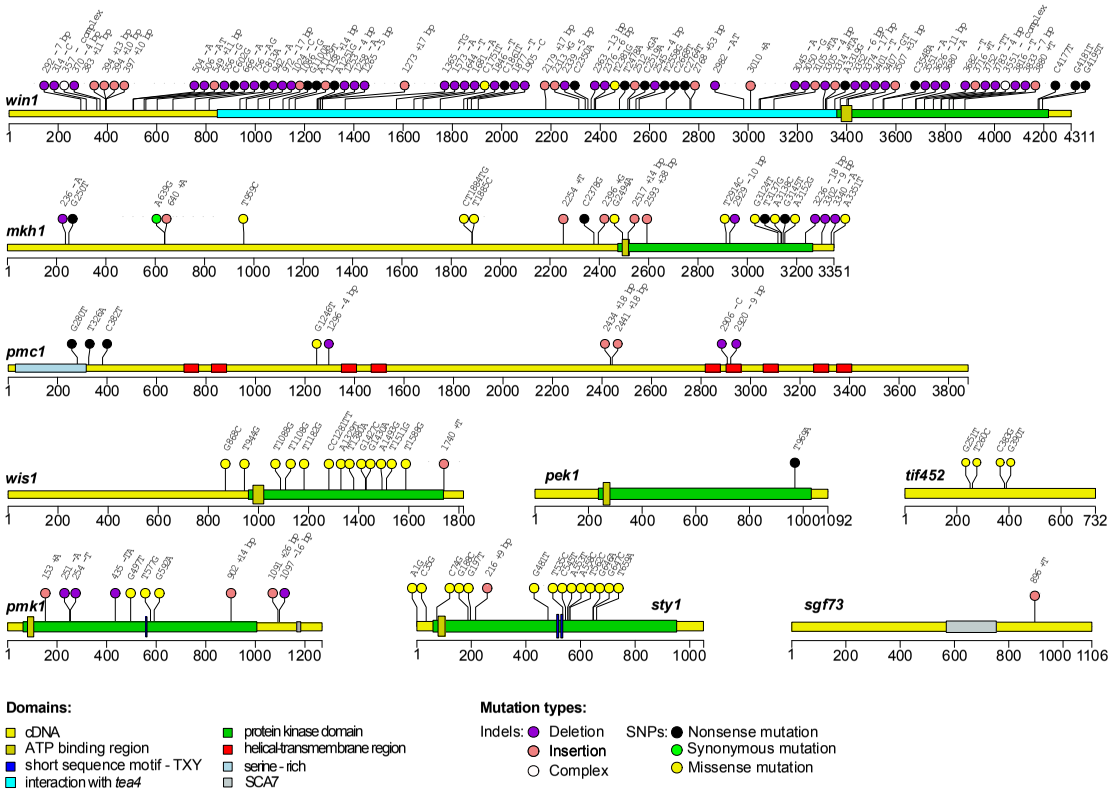
win1
mkh1
pmc1
wis1
pek1
tif452
pmk1
sty1
sgf73
Domains:
cDNA
ATP binding region
short sequence motif - TXY
interaction with tea4
protein kinase domain
helical-transmembrane region
serine - rich
SCA7
Mutation types:
Indels: Deletion
Insertion
Complex
SNPs: Nonsense mutation
Synonymous mutation
Missense mutation

Figure S2

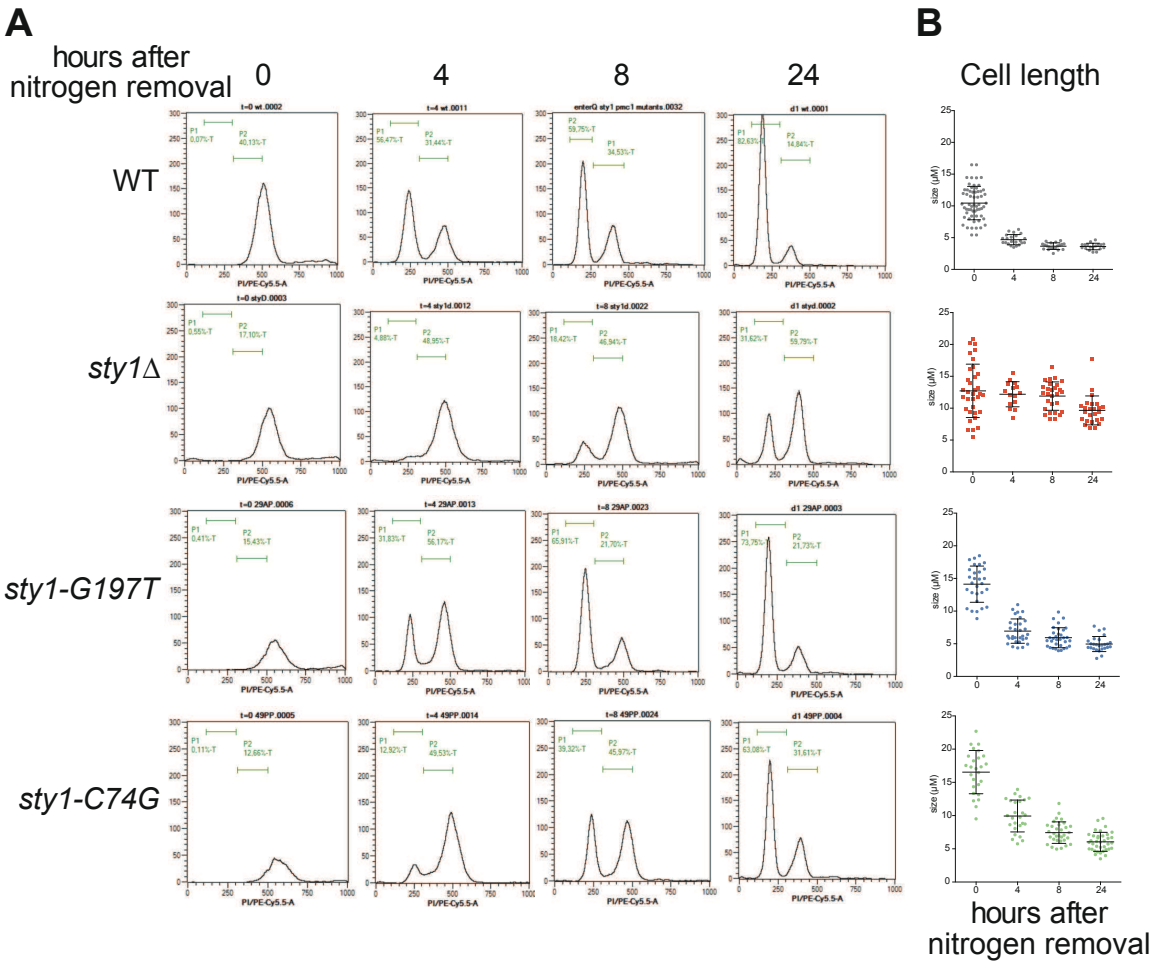
A
hours after nitrogen removal
0
4
8
24
WT
sty1Δ
sty1-G197T
sty1-C74G
B
Cell length
size (μM)
hours after nitrogen removal

Figure S3

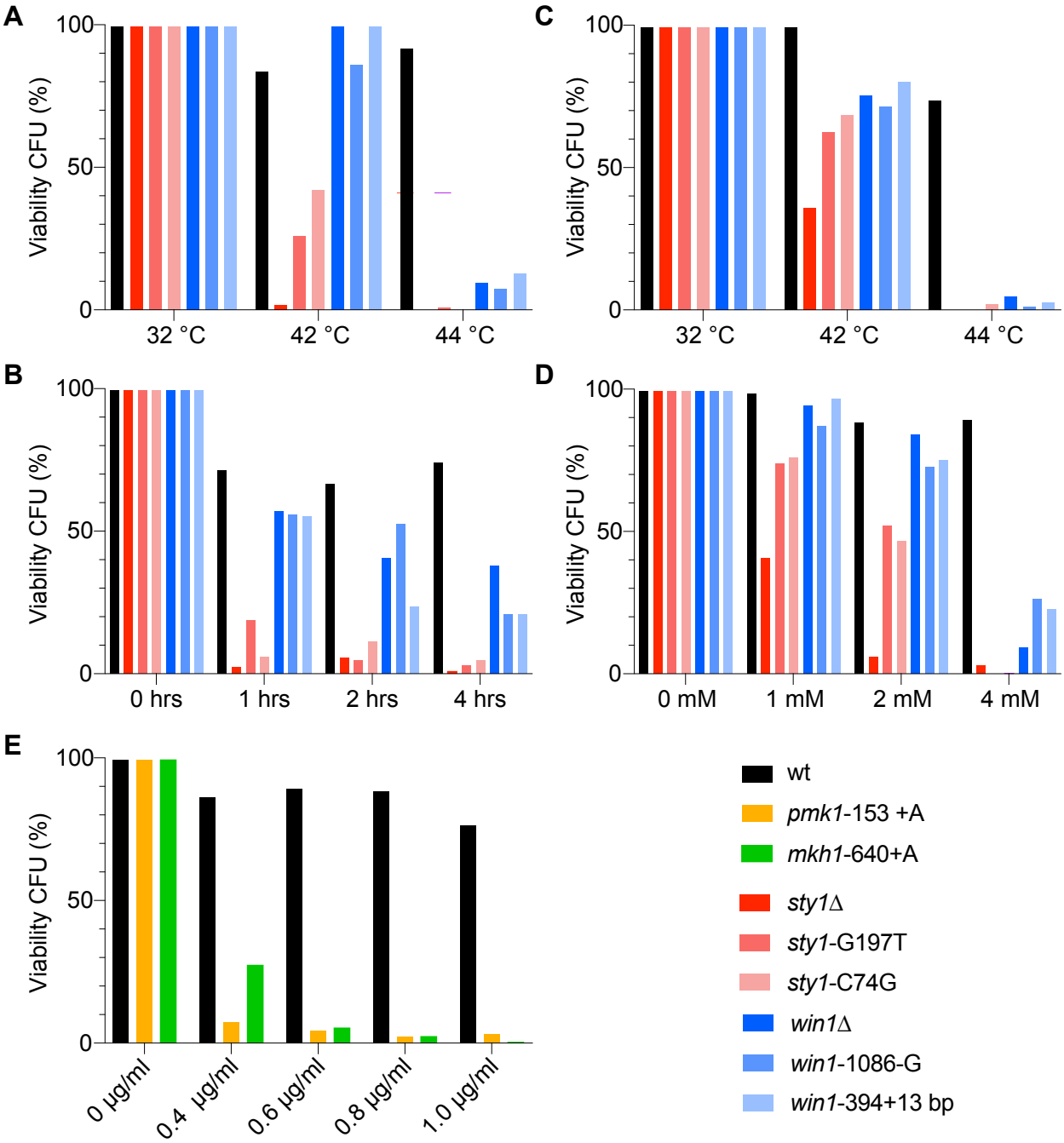
A
C
B
D
E
Viability CFU (%)
100
50
0
32 °C
42 °C
44 °C
0 hrs
1 hrs
2 hrs
4 hrs
0 mM
1 mM
2 mM
4 mM
0 µg/ml
0.4 µg/ml
0.6 µg/ml
0.8 µg/ml
1.0 µg/ml
wt
pmk1-153 +A
mkh1-640+A
sty1Δ
sty1-G197T
sty1-C74G
win1Δ
win1-1086-G
win1-394+13 bp

Figure S4

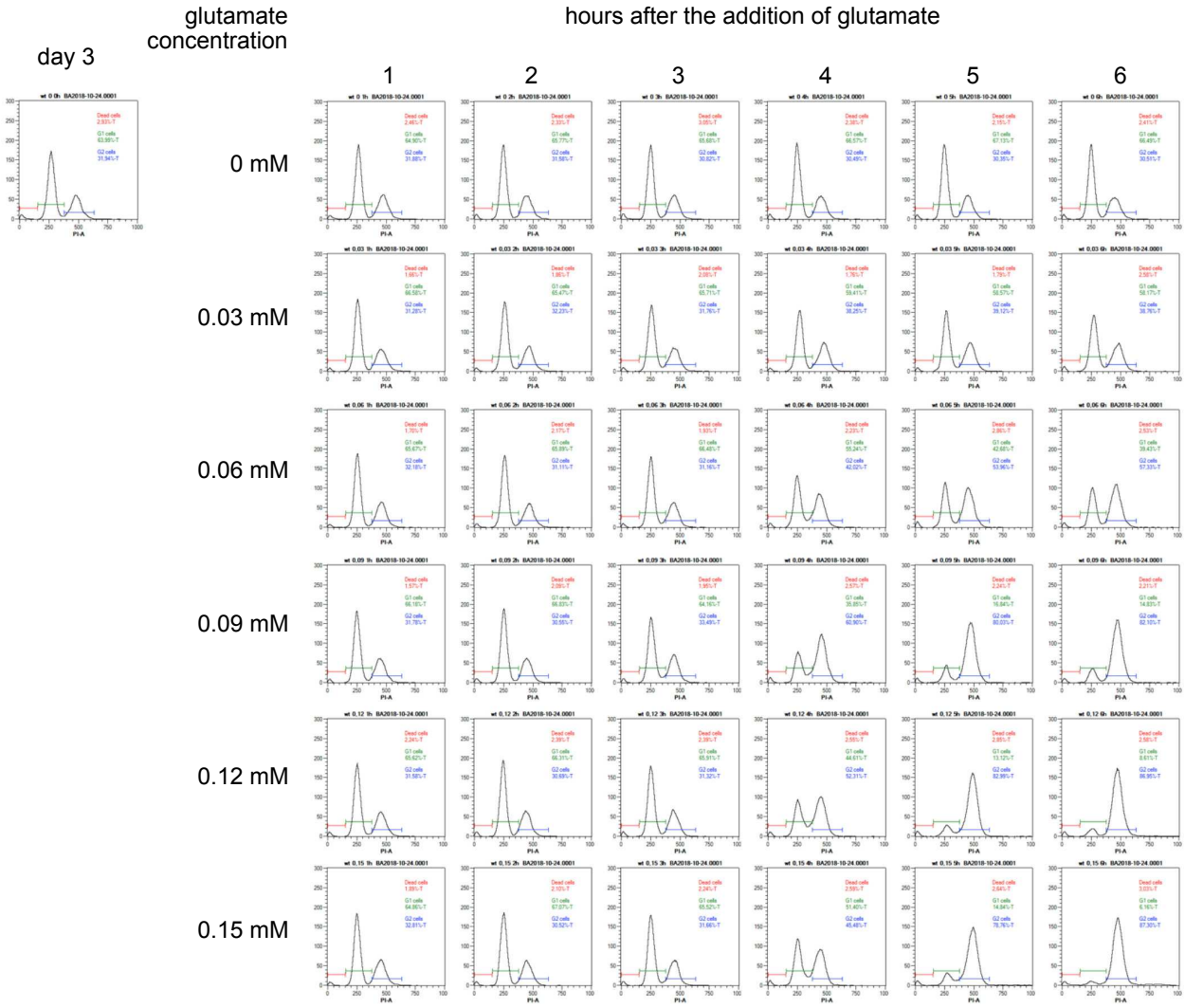
day 3
glutamate concentration
hours after the addition of glutamate
1
2
3
4
5
6
0 mM
0.03 mM
0.06 mM
0.09 mM
0.12 mM
0.15 mM

Figure S5

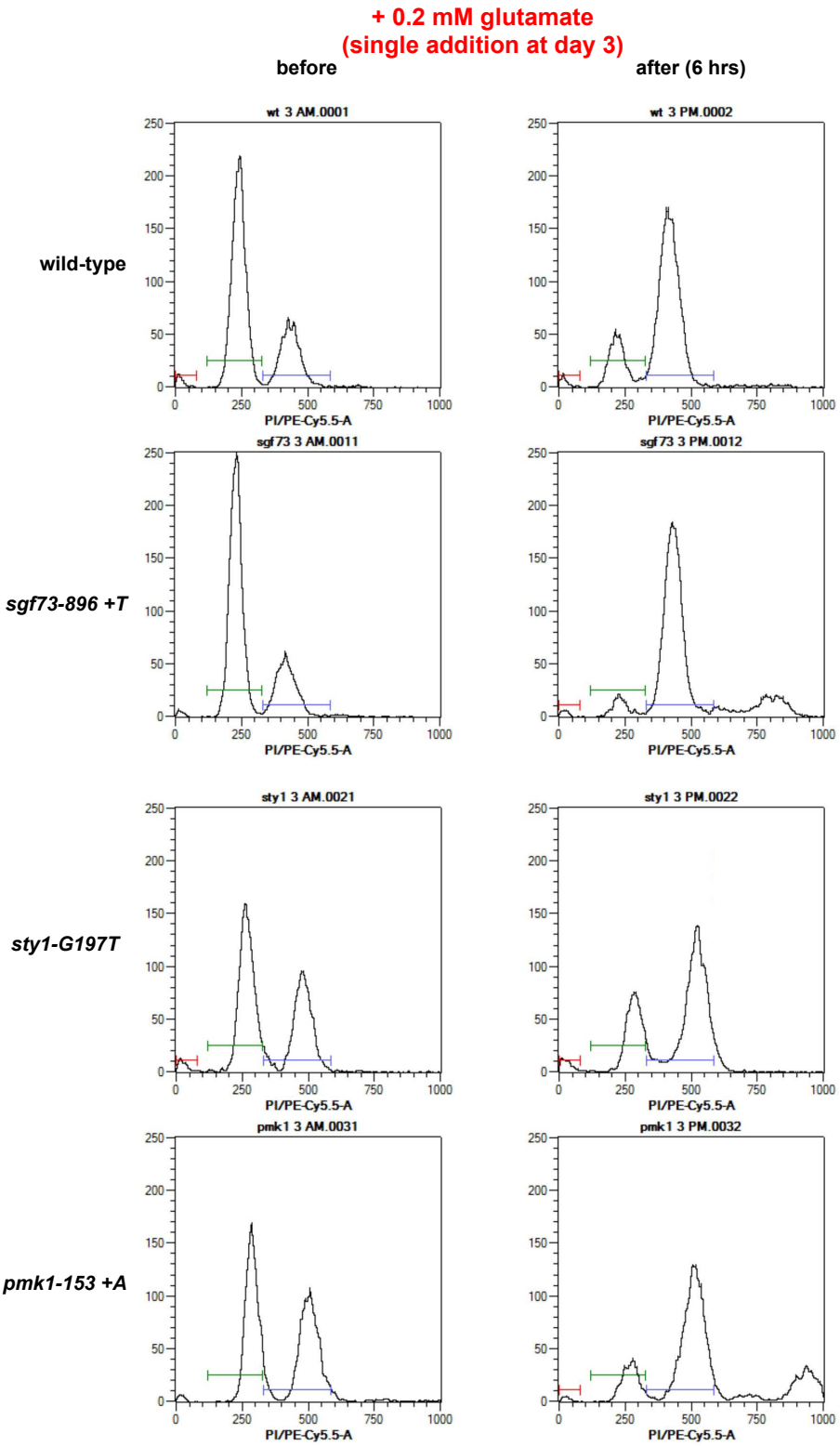
+ 0.2 mM glutamate
(single addition at day 3)
before
after (6 hrs)
wild-type
sgf73-896 +T
sty1-G197T
pmk1-153 +A
wt 3 AM.0001
wt 3 PM.0002
sgf73 3 AM.0011
sgf73 3 PM.0012
sty1 3 AM.0021
sty1 3 PM.0022
pmk1 3 AM.0031
pmk1 3 PM.0032
PI/PE-Cy5.5-A

Figure legends

Fig 1. Viability and distribution of mutations in quiescence.

(A) Viability curves (from at least 5 independent cultures of the same strain) in unrefreshed (blue) and refreshed (red) medium. The red curve was determined in [6]. Three phases are depicted in unrefreshed medium and two in the refreshed medium. (B) Distribution of the number of mutations per genome after 3 months of quiescence in the 36 randomly picked (R) colonies and in the 12 colonies selected for their sensitivity to various agents. (C) Win1/Wis1/Sty1 is the stress-activated kinase (SAPK) module essential for stress response. The Wis4 SAPKKK is parallel to Win1, but was not found in our study. Mkh1/Pek1/Pmk1 is the mitogen-activated kinase (MAPK) module essential for membrane, cell wall and stress response. Pmc1 is the vacuole Ca++ efflux protein that is depleting the cytosol of Ca++, regulating calcineurin. Sgf73 is a subunit of the transcriptional SAGA complex that has been previously connected to the transcriptional hypoxic-response upon S/MAPK activation. eIF4E/tif452 is binding mRNA 5'-CAP structure and is a target for Tor (target of rapamycin) and S/MAPK signaling.

Fig 2. Targeted resequencing of genes in the S/MAPK pathways.

(A) Schematic view of the strategy indicating that the same progenitor strain was used in 3 independent cultures (in addition of culture 0) and in 1 culture split at day 1 of quiescence in 6 parallel subcultures. Samples were analyzed after 2 and 3 months of quiescence. Distribution of mutations of cultures 0 to 3 after 2 months (B) and after 3 months (C). In red, are depicted the mutations confirmed by Sanger sequencing of the isolated mutants. (D) Distribution of mutations of the subcultures after 2 months of quiescence. (E) Distribution of the number of SNVs and indels in the targeted genes.

Fig 3. Quiescence survival of single and co-cultured strains.

(A) Comparison of the survival of single mutants with the wild-type control during quiescence. Independent cultures are indicated by the presence of error bars. The star (*) indicates the presence of the kanamycin marker in the background (B) Co-cultures where the wild-type is contaminated at day 1 of quiescence with 0.1% of the indicated strain marked (*) with the kanamycin gene (red). The black curve indicates the viability of the population.

Fig 4. Sub-limiting concentration of glutamate promotes quiescence exit of the S/MAPK mutants.

At day 3 of quiescence, glutamate was added twice a day (0.02 mM). (A) Increase in OD_{600nm}. (B) Plating efficiency. (C) FACS analysis at day 3 prior to glutamate addition indicating that most cells exhibit a 1C DNA content. The DNA content is followed at day 4, 5 and 6 after glutamate addition. (D) Calcofluor staining of the populations at day 5.

Fig 5. Functional analogy between RpoS and S/MAPK.

The green color indicates a low activity of the functional analogues that leads to growth, while the red color points to an elevated activity that results in an arrest that eventually leads to genetic instability.

Fig S1. Position and nature of the mutations found in the 9 targeted genes after resequencing.

The different types of mutation and known domains are indicated by colors.

Fig S2. Analysis of quiescence entry of *sty1* mutants. (A) DNA content analysis by FACS following removal of nitrogen (t= 0h). (B) Cell size determined by microscopy (n>30) following nitrogen removal.

Fig S3. Sensitivity to various agents during growth and quiescence.

(A) The growing strains were incubated for 2 hours at the indicated temperature prior to plating. (B) Viability of the growing strains following exposure to 1 mM H_2O_2 for the indicated times. (C) Viability of 1-day-old quiescent strains incubated for 2 hours at the indicated temperature prior to plating. (D) Viability of 1-day-old quiescent strains following exposure for 2 hours in the presence of the indicated amounts of H_2O_2 prior to plating. (E) Viability of growing strains after 16 hours of exposure to various concentrations of caspofungin. All the strains were plated on rich medium and incubated at 32 °C for 3 days and scored.

Fig S4. Effect of glutamate concentration on the cell cycle of a 3-day-old quiescent

culture.

FACS analysis of the DNA content of a wild-type strain followed for 6 hours after the addition of a given amount of glutamate.

Fig S5. Effect of glutamate addition on the cell cycle of 3-day-old quiescent cultures of S/MAPK mutants.

FACS analysis of the DNA content of strains determined 6 hours after the addition of 0.2 mM of glutamate.

Tables Table 1. Distribution of the mutants of S/MAPK pathway among 48 strains sequenced after 3 months of quiescence.

Table S1. Mutations found after 3 months of quiescence in the 48 genomes that were sequenced.

Table S2. List of primers.

Table S3. Sensitivity of the 12 mutant strains (P) to various agents.

Table S4. Mutations identified in the targeted resequencing experiment.

Table S5. List of strains.

Table 1: Distribution of the mutants of S/MAPK pathway among 48 strains sequenced after 3 months of quiescence				
genes	phenotype	random	function	human homologue
win1	1	2	SAPKKK	MAP3K4
wis1	-	2	SAPKK	MAP2K1
sty1	1	1	SAPK	p38
mkh1	-	4	MAPKKK	MEKK1
pek1	-	1	MAPKK	MEK2
pmk1	-	2	MAPK	ERK
pmc1	3	3	Calcium efflux	PMCA
sgf73	4	-	SAGA subunit	ATXN7
tif452	-	1	CAP binding	eIF4E

Table S1

Table S1: Mutations found after 3 months of quiescence in the 48 genomes that were sequenced.							
Strain	**Chromosome**	**Position**	**Reference**	**Alternative**	**Mutation type**	**Gene**	**Allele**
1R	II	945943	A	T	SNP	*gap1*	*gap1*- T1460A
2R	-	-	-	-	-	-	
3R	II	1532631	A	G	SNP	SPBC83.12	
4R	I	616209	G	GT	Insertion	*mkh1*	*mkh1*-640+A
	II	1048712	G	A	SNP	*dre2* (predicted)	*dre2*-C719T
5R	I	1591589	T	A	SNP	*thi4*	*thi4*-T1490A
6R	-	-	-	-	-	-	
7R	-	-	-	-	-	-	
8R	I	207717	C	A	SNP	*sty1*	*sty1*-G197T
	III	175767	A	ATACATCTAA	Insertion	SPCC1235.01	
9R	-	-	-	-	-	-	
10R	I	2714004	TAACCCACAA	T	Deletion	*pmc1*	*pmc1*-2920 -9 bp
11R	-	-	-	-	-	-	
12R	III	1493950	A	G	SNP	*pfl4*	*pfl4*-T818C
13R	-	-	-	-	-	-	
14R	I	255219	A	G	SNP	SPNCRNA.630 (predicted)	
	II	693417	-36bp		Deletion	SPBPJ4664.02	
	I	613911	CTATGCTTAGA	C	Deletion	*mkh1*	*mkh1-2929 -10 bp*
15R	II	4313731	T	A	SNP	*pek1*	*pek1*- T969A
	III	903386	GAAA	G	Deletion	*mcm4*	
16R	-	-	-	-	-	-	
17R	-	-	-	-	-	-	
18R	II	731112	T	TA	Insertion	*pmk1*	*pmk1*-153+A
19R	I	2715686	C	A	SNP	*pmc1*	*pmc1*-G1246T
	II	3860184	TCTAGT	T	Deletion	Intergenic	
20R	III	1493950	A	G	SNP	*pfl4*	*pfl4*-T818C
21R	II	1134749	G	T	SNP	*tif452*	*tif452*-G251T
22R	I	616209	G	GT	Insertion	*mkh1*	*mkh1*-640+A
	I	2245479	T	TCCC	Insertion	Intergenic	
23R	II	53302	G	C	SNP	Intergenic	
	I	760579		-AT	Deletion	Intergenic	
	I	801095		-AAGTATATAT	Deletion	Intergenic	
24R	I	5090834	T	TCTACTACATCCTC	Insertion	*win1*	*win1*-394 +13 bp
25R	-	-	-	-	-	-	
26R	II	1146497	C	CA	Insertion	*wis1*	

Table S1 continue

27R	-	-	-	-	-	-	
28R	II	4538083	GA	G	Deletion	Intergenic	
29R	I	5091713	A	ATATCCTTCACGTCGTTC	Insertion	*win1*	*win1*-1273 + 17bp
30R	I	614355	C	T	SNP	*mkh1*	*mkh1*-G2494A
	II	1649054	A	C	SNP	*rec6*	*rec6*-T533G
31R	-	-	-	-	-	-	
32R	II	1146497	C	CA	Insertion	*wis1*	
33R	II	4255819	T	G	SNP	SPBC1652.02-antisense-1 (predicted)	
	I	2714492	C	CAATATTATCACCAGTAAC	Insertion	*pmc1*	*pmc1*-2441+18bp
34R	II	731112	T	TA	Insertion	*pmk1*	*pmk1*-153+A
35R	II	1049917	T	TGTAA	Insertion	*dre2* (predicted)	
36R	II	1665445	C	CTTTAT	Insertion	intergenic	
1P	I	2716606	A	T	SNP	*pmc1*	*pmc1*-T326A
2P	I	2714026	AG	A	Deletion	*pmc1*	*pmc1*-2906-C
3P	III	2122890	T	TA	Insertion	*sgf73*	*sgf73-896+T*
4P	III	2122890	T	TA	Insertion	*sgf73*	*sgf73-896+T*
	I	1544016	T	A	SNP	*pabp*	*pabp*-T1152A
5P	III	2122890	T	TA	Insertion	*sgf73*	*sgf73-896+T*
6P	I	207840	G	C	SNP	*sty1*	*sty1*-G74C
	I	2499161	TG	T	Deletion	SPAC23H3.04	
	II	2437855	A	C	SNP	*map4*	*map4*-A2220C
	III	1493950	A	G	SNP	*pfl4*	*pfl4*-T818C
7P	III	2122890	T	TA	Insertion	*sgf73*	*sgf73-896+T*
8P	I	2716550	G	A	SNP	*pmc1*	*pmc1*-C382T
9P	I	5091526	TG	T	Deletion	*win1*	*win1*-1086-G
10P	III	648242	T	C	SNP	*cut1*	*cut1*-T4313C
	II	4344813	A	ATTTTCTTC	Insertion	*qcr6*	*qcr6*-T325+6 bp
11P	III	748812	A	T	SNP	SPCC14G10.04	
12P	III	748812	A	T	SNP	SPCC14G10.04	
	III	2433242	T	A	SNP	SPCC569.02c-antisense-1 (predicted)	
	III	99099	A	AACTATGCAAGGGACCATGAAC	Insertion	*meu23*	*meu23*-T387 +21bp
	III	2433240	A	G	SNP	SPCC569.02c-antisense-1 (predicted)	
	III	2433279	A	G		SPCC569.02c-antisense-1 (predicted)	
	III	2433281	A	C		SPCC569.02c-antisense-1 (predicted)	

Table S2

Table S2: List of primers used for the targeted resequencing of the 9 genes of S/MAPK path		
Primer name	**Gene targeted**	**Primer Sequence 5' > 3'**
OL1451	*sgf73*	AAAGTCGAAAATGCGTGG
OL1452	*sgf73*	TGTTTTGCTTGCAGCTTGT
OL1453	*sgf73*	TTCTTTTGCAGTTTCGAGG
OL1454	*sgf73*	TAAATCGACAGCTAAGGG
OL1455	*sgf73*	TTCTTTTCATGATTCCCAG
OL1456	*sgf73*	AAACTCGGTTCTTATCAA
OL1073	*win1*	TAGTTGCATTGACTTCGCT
OL1074	*win1*	TGGCCTTCTGTGATTTTCTT
OL1075	*win1*	CATCGTCGCTCTTTGACT
OL1076	*win1*	CTGTGCATATAATCGTCTTCCT
OL1077	*win1*	CTTCTTCCTCTTCCATTCC
OL1078	*win1*	CGAGTCCTCCTCATCATAA
OL1079	*win1*	CTTCTCTAAGCATTCGTC
OL1080	*win1*	TAGCACATCAACCATACC
OL1081	*win1*	GTGGATGGAAATATGGTGT
OL1082	*win1*	TGGTCCGTTTGAAATTTGAG
OL1083	*win1*	GGTTGGTAATGAGGAAATGG
OL1084	*win1*	TTGTTGAATGATATGGACGG
OL1085	*win1*	CGTCTTCTTTCTTTTCCGT
OL1086	*win1*	ATATTTCACCAACCAGCG
OL1087	*win1*	CCACATCGAACACGGATT
OL1088	*win1*	CGCATATGGAGGTACACTTT
OL1089	*win1*	CGAACATGAAGGAGCATAC

OL1090	*win1*	CACATCAAGCAATGACAAAG
OL1091	*win1*	CTCACTTGTTGATTCTGC
OL1092	*win1*	CCACACATTTTCCAACCT
OL1093	*win1*	CAGTTGGGTTGGATTCAT
OL1094	*win1*	CCTGTTCTCCTTTGTCGT
OL1095	*win1*	AAAGTAATAGAAGGGACCGA
OL1096	*win1*	CCTCAATTCTACCGTAAC
OL1097	*win1*	GAAGTGCATCGTGAAAAAG
OL1098	*win1*	AATATCCATAGCACCAACC
OL1099	*win1*	GCAGCATCTAGACCAAAA
OL1100	*win1*	TTCGACTACGGATGAGTT
OL1101	*win1*	CGTTGTTTTGTTTCTGATCCC
OL1102	*win1*	TCTCTTCCTAGCGCCGTA
OL1509	*wis1*	AACAGAGCAGGCAATTAGA
OL1510	*wis1*	ACATGGCTCCTGAAAGAA
OL1511	*wis1*	GATAAGCTCCTAAAGCCA
OL1512	*wis1*	TGGTGCCTTTTTTGTGGA
OL1513	*wis1*	ACTCCTTCGTCTTTGATACC
OL1514	*wis1*	CTAAACATTCCTCCCACCC
OL1515	*wis1*	GAAAATGTGGAAAAAGGGG
OL1516	*wis1*	ACAGGAGAAATTGAAGGC
OL1517	*wis1*	TCCGGCATTGATTTTGATCT
OL1518	*wis1*	CTTCTCCAAATAATCAACCC
OL1041	*sty1*	CATAACATACCCCGAGAACA
OL1042	*sty1*	CCGAGACCACGTTAACCA
OL1043	*sty1*	ATTACTTCCATAGGCGGC
OL1044	*sty1*	ACTACTTACATCGCGACC

OL1045	*sty1*	TGGGTTTCAGATCACGGT
OL1046	*sty1*	CCTTTGGCCTCGTTTGTT
OL1047	*sty1*	AACAGCGACATTCATTCCA
OL1048	*sty1*	ACATACCTCCTTACCACAAC
OL1329	*mkh1*	CGAGGAAACGCTAAGTAA
OL1330	*mkh1*	GCAAACCTGTCCATGCAA
OL1331	*mkh1*	TTCCAACACTACACATCC
OL1332	*mkh1*	TAGTGCAATATCTGGGTTTC
OL1333	*mkh1*	AATTCCGCAAACATCGAC
OL1334	*mkh1*	AAATACGACATAACGCGAG
OL1335	*mkh1*	TACAATCCTAGAGCCCCAAA
OL1336	*mkh1*	TCGCCTAAAACTCCTGAA
OL1337	*mkh1*	CCCAGTTACCAGAATTGA
OL1338	*mkh1*	CCGGACATAACGAAGCTA
OL1339	*mkh1*	GCTTCCACACTTTCCTTT
OL1340	*mkh1*	GACGTTTTCGAGGGTTTG
OL1341	*mkh1*	GCCATTTCTCCTTTAGCAC
OL1342	*mkh1*	GGCGGGGCTCAATACATA
OL1343	*mkh1*	CACTATCCATACCCGATTCT
OL1344	*mkh1*	CAAATTCGAACCCATTCCA
OL1345	*mkh1*	TACCCACTCACCTTGATCC
OL1346	*mkh1*	CTCTGGTTTCCGCTCTTC
OL1347	*mkh1*	CTTTTGAGGGACGAATTTTG
OL1348	*mkh1*	GTTCTGGGTATATGGCTG
OL1049	*pek1*	GGTTGTTTGTTTGCGAGG
OL1050	*pek1*	TATCCCGGCTCTCCTTTC
OL1051	*pek1*	TGGTGTTTTCTAGCGAGT

OL1052	*pek1*	TTTGTATATCGCGTCGAG
OL1053	*pek1*	GGAATATTGCGGAGCAGG
OL1054	*pek1*	AGGTAAAAGGGGAGGTGG
OL1055	*pek1*	GGTTTAACATTGATGGAGG
OL1056	*pek1*	AACAAGCGAACTGGAAGA
OL1057	*pek1*	AGAGTTCCTTCGTCAAGT
OL1058	*pek1*	AAGCTAGCAAGGCGTAAA
OL1059	*pmk1*	TTTTTCCACATCCCTTTTGCC
OL1060	*pmk1*	AATCAATCACAGGAAGCCG
OL1061	*pmk1*	GAGAGAGATAAAACTGCTGA
OL1062	*pmk1*	TCGCGTAACATACCAACT
OL1063	*pmk1*	TGCATTTACGATCTCGAC
OL1064	*pmk1*	TGATAGCTGCTGAACGAA
OL1065	*pmk1*	TGGTTTTATGACGGAGTATG
OL1066	*pmk1*	GAAATACGTCTGTTGGGG
OL1067	*pmk1*	ACAGGAGTATGTTCGAAG
OL1068	*pmk1*	AGGTTTGAGAGGATGAAG
OL1069	*pmk1*	CTCATCCAACAAACCCAAC
OL1070	*pmk1*	GCAAGAAAAGGGAGCACA
OL1201	*pmk1*	CTTGCATTTACGATCTCGAC
OL1202	*pmk1*	ACACTCCAAACATCAATACC
OL1173	*tif452*	AACCCAATTACGACCACC
OL1174	*tif452*	CCCCAAAACTCTTCCACT
OL1175	*tif452*	AAAAACACACCCCCTTCA
OL1176	*tif452*	CACCAGTAACTTCTTTCCCA
OL1177	*tif452*	ACTGCTGTGATATCGACT
OL1178	*tif452*	TCGTAAATGAACACCCCT

OL1293	*pmc1*	GGCGATTTCCAACGAGAA
OL1294	*pmc1*	GAACCCACATCTCCCAAC
OL1295	*pmc1*	GAGTTGTTGAGTAGGTGG
OL1296	*pmc1*	CGGAGATTGGATAACAAG
OL1297	*pmc1*	GCACCTCCGAAAAAAACAA
OL1298	*pmc1*	TCGACTGACCAAAGCTCT
OL1299	*pmc1*	TCTCAGGTTTCCTCTTTAACAC
OL1300	*pmc1*	TTGCACGCTCATCTCCTT
OL1301	*pmc1*	CTTTTTTTAGTGCAGGCG
OL1302	*pmc1*	TCCCAAAGATATTCCCACCA
OL1303	*pmc1*	GTCAAACACACGATAGCAT
OL1304	*pmc1*	ACTTCGGGACTTAACTCT
OL1305	*pmc1*	CCTTGGGGTGTCAGAATTA
OL1306	*pmc1*	AGAACAAGGGTCAAGAGT
OL1307	*pmc1*	AGCAAAAGCCAAAGCCAA
OL1308	*pmc1*	GAAAGAACATCGCCGGAC
OL1309	*pmc1*	AATTAACACCGACAGCAG
OL1310	*pmc1*	GTGTCGAATGGGTGGAAG
OL1311	*pmc1*	CAGTCATTCACACCACCCA
OL1312	*pmc1*	ATTTCTACTCACGAACCTCA
OL1313	*pmc1*	CTCATCTGCAATTTATCGGC
OL1314	*pmc1*	TTCCTCGGTGTTCCTTCT
OL1315	*pmc1*	CCACTTCGAGAGCTATTT
OL1316	*pmc1*	TCTCCTCTTCATCTTCTCTT

Table S3. Sensitivity of the 12 mutant strains (P) to various agents												
Strain name	**18 °C**	**25 °C**	**32 °C**	**37 °C**	**Sorbitol 2M**	**HU 4 mM**	**SDS 0.01%**	**TBZ 15 µg/ mL**	**KCl 0.8 M**	**Ca(NO3)2 0.15 M**	**CaCl2 0.3 M**	**gene asociated with the phenotype**
PB1623	+	+	+	+	+	+	+	+	+	+	+	WT
1P	+	+	+	+	+	NA	--	--	+	--	--	*pmc1*
2P	+	+	+	+/-	+	+	--	--	+	--	--	*pmc1*
3P	-	+	+	+	+	-	+	+/-	+	+	+	*sgf73*
4P	-	+	+	+	+	--	+	+	+	+	+	*sgf73*
5P	-	+	+	+	+	--	+	+	+	+	+	*sgf73*
6P	+	+	+	--	+	+	+	--	+	+	+	*sty1*
7P	-	+	+	+	+	--	+	+	+	+	+	*sgf73*
8P	+	+	+	+	+	+	--	--	+	--	--	*pmc1*
9P	+	+	+	--	+	+	+	+	+/-	+	+	*win1*
10P	+/-	+	+	--	+	+	+	+	+	NA	NA	*cut1* + *qcr6* (ND)
11P	--	+/-	+	--	+/-	+	+	+	+	NA	NA	SPCC14G10.04
12P	--	+	+	--	+	+	+	+	+	NA	NA	SPCC569.02c + *meu23* (ND)

Table S4

Table S4. Mutations identified in the targeted resequencing experiment									
Sample	**Mutation type**	**Gene**	**cDNA**	**Frequiency**	**Ref**	**VarAllele**	**Mutation**	**time in quiescence**	**P-value < 0.05**
culture_0	Insertion	*sgf73*	896	0,9%	T	+A	+T	2_months	9,69E-23
culture_0	Insertion	*win1*	394	0,2%	T	+CTACTACATCCTC	+CTACTACATCCTC	2_months	2,96E-02
culture_0	Insertion	*win1*	1273	0,3%	A	+TATCCTTCACGTCGTTC	+TATCCTTCACGTCGTTC	2_months	2,44E-02
culture_0	Insertion	*mkh1*	640	13,0%	G	+T	+A	2_months	0,00E+00
culture_0	SNP	*mkh1*	959	1,4%	A	G	T>C	2_months	1,13E-43
culture_0	SNP	*mkh1*	1885	0,2%	A	G	T>C	2_months	4,80E-02
culture_0	SNP	*mkh1*	2914	0,4%	A	G	T>C	2_months	3,57E-03
culture_0	SNP	*mkh1*	3351	0,4%	T	A	A>T	2_months	1,32E-14
culture_0	Deletion	*pmk1*	254	0,7%	A	-T	-T	2_months	1,06E-02
culture_0	SNP	*tif452*	251	0,2%	G	T	G>T	2_months	3,25E-05
total = 17.7%									
culture_0	Insertion	*sgf73*	896	4,3%	T	+A	+T	3_months	2,12E-169
culture_0	Insertion	*win1*	394	1,5%	T	+CTACTACATCCTC	+CTACTACATCCTC	3_months	5,40E-80
culture_0	Insertion	*win1*	549	0,3%	T	+GCACAGAGGAC	+GCACAGAGGAC	3_months	1,66E-05
culture_0	Deletion	*win1*	756	0,2%	C	-AG	-AG	3_months	2,20E-02
culture_0	Insertion	*win1*	1158	0,3%	G	+TATGGTTGATGTGC	+TATGGTTGATGTGC	3_months	4,60E-02
culture_0	Insertion	*win1*	1273	1,5%	A	+TATCCTTCACGTCGTTC	+TATCCTTCACGTCGTTC	3_months	6,51E-13
culture_0	Deletion	*win1*	1573	0,7%	C	-A	-A	3_months	2,01E-10
culture_0	SNP	*win1*	2348	0,2%	C	A	C>A	3_months	1,72E-03
culture_0	SNP	*win1*	2556	0,2%	T	G	T>G	3_months	2,89E-02

culture_0	Insertion	*win1*	3010	0,9%	T	+A	+A	3_months	7,55E-65
culture_0	SNP	*sty1*	74	0,6%	G	C	C>G	3_months	1,12E-11
culture_0	SNP	*sty1*	197	0,5%	C	A	G>T	3_months	6,15E-12
culture_0	Insertion	*mkh1*	640	9,0%	G	+T	+A	3_months	6,41E-291
culture_0	SNP	*mkh1*	959	0,9%	A	G	T>C	3_months	2,07E-29
culture_0	Insertion	*pmk1*	1091	0,3%	C	+CAACAAACCCAACAGTCAACATCCCG	+CAACAAACCCAACAGTCAACATCCCG	3_months	2,80E-05
culture_0	SNP	*tif452*	251	0,7%	G	T	G>T	3_months	2,11E-40
total = 22.1%									
culture_1	Insertion	*win1*	1273	0,3%	A	+TATCCTTCACGTCGTTC	+TATCCTTCACGTCGTTC	2_months	1,73E-02
culture_1	Insertion	*win1*	3010	0,9%	T	+A	+A	2_months	3,13E-79
culture_1	Insertion	*sty1*	216	0,4%	C	+TTTAATAGT	+ACTATTAAA	2_months	5,70E-13
culture_1	SNP	*sty1*	647	1,1%	C	G	G>C	2_months	5,47E-18
culture_1	SNP	*mkh1*	639	1,9%	T	C	A>G	2_months	7,29E-63
culture_1	Insertion	*mkh1*	640	21,3%	G	+T	+A	2_months	0,00E+00
culture_1	SNP	*mkh1*	2378	0,8%	G	C	C>G	2_months	1,97E-36
culture_1	SNP	*mkh1*	3138	0,3%	T	G	A>C	2_months	8,15E-08
culture_1	Deletion	*mkh1*	3236	1,6%	A	-GCATTCACAGTAAAGCAT	-ATGCTTTACTGTGAATGC	2_months	1,34E-102
culture_1	SNP	*pmk1*	497	1,2%	G	T	G>T	2_months	1,13E-27
total = 29.8%									
culture_1	SNP	*win1*	2666	1,2%	C	T	C>T	3_months	3,02E-59
culture_1	Insertion	*win1*	3010	1,2%	T	+A	+A	3_months	2,62E-56
culture_1	Insertion	*sty1*	216	1,8%	C	+TTTAATAGT	+ACTATTAAA	3_months	6,60E-52
culture_1	Insertion	*mkh1*	640	10,2%	G	+T	+A	3_months	4,73E-234

culture_1	Deletion	*mkh1*	3236	0,2%	A	-GCATTCACAGTAAAGCAT	-ATGCTTTACTGTGAATGC	3_months	1,91E-03
culture_1	SNP	*pmk1*	577	6,1%	T	G	T>G	3_months	5,94E-146
total = 20.7%									
culture_2	Insertion	*sgf73*	896	9,6%	T	+A	+T	2_months	0,00E+00
culture_2	Insertion	*win1*	393	0,6%	A	+TCTACTACATCCT	+TCTACTACATCCT	2_months	7,32E-19
culture_2	SNP	*win1*	811	0,8%	C	A	C>A	2_months	5,50E-38
culture_2	Deletion	*win1*	2339	0,8%	T	-ACGTA	-ACGTA	2_months	6,53E-18
culture_2	SNP	*win1*	2379	0,3%	T	G	T>G	2_months	5,01E-10
culture_2	SNP	*sty1*	188	3,7%	C	G	G>C	2_months	1,30E-146
culture_2	SNP	*mkh1*	250	4,7%	C	A	G>T	2_months	2,41E-227
culture_2	Insertion	*mkh1*	640	27,0%	G	+T	+A	2_months	0,00E+00
culture_2	Insertion	*mkh1*	2517	1,2%	A	+TACCTTACCATAAG	+CTTATGGTAAGGTA	2_months	2,19E-34
culture_2	SNP	*mkh1*	3145	0,2%	C	A	G>T	2_months	1,06E-02
culture_2	Deletion	*pmk1*	251	1,7%	T	-A	-A	2_months	2,26E-24
culture_2	SNP	*pmk1*	592	2,5%	G	A	G>A	2_months	3,35E-100
culture_2	Deletion	*pmk1*	1097	10,4%	A	-ACCCAACAGTCAACAT	-ACCCAACAGTCAACAT	2_months	2,58E-317
culture_2	Insertion	*pmc1*	2441	1,2%	G	+CAGTAACAATATTATCAC	+GTGATAATATTGTTACTG	2_months	8,66E-12
total = 64.7%									
culture_2	Insertion	*sgf73*	896	43,5%	T	+A	+T	3_months	0,00E+00
culture_2	Deletion	*win1*	2339	0,2%	T	-ACGTA	-ACGTA	3_months	1,75E-04
culture_2	SNP	*sty1*	188	0,7%	C	G	G>C	3_months	5,97E-27
culture_2	Insertion	*mkh1*	640	5,3%	G	+T	+A	3_months	1,39E-199
culture_2	SNP	*pmk1*	592	2,7%	G	A	G>A	3_months	2,86E-100

total = 52,4%									
culture_3	Insertion	*win1*	383	0,5%	G	+ATACTAGTAAT	+ATACTAGTAAT	2_months	1,12E-15
culture_3	Insertion	*win1*	394	1,6%	T	+CTACTACATC	+CTACTACATC	2_months	1,15E-77
culture_3	Deletion	*win1*	504	1,7%	C	-A	-A	2_months	1,00E-162
culture_3	Deletion	*win1*	556	0,6%	A	-G	-G	2_months	2,48E-19
culture_3	Insertion	*win1*	1273	0,6%	A	+TATCCTTCACGTCGTTC	+TATCCTTCACGTCGTTC	2_months	8,84E-07
culture_3	SNP	*win1*	1859	0,6%	C	T	C>T	2_months	2,15E-18
culture_3	Deletion	*win1*	2363	3,8%	G	-TTGATTCCCCTAA	-TTGATTCCCCTAA	2_months	0,00E+00
culture_3	Deletion	*win1*	2545	0,7%	C	-CGTT	-CGTT	2_months	3,27E-26
culture_3	Insertion	*win1*	2768	0,7%	A	+ATCTAAAATTAAGATTAAAGCTGGAATTAAAGTCCAAATGAATTCAACAATTG	+ATCTAAAATTAAGATTAAAGCTGGAATTAAAGTCCAAATGAATTCAACAATTG	2_months	2,24E-25
culture_3	Deletion	*win1*	3680	3,5%	C	-A	-A	2_months	1,28E-90
culture_3	SNP	*win1*	4179	0,2%	G	T	G>T	2_months	1,29E-04
culture_3	Deletion	*mkh1*	236	1,2%	A	-T	-A	2_months	3,22E-58
culture_3	Insertion	*mkh1*	640	15,8%	G	+T	+A	2_months	0,00E+00
culture_3	Complex	*mkh1*	1884	0,2%	G	A	CT>TG	2_months	4,53E-04
culture_3	Insertion	*mkh1*	2254	0,7%	G	+A	+T	2_months	1,15E-03
culture_3	SNP	*mkh1*	3124	0,2%	C	A	G>T	2_months	2,59E-02
culture_3	SNP	*mkh1*	3137	0,5%	A	C	T>G	2_months	4,67E-16
culture_3	Deletion	*pmk1*	435	0,7%	T	-TA	-TA	2_months	1,49E-13
culture_3	Insertion	*pmk1*	902	0,2%	A	+GACGTATTTCGGTT	+GACGTATTTCGGTT	2_months	5,64E-03
total = 34.0%									
culture_3	Insertion	*win1*	383	0,2%	G	+ATACTAGTAAT	+ATACTAGTAAT	3_months	1,40E-07
culture_3	Insertion	*win1*	394	1,1%	T	+CTACTACATC	+CTACTACATC	3_months	2,14E-93

culture_3	Deletion	*win1*	504	1,1%	C	-A	-A	3_months	1,14E-153
culture_3	Deletion	*win1*	556	0,7%	A	-G	-G	3_months	3,91E-42
culture_3	Insertion	*win1*	1273	0,2%	A	+TATCCTTCACGTCGTTC	+TATCCTTCACGTCGTTC	3_months	1,78E-02
culture_3	SNP	*win1*	1859	0,8%	C	T	C>T	3_months	5,76E-57
culture_3	Deletion	*win1*	2363	3,8%	G	-TTGATTCCCCTAA	-TTGATTCCCCTAA	3_months	0,00E+00
culture_3	Deletion	*win1*	2545	0,9%	C	-CGTT	-CGTT	3_months	1,55E-60
culture_3	Insertion	*win1*	2768	0,6%	A	+ATCTAAAATTAAGATTAAAGCTGGAATTAAAGTCCAAATGAATTCAACAATTG	+ATCTAAAATTAAGATTAAAGCTGGAATTAAAGTCCAAATGAATTCAACAATTG	3_months	4,17E-36
culture_3	Deletion	*win1*	3680	4,4%	C	-A	-A	3_months	2,17E-146
culture_3	Deletion	*mkh1*	236	1,4%	A	-T	-A	3_months	1,43E-105
culture_3	Insertion	*mkh1*	640	21,5%	G	+T	+A	3_months	0,00E+00
culture_3	Insertion	*mkh1*	2593	0,2%	C	+GGCCATTAATAGTTTGTGGTATTTCAACTTGCTTTACT	+AGTAAAGCAAGTTGAAATACCACAAACTATTAATGGCC	3_months	2,01E-03
culture_3	Deletion	*mkh1*	3340	1,2%	C	-T	-A	3_months	6,81E-89
culture_3	Deletion	*pmk1*	435	0,3%	T	-TA	-TA	3_months	4,45E-06
culture_3	SNP	*pmc1*	280	0,2%	C	A	G>T	3_months	1,79E-03
total = 38.6%									
subculture_1	Complex	*win1*	357	1.2%	A	-TCGTGCT*T>A*T>A*C>A	-TCGTGCT*T>A*T>A*C>A	2_months	6,00E-213
subculture_1	Insertion	*win1*	394	3.4%	T	+CTACTACATCCTC	+CTACTACATCCTC	2_months	0,00E+00
subculture_1	Insertion	*win1*	397	0.2%	A	+CTACATCCTC	+CTACATCCTC	2_months	6,41E-13
subculture_1	Deletion	*win1*	506	0.2%	A	-AT	-AT	2_months	2,90E-18
subculture_1	SNP	*win1*	602	0.2%	C	G	C>G	2_months	3,77E-06

subculture_1	Insertion	*win1*	1273	0.3%	A	+TATCCTTCACGTCGTTC	+TATCCTTCACGTCGTTC	2_months	6,94E-04
subculture_1	SNP	*win1*	2478	1.8%	T	A	T>A	2_months	0,00E+00
subculture_1	Insertion	*win1*	3010	2.5%	T	+A	+A	2_months	0,00E+00
subculture_1	Deletion	*win1*	3305	0.5%	G	-AGAA	-AGAA	2_months	1,55E-72
subculture_1	Insertion	*win1*	3314	0.3%	C	+TA	+TA	2_months	1,62E-35
subculture_1	SNP	*win1*	3319	0.3%	A	G	A>G	2_months	4,13E-31
subculture_1	Insertion	*win1*	3544	0.2%	C	+GTATCGTATTATG	+GTATCGTATTATG	2_months	9,61E-13
subculture_1	Deletion	*win1*	3752	0.3%	C	-TT	-TT	2_months	5,54E-06
subculture_1	SNP	*win1*	4195	0.3%	G	T	G>T	2_months	2,85E-31
subculture_1	SNP	*wis1*	868	1.6%	C	G	G>C	2_months	0,00E+00
subculture_1	SNP	*wis1*	1108	3.4%	A	C	T>G	2_months	0,00E+00
subculture_1	SNP	*wis1*	1493	0.3%	T	C	A>G	2_months	4,84E-14
subculture_1	Insertion	*wis1*	1740	1.0%	T	+A	+T	2_months	1,94E-57
subculture_1	SNP	*sty1*	562	0.2%	A	G	T>C	2_months	5,44E-06
subculture_1	Insertion	*mkh1*	640	0.6%	G	+T	+A	2_months	2,15E-57
subculture_1	SNP	*tif452*	390	4.3%	G	T	G>T	2_months	0,00E+00
total = 23.1%									
subculture_2	Insertion	*win1*	394	2.4%	T	+CTACTACATCCTC	+CTACTACATCCTC	2_months	0,00E+00
subculture_2	SNP	*win1*	1100	1.0%	G	A	G>A	2_months	4,16E-206
subculture_2	Insertion	*win1*	1273	0.6%	A	+TATCCTTCACGTCGTTC	+TATCCTTCACGTCGTTC	2_months	2,96E-32
subculture_2	SNP	*win1*	2519	0.4%	C	A	C>A	2_months	1,50E-57
subculture_2	Deletion	*win1*	3489	1.1%	T	-C	-C	2_months	1,62E-131
subculture_2	Deletion	*win1*	3833	0.2%	G	-AACAGTT	-AACAGTT	2_months	2,25E-09
subculture_2	SNP	*wis1*	1380	4.6%	A	T	T>A	2_months	0,00E+00
subculture_2	SNP	*wis1*	1511	1.0%	A	C	T>G	2_months	5,00E-286

subculture_2	SNP	*sty1*	553	12.5%	T	A	A>T	2_months	0,00E+00
total = 23.8%									
subculture_3	Deletion	*win1*	292	0.6%	A	-CAGCCTC	-CAGCCTC	2_months	1,59E-79
subculture_3	Insertion	*win1*	394	0.4%	T	+CTACTACATCCTC	+CTACTACATCCTC	2_months	8,93E-42
subculture_3	Deletion	*win1*	1007	0.2%	C	-GATCT	-GATCT	2_months	1,32E-07
subculture_3	Insertion	*win1*	1273	1.8%	A	+TATCCTTCACGTCGTTC	+TATCCTTCACGTCGTTCC	2_months	2,71E-84
subculture_3	Deletion	*win1*	1365	0.8%	A	-TG	-TG	2_months	1,12E-31
subculture_3	Deletion	*win1*	1846	0.8%	A	-T	-T	2_months	7,47E-185
subculture_3	Deletion	*win1*	1877	1.6%	A	-T	-T	2_months	0,00E+00
subculture_3	Insertion	*win1*	2179	1.8%	C	+TTCCGAAAATTGATGAG	+TTCCGAAAATTGATGAG	2_months	2,01E-31
subculture_3	Insertion	*win1*	3010	2.8%	T	+A	+A	2_months	0,00E+00
subculture_3	Insertion	*win1*	3105	0.7%	G	+T	+T	2_months	7,29E-41
subculture_3	Insertion	*win1*	3716	0.6%	G	+T	+T	2_months	2,92E-27
subculture_3	Insertion	*win1*	3880	0.6%	A	+T	+T	2_months	4,28E-24
subculture_3	SNP	*win1*	4177	0.5%	C	T	C>T	2_months	3,36E-91
subculture_3	SNP	*wis1*	944	9.2%	A	C	T>G	2_months	0,00E+00
subculture_3	Complex	*wis1*	1281	8.5%	GG	AA	AA	2_months	0,00E+00
subculture_3	SNP	*wis1*	1329	0.4%	T	A	A>T	2_months	1,91E-24
subculture_3	Insertion	*wis1*	1740	6.2%	T	+A	+T	2_months	0,00E+00
subculture_3	SNP	*sty1*	1	1.0%	T	C	A>G	2_months	5,77E-103
subculture_3	SNP	*sty1*	481	3.5%	C	A	G>T	2_months	0,00E+00
subculture_3	SNP	*sty1*	535	1.4%	A	G	T>C	2_months	0,00E+00
subculture_3	Insertion	*mkh1*	640	1.0%	G	+T	+A	2_months	1,76E-144
subculture_3	SNP	*mkh1*	1885	0.2%	A	G	T>C	2_months	8,16E-08
subculture_3	Deletion	*pmc1*	1296	0.1%	T	-TCTG	-CAGA	2_months	2,32E-02

total = 43.4%									
subculture_4	Deletion	*win1*	241	0.2%	C	-AAGGCGAGCGCCAAAGAGGACTTATTTTCAGAAGCTTTCAGAATGGCTG	-AAGGCGAGCGCCAAAGAGGACTTATTTTCAGAAGCTTTCAGAATGGCTG	2_months	8,39E-19
subculture_4	Insertion	*win1*	394	0.5%	T	+CTACTACATCCTC	+CTACTACATCCTC	2_months	4,48E-52
subculture_4	Deletion	*win1*	2982	2.4%	C	-AT	-AT	2_months	3,69E-312
subculture_4	Insertion	*win1*	3010	0.8%	T	+A	+A	2_months	3,73E-83
subculture_4	Deletion	*win1*	3045	1.2%	G	-A	-A	2_months	1,68E-129
subculture_4	Deletion	*win1*	3050	0.8%	T	-G	-G	2_months	1,17E-71
subculture_4	Deletion	*win1*	3097	0.2%	T	-GC	-GC	2_months	5,36E-04
subculture_4	Deletion	*win1*	3352	3.6%	G	-ATTCGA	-ATTCGA	2_months	0,00E+00
subculture_4	Deletion	*win1*	3374	0.6%	C	-TTATAGGTAGCGGTTCT	-TTATAGGTAGCGGTTCT	2_months	2,16E-77
subculture_4	Insertion	*win1*	3507	0.5%	A	+AATGTTAGTACTTGAACTCTTTGATCATCCT	+AATGTTAGTACTTGAACTCTTTGATCATCCT	2_months	5,87E-53
subculture_4	Deletion	*win1*	3617	0.5%	C	-TTTTCGAATTTCTACG	-TTTTCGAATTTCTACG	2_months	7,73E-52
subculture_4	Deletion	*win1*	3618	0.2%	T	-TTTCGAA	-TTTCGAA	2_months	1,13E-16
subculture_4	Deletion	*win1*	3682	0.8%	A	-T	-T	2_months	5,36E-49
subculture_4	Deletion	*win1*	3817	0.3%	T	-TC	-TC	2_months	1,06E-09
subculture_4	SNP	*wis1*	1588	1.9%	A	C	C	2_months	0,00E+00
subculture_4	Insertion	*wis1*	1740	1.2%	T	+A	+A	2_months	2,56E-167
subculture_4	SNP	*sty1*	35	1.0%	G	C	C	2_months	3,24E-122
subculture_4	Insertion	*mkh1*	640	1.6%	G	+T	+T	2_months	7,16E-247
subculture_4	Insertion	*mkh1*	2396	0.8%	G	+C	+C	2_months	2,87E-157
subculture_4	Insertion	*mkh1*	2846	0.2%	T	+TTAGA	+TTAGA	2_months	4,00E-02

subculture_4	SNP	*mkh1*	3152	0.2%	T	C	C	2_months	1,93E-06
total = 19.5%									
subculture_5	Deletion	*win1*	314	0.7%	A	-C	-C	2_months	5,12E-95
subculture_5	Deletion	*win1*	370	0.2%	C	-GTAA	-GTAA	2_months	2,78E-08
subculture_5	Insertion	*win1*	394	4.0%	T	+CTACTACATCCTC	+CTACTACATCCTC	2_months	0,00E+00
subculture_5	Deletion	*win1*	942	0.7%	C	-A	-A	2_months	6,42E-94
subculture_5	Deletion	*win1*	1024	2.0%	G	-C	-C	2_months	0,00E+00
subculture_5	SNP	*win1*	1129	0.4%	A	T	A>T	2_months	1,33E-45
subculture_5	SNP	*win1*	1251	0.2%	A	G	A>G	2_months	1,47E-02
subculture_5	Deletion	*win1*	1258	0.9%	T	-A	-A	2_months	3,32E-54
subculture_5	Deletion	*win1*	1265	2.4%	G	-AACGT	-AACGT	2_months	2,37E-189
subculture_5	Insertion	*win1*	1273	0.8%	A	+TATCCTTCACGTCGTTC	+TATCCTTCACGTCGTTC	2_months	1,43E-37
subculture_5	Deletion	*win1*	2376	0.2%	A	-TATACT	-TATACT	2_months	8,56E-05
subculture_5	Insertion	*win1*	3010	1.8%	T	+A	+A	2_months	0,00E+00
subculture_5	Deletion	*win1*	3142	0.2%	C	-CTTGTTCGAAATAATTCCGACCGAAGTCGTTTAT	-CTTGTTCGAAATAATTCCGACCGAAGTCGTTTAT	2_months	3,77E-03
subculture_5	Deletion	*win1*	3407	0.5%	C	-GT	-GT	2_months	6,46E-59
subculture_5	Deletion	*win1*	3626	0.3%	T	-TTCTACGTTAC	-TTCTACGTTAC	2_months	4,45E-26
subculture_5	Insertion	*win1*	3922	0.3%	A	+GGAACACCTACGTATAT	+GGAACACCTACGTATAT	2_months	1,44E-09
subculture_5	SNP	*win1*	4177	0.9%	C	T	C>T	2_months	1,02E-204
subculture_5	SNP	*wis1*	1088	1.0%	A	C	T>G	2_months	5,31E-116
subculture_5	SNP	*wis1*	1182	5.2%	A	C	T>G	2_months	0,00E+00
subculture_5	SNP	*wis1*	1427	0.7%	C	G	G>C	2_months	5,14E-50
subculture_5	SNP	*wis1*	1430	0.2%	C	T	G>A	2_months	2,63E-02

subculture_5	SNP	*sty1*	545	13.2%	G	A	C>T	2_months	0,00E+00
subculture_5	SNP	*sty1*	558	1.4%	T	G	A>C	2_months	0,00E+00
subculture_5	SNP	*sty1*	646	0.7%	C	T	G>A	2_months	9,02E-130
subculture_5	SNP	*sty1*	659	10.2%	A	T	T>A	2_months	0,00E+00
subculture_5	Insertion	*mkh1*	640	1.6%	G	+T	+A	2_months	0,00E+00
subculture_5	Deletion	mkh1	3302	0.2%	G	-TTGAATTCT	-AGAATTCAA	2_months	2,16E-06
total = 50.9%									
subculture_6	Deletion	*win1*	292	0.8%	A	-CAGCCTC	-CAGCCTC	2_months	8,24E-121
subculture_6	Insertion	*win1*	394	4.5%	T	+CTACTACATCCTC	+CTACTACATCCTC	2_months	0,00E+00
subculture_6	Insertion	*win1*	397	1.4%	A	+CTACATCCTC	+CTACATCCTC	2_months	5,06E-294
subculture_6	Deletion	*win1*	666	0.6%	G	-A	-A	2_months	7,66E-43
subculture_6	Deletion	*win1*	972	0.7%	A	-TATGTTGACTTCAGTTC	-TATGTTGACTTCAGTTC	2_months	8,61E-99
subculture_6	Deletion	*win1*	1253	0.5%	C	-TTGA	-TTGA	2_months	8,32E-13
subculture_6	Insertion	*win1*	1273	0.4%	A	+TATCCTTCACGTCGTTC	+TATCCTTCACGTCGTTC	2_months	5,44E-06
subculture_6	Deletion	*win1*	1644	0.6%	A	-T	-T	2_months	5,80E-08
subculture_6	Deletion	*win1*	1681	0.8%	C	-A	-A	2_months	6,91E-152
subculture_6	SNP	*win1*	1749	0.9%	C	T	C>T	2_months	5,12E-184
subculture_6	Deletion	*win1*	1905	1.0%	T	-C	-C	2_months	8,92E-195
subculture_6	Insertion	*win1*	2313	4.8%	C	+G	+G	2_months	0,00E+00
subculture_6	Insertion	*win1*	2512	0.7%	G	+GA	+GA	2_months	1,57E-68
subculture_6	SNP	*win1*	2762	2.2%	C	T	C>T	2_months	0,00E+00
subculture_6	Insertion	*win1*	3010	1.1%	T	+A	+A	2_months	2,47E-254
subculture_6	Insertion	*win1*	3105	1.2%	G	+TA	+TA	2_months	4,04E-96
subculture_6	Deletion	*win1*	3401	1.2%	G	-T	-T	2_months	4,04E-182

subculture_6	Insertion	*win1*	3507	1.2%	A	+AATGTTAGTACTTGAACTCTTTGATCATCCT	+AATGTTAGTACTTGAACTCTTTGATCATCCT	2_months	1,95E-173
subculture_6	SNP	*win1*	3546	1.2%	C	A	C>A	2_months	7,68E-165
subculture_6	Deletion	*win1*	3551	1.1%	T	-A	-A	2_months	5,04E-156
subculture_6	Deletion	*win1*	3682	1.3%	A	-T	-T	2_months	4,67E-78
subculture_6	Deletion	*win1*	3783	0.4%	C	-AGAT	-AGAT	2_months	8,43E-12
subculture_6	Complex	*win1*	3784	1.0%	T	T>C*-C	-T>C*-C	2_months	1,50E-50
subculture_6	Deletion	*win1*	3816	1.3%	C	-T	-T	2_months	4,48E-71
subculture_6	SNP	*win1*	4177	0.4%	C	T	C>T	2_months	1,27E-48
subculture_6	Insertion	*wis1*	1740	1.2%	T	+A	+T	2_months	4,31E-108
subculture_6	SNP	*sty1*	535	4.8%	A	G	T>C	2_months	0,00E+00
subculture_6	Insertion	*mkh1*	640	2.2%	G	+T	+A	2_months	0,00E+00
subculture_6	SNP	*tif452*	260	1.0%	T	C	T>C	2_months	1,75E-295
subculture_6	SNP	*tif452*	383	0.5%	C	G	C>G	2_months	5,97E-28
total = 41.0%									

Table S5

Table S5 : strains used in this study	
Strain	Relevant genotype
PB1623	*Msmt0*
PB2262	*Msmt0 SPBC31A8.02::mCherry::KanR*
PB2740	*Msmt0 win1-394 +13 bp SPBC31A8.02:: mCherry:KanR*
PB2741	*Msmt0 mkh1-2929 -10 bp SPBC31A8.02::mCherry::KanR*
PB2850	*PΔ17 sty1-G197T SPBC31A8.02::mCherry::KanR*
PB2851	*Msmt0 sty1-C74G SPBC31A8.02::mCherry::KanR*
PB2739	*Msmt0 sgf73-896+T SPBC31A8.02::mCherry::KanR*
PB2532	*Msmt0 sgf73-896+T*
PB2921	*Msmt0 sty1-G197T*
PB2926	*Msmt0 sty1-C74G*
PB2928	*Msmt0 pmk1-153+A*
PB2310	*Msmt0 sty1::ura4+*
PB3242	*Msmt0 mkh1-640+A*
PB2932	*Msmt0 win1-1086-G*
PB2933	*Msmt0 win1-394 +13 bp*
PB2457	*PΔ17 win1::KanR*

DISSCUSSION AND PERSPECTIVES

5 DISCUSSION AND PERSPECTIVES

5.1 Improving mutation calling by amplifying and sequencing an identical pool of colonies twice

5.1.1 How to distinguish a real mutation from a sequencing artifact in the pool of colonies?

Calling low-frequency variants from targeting re-sequencing data is a challenging task which requires both searching for an optimal algorithm for variant calling (NISC Comparative Sequencing Program et al., 2015). Depending on the conditions, the error rate produced by MiSeq and HiSeq sequencing (Illumina technology) has been reported to range from ~0.1% (Fox et al., 2014) to 2.6% (May et al., 2015) of misinterpreted nucleotides for substitutions and <0.001% for indels (May et al., 2015). Illumina technology is robust against errors generated during sequencing homopolymeric regions, but nevertheless the error rate is 1000 fold higher compared to that in any random region and reaches 0.2% at 10 nucleotides in length (Minoche et al., 2011). Varscan contains several build-in filters: *strand filter* to ignore variants with >90% support on one strand, *pvalue* – Fisher's Exact Test based on the read counts supporting the reference and the variant allele, *min-avg-qual* - minimum average position to count a read. In order to improve the quality of variant calling, I have developed several new filters: first, I have increased the sensitivity of the filter by discarding variants with >20% distribution on both read. I have considered that a mutation should have similar properties than the reference allele. Thus, I have considered that a mutation should have the same base quality as the reference at a given position. In addition, the proportion of a variant called from the forward (+) and the reverse (-) direction of a paired-end read should be equivalent to that of the reference allele (filter_reads_proportion_indels) (filter_reads_proportion_SNVs).

The sequencing quality can be affected by batch effect. To date, no systematic or heuristic algorithms exist to detect and filter batch effects or even remove associations impacted by batch effects in whole genome sequencing data (Tom et al., 2017). Amplifying and sequencing the same dataset twice increased the quality of the analysis and the mutation detection in 6 subcultures (Figure 24). Discarding the variants that are not present in both sets of sequencing affects only variants present at a minor frequency (<0.5%), while more abundant alleles are always found in both datasets. Applying statistical analysis on the pairs of mutation frequencies called independently from duplicates with Student's t-test provides a p-value >0.05 (in

particular, the minimum p-value was reported for subculture 6 p=0.82), thus allowing discarding the null hypothesis (two sequencing runs are independent of one other, e.g., they have been done on the same pool of colonies) (Figure 25). The difference in frequency per individual allele within the duplicates ranges from 0 to 0.4%, supporting the notion that precise mutation detection at a variant frequency below 0.5% is complicated.

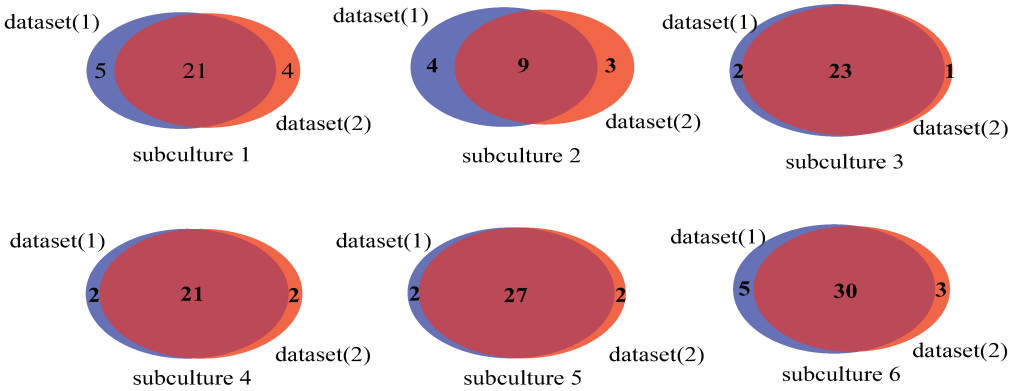

Figure 22: Overlap of the independent experiments.

The Venn diagrams show the number of alleles that are either unique to each individual experiment (red and blue) or shared between 2 sequencing runs within the subcultures (deep purple).

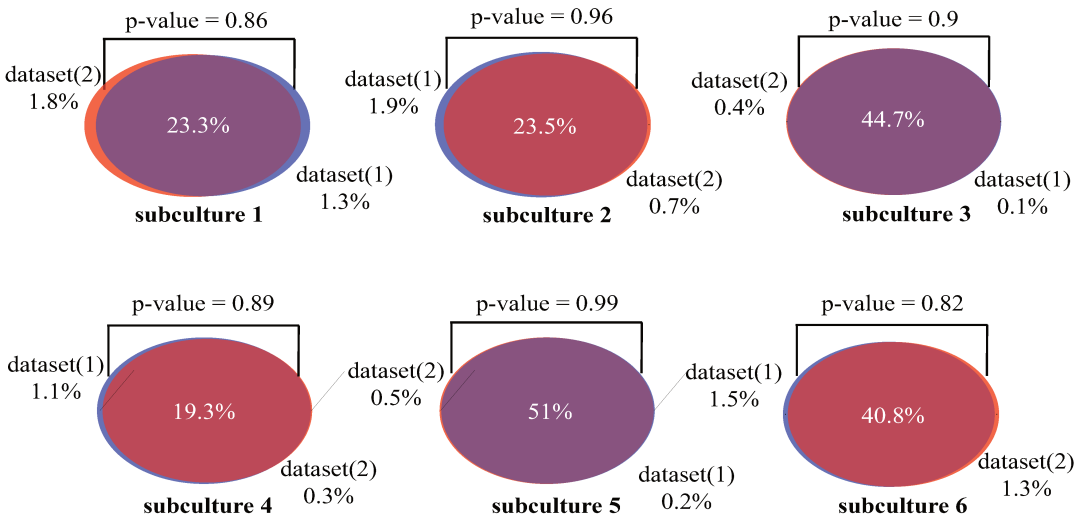

Figure 23: The outliers are at a low frequency and may represent sequencing errors.

The percentage in the middle correspond to the sum of the mean frequency of the shared alleles in the population, whereas those to the edges refer to the sum of the mean frequency of the unique alleles. The p-value was calculated according to the two-tailed Student test. For all the samples, p>0.05, indicating that the datasets are not independent (i.e. they come from the same population).

With this in hand, we can also imagine to amplify and sequence directly the genomic DNA extracted from the quiescnece cells. We predict that any mutations present above 0.5% of the cell population in the pool of the cells can be identify. We leave this issue open for further studies.

5.2 Mutations found in long-term quiescence share similarities with the GASP adaptive mutations *in E. coli*, but differ from the persistence phenotype.

Prior to the decoding of the DNA structure by Watson and Crick in 1954, two hypotheses have existed regarding the origin of mutations. Mutations can arise stochastically and undergo a selection process or appear in response to an environmental influence. In 1943, Luria and Delbrück (Luria and Delbrück, 1943) demonstrated that mutations arise in bacterial cultures before the cells are exposed to selective pressure, thus establishing the dogma that every cell in a culture has a constant probability of acquiring a mutation, and that this probability is independent of any advantage that the mutation confers (Newcombe, 1949). Despite occasional reports on stationary-phase mutations in bacteria (Grigg and Stuckey, 1966; Ryan, 1955), a spontaneous mutation was thought to occur exclusively under defined circumstances: in growing cells (usually measured as mutations per cell per generation) before the cell faces a situation in which the mutation might prove useful and in any gene, irrespective of the usefulness of the mutation.

5.2.1 The GASP Phenotype

Here, I further develop the GASP phenotypes that rapidly stated into the above manuscript. The standard description of the bacterial life cycle consists of three or four phases: lag phase, exponential (logarithmic) phase, stationary phase and death. However, in the laboratory, there are five phases that include an extended (or long-term stationary) phase after the majority of the population (99%) has died (Finkel, 2006) (Figure 26). Unlike the early stationary phase, in which there is little cell division, the long-term stationary phase is a highly dynamic period in which the ‘birth’ and ‘death’ rates are balanced. Experiments focusing on the populations of long-term *E. coli* stationary cultures have uncovered GASP (Growth Advantage in Stationary Phase) a phenomenon in which aged cells from long-term cultures outcompete cells from younger cultures (Zambrano et al., 1993).

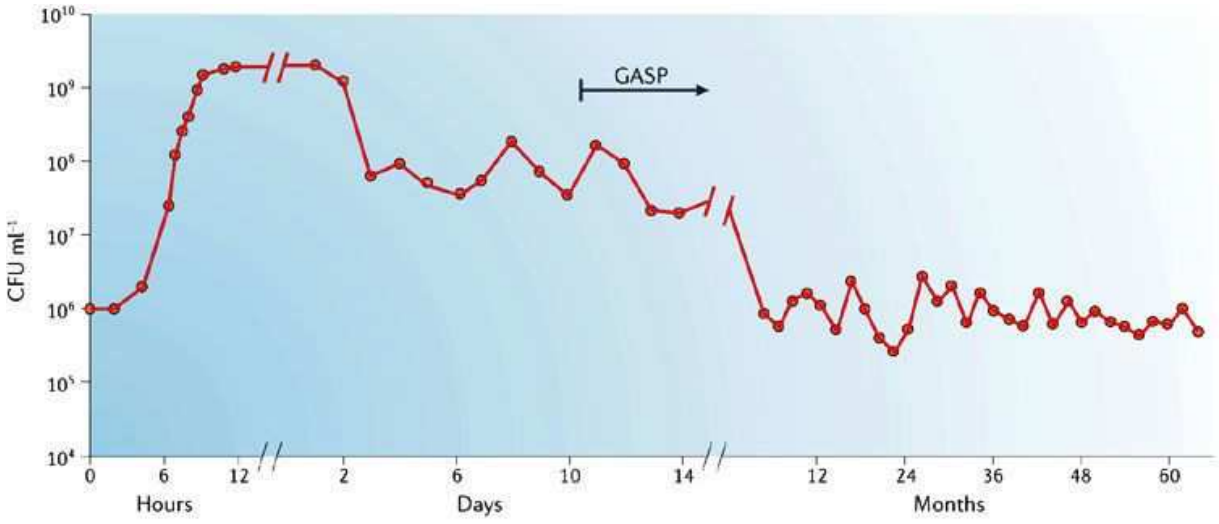

Figure 24: The overview of a GASP experiment (Finkel, 2006).

The five phases of the bacterial life cycle. Once bacteria are inoculated into fresh medium, there is an initial lag period followed by exponential-phase growth. After remaining at high density for 2 or 3 days, cells enter death phase. After ~99% of the cells die, the survivors can be maintained under long-term stationary-phase culture conditions for months or years. The arrow indicates the time after which cells expressing the growth advantage in stationary phase (GASP) phenotype are observed.

In a typical GASP experiment, a sample of *E. coli* incubated aerobically in LB medium for 10 days at 37 °C is transferred into a culture of 1-day-old cells (usually a 1:1000 ratio). Within a few days, the minority of aged cells will increase in number, with a concomitant reduction in the number of 'young' cells (Zambrano et al., 1993). By regularly providing distilled water to maintain the volume and osmolarity, aerobically grown cultures can be maintained at densities of ~10^6 CFU per ml for more than five years with no addition of nutrients. The defining characteristic of GASP strains is their ability to confer growth under starvation conditions to a subpopulation when the rest of the population remains static or is in decay.

The competitive advantage of cells expressing the GASP phenotype is genetically determined and is not due to physiological adaptation to the stationary-phase environment or due to epigenetic factors (Zambrano et al., 1993). Subsequently, 4 genes responsible for the GASP phenotype have been identified: *rpoS* (general stress response factor – functional analog of the MAPK stress response factors), *lrp*, which mediates a global response to leucine, probably in cooperation with the stringent response (Traxler et al., 2008). Both genes, *rpoS* and *lrp*, coordinate metabolic and physiological responses to environmental stress by co-regulating genes of related function (e.g., selection favors pleiotropic mutations that have a higher fitness potential). Additional mutations were mapped in the *ybeJ–gltJKL* cluster encoding high-affinity

aspartate and glutamate transporters, respectively. Although each of these genes is involved in different processes, each GASP mutation results in an increased ability to catabolize one or more amino acids (Finkel and Kolter, 1999; Zambrano et al., 1993). Similarly, the adaptive mutations affecting amino-acid metabolism has been identified in *spoT*, the gene that regulates the concentration of the effector molecule ppGpp (Cooper et al., 2003), under low glucose growth.

Since mutations arising during GASP affect amino-acid metabolism, it has been proposed that GASP-mutations are forcing scavenging during prolonged periods of starvation in the stationary phase. Indeed, it has been demonstrated that GASP mutants grow by outcompeting their parents on amino acid sources (Zinser and Kolter, 1999). Interestingly, a recent report demonstrates that *E. coli* consumes DNA during starvation, and mutants that cannot consume DNA suffer a significant fitness loss (Finkel and Kolter, 2001).

The type of mutation that arises during the stationary phase is a partial loss of function. Thus, the *lrp* GASP allele when overexpressed behaves as a dominant negative and forms inactive multimers when mixed with wild-type proteins (Zinser and Kolter, 2000). If any loss-of-function allele can confer the GASP phenotype, then recessive mutations should occur at a higher frequency in the population. Due to the presence of the wild-type products of the gene produced prior to the mutation, the effect of the mutation will not manifest immediately in the cell, while dominant mutation will exert their effect more rapidly after their products are made, and therefore give them a head start in the population. As an alternative explanation, partial loss of function could be due to the necessity to maintain some of the function to retain viability in the non-dividing stage.

(Zinser and Kolter, 2004) have considered the possibility of how dominant or recessive mutation arise in conditions of long-term stationary phase. The mutation rate will favor the appearance of recessive over dominant mutations. On the contrary, the phenotypic lag of the adaptive mutations will support dominant mutations. Finally, stochastic death due to fitness-independent factors in the population will promote dominant mutations as well. To sum up, selection may bolster dominant mutations over recessive ones due to the influence of the phenotypic lag.

The pathways that generate mutations in GASP cells could be similar to those implicated in the formation of Lac revertants. Two models have been developed to explain the origin of the

GASP mutations. One model proposes that MMR, or perhaps the very short patch repair (VSR) system (Bhagwat and Lieb, 2002; Macintyre et al., 1999) will handle the lesion. However, since it cannot determine the old from the new strand, half of the time the wrong strand will be repaired, leading to mutations. Just like a deficient MMR accumulates mutations, mutagenic SOS polymerases can also introduce genetic diversity and induce a hypermutable state (Yeiser et al., 2002).

Therefore, the formation of persistent cells in budding yeast by DNA damage could involve a similar path (activation of the stress-response pathway, resistance to a variety of stress, accumulation of the mutations) to the persistence formation in the context of the SOS response in prokaryotes. The phenomenon described in this study is the opposite of persistence and is similar to GASP. Persister cells are a small subpopulation of non-dividing or slow-dividing cells in a growing population that acquires resistance to severe stress and under conditions that favor the activation of stress response signaling pathways. In long-term fission yeast quiescence and bacterial GASP, the stress response pathways are downregulated and a small subpopulation of cells acquires the ability to proliferate, while the majority of the population declines.

Mutations in the SAP/MAP-kinase stress-response pathway in fission yeast results in a similar behavior to that reported for GASP mutants in *E. coli*. They appear at a low frequency in the population during the non-growing stage. Since the majority of the population dies, nutrients are released and selection favors mutants with an enhanced ability to scavenge these nutrients. Which component of the dead cells released in the medium is taken up by the mutants is a complicated question. Amino-acids (Zinser and Kolter, 1999; Zinser et al., 2003) or DNA (Finkel and Kolter, 2001) have been proposed.

RpoS, the general stress-response factor in bacteria has been reported as responsible for the generation of the phenotypic diversity in aging colonies in *E. coli* (Saint-Ruf et al., 2014) via island formation. In standard LB liquid medium, 16 isolates showed a growth rate comparable to that of the parental strain, and 9 isolates grew significantly more slowly demonstrating that a gain of fitness in non-dividing conditions may result in fitness loss during growth. Island formation was shown to be a genetically controlled process, in that it is regulated by the RpoS sigma factor.

The major type of mutations in quiescent fission yeast is insertions or deletions of 1 nucleotide. This mutation signature is similar to that observed in bacterial stress-induced mutations or

adaptive mutations. Stress-induced mutagenesis is a process in which cells upregulate their mutation rate in response to stress while adaptive mutations is a phenomenon during which beneficial mutations appear at a higher rate under a non-lethal selection process.

Adaptive mutations were first described by (Shapiro, 1984) supported by (Cairns et al., 1988) in a system where bacteriophage Mu is inserted in a fusion between the *ara* promoter and the *lac* operon in *E. coli*. Incubation for several days with arabinose and lactose (but not with either alone) led to the frequent excision of Mu and hence to colonies that could grow on this medium at a higher frequency than would be expected by spontaneous mutagenesis. The best-studied assay to investigate adaptive mutations was developed in Foster's lab in the experiments with lactose revertants in *E. coli* (Cairns and Foster, 1991)}. In this system, *E. coli* contains a lacZ gene on an episome with a frameshift insertion that makes it is unable to grow on a medium lacking lactose. In the typical adaptive experiment, Lac- cells are plated on lactose minimum medium from the second day of the incubation, and Lac+ revertants start to appear. The revertants contain almost exclusively a +1-nucleotide insertion in a homopolymeric run. (Davis, 1989) has demonstrated that transcription induced by the substrate introduces a bias in the random process of mutation, because the resulting single-stranded region of DNA is more mutable. The major difference of adaptive and spontaneous mutations is that they appear with time while the total number of cells does not change.

In quiescent *S. pombe* cells, insertion or deletion of one nucleotide were also a very frequent event. Out of the 199 mutations detected in the 9 re-sequenced genes, 54 were either insertion or deletion of 1 nucleotide (27.1%). Among the 5 “hotspot” mutations (*win1*-394+13 bp*, win1*-1273+17 bp, *mkh1*-640+A, *sgf73*-896+T, *win1*-3010+A) that have been reported from the first batch of sequencing (4 independent cultures), 3 are insertion or deletion of one nucleotide. The *mkh1*-640+A mutation was found in all four cultures, *sgf73*-896+T in cultures 0 and 2, *win1*-3010+A in cultures 0 and 1.

There are several lines of evidence indicating that Lac adaptive mutation originates from non-dividing cells. (Foster and Trimarchi, 1994; Rosenberg et al., 1994) show that the sequence of Lac adaptive mutations differs from growth-dependent Lac reversions. Several mechanisms and models have been proposed to explain the origin of adaptive mutations, but the main hypothesis claims that 85% of the adaptive mutations described so far are RpoS-dependent. Although the expression of RpoS-dependent genes aims to protect the cell, it is also responsible for increasing

the mutation rate in stress situations by repressing mismatch repair (MMR) and inducing the error-prone DNA polIV. Also, it has been reported that mutant cells lacking any of the SOS DNA polymerases (PolIV, PolV and PolII) do not acquire the GASP phenotype (Yeiser et al., 2002).

Implication of DNA-repair mechanisms could be under the control of the SOS response induced after DNA damage or inhibition of DNA replication. Induction of the SOS response derepresses at least 42 genes usually repressed by the transcriptional repressor LexA, that function in DNA repair, recombination, mutation, translesion DNA synthesis and prevention of cell division. In the work of Cairns using LexA mutants resistant to RecA cleavage, a 3-fold reduction in the revertant rate was reported, demonstrating the role of the SOS response in the generation of adaptive mutations (Cairns and Foster, 1991).

Attempts to describe adaptive mutations in eukaryotes are limited to a few budding yeast assays, and a small amount of mechanistic information has been reported. (Baranowska et al., 1995; Greene and Jinks-Robertson, 1999; Hall, 1992; Heidenreich, 1998; Heidenreich and Wintersberger, 1997; 2001; Steele and Jinks-Robertson, 1992). Adaptive mutation experiments using *S. cerevisiae* rely on the starvation for an essential amino acid or nucleobase. Depletion of internal reserves arrests the cell cycle and only cells that have already acquired prototrophy continue to grow. (Steele and Jinks-Robertson, 1992) have examined Lys+ prototrophic revertants in a haploid yeast strain containing a defined *lys2* frameshift mutation. When cells were plated on a medium lacking lysine, Lys+ revertant colonies accumulate in a time-dependent manner in the absence of any detectable increase in cell number. This experiment provides evidence that the phenomenon of adaptive mutations or stress-induced mutations is not limited to prokaryotic systems.

Although there are no direct homologues of the SOS-response mutagenesis mechanism in eukaryotes, there is evidence demonstrating that replication dependent and replication independent mutations are different. Thus, Heidenreich has indicated a difference in the mutational profile of non dividing and growing yeast (Heidenreich and Wintersberger, 1997). Deletion of the genes in the Non-homologous end-joining pathway results in a two-fold reduction in replication independent mutations in haploid cells, with a profile similar to that observed for the lac+ system in *E. coli* (Heidenreich and Wintersberger, 1997).

Adaptive mutations are connected to stress-response kinases in different yeast species. (Payen et al., 2016) have used high-throughput techniques to demonstrate that loss-of-function mutations are enriched in budding yeast haploid cells. A fitness increase of at least 10% was found in mutants of the stress response pathways, including *SGF73* in sulfate-limited conditions and several MAP kinases (*PBS2*, *HOG1*, *SSK2*) in glucose-limited conditions (Payen et al., 2016). The S/MAPK pathways may be part of the global mechanism regulating the genetics of quiescence.

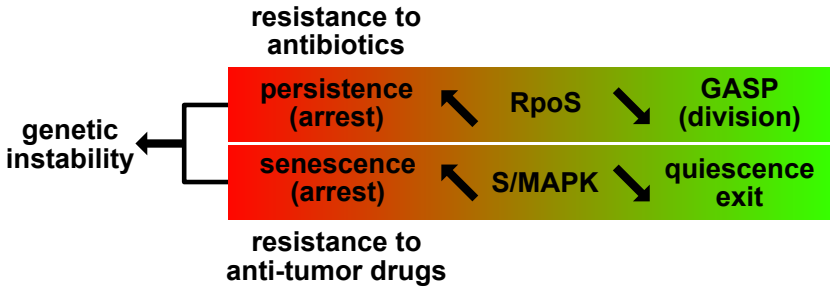

Figure 25: Comparation between the RpoS persistence in bacteria and S/MAPK quiescence in fission yeast.

The green color indicates a low activity of the functional analogues that leads to growth, while the red color points to an elevated activity that results in an arrest that eventually leads to genetic instability.

5.3 Do components of the medium have an impact on quiescence exit?

It is known that the type of nitrogen source used in the medium impacts cell cycle progression in *S. pombe* (Carlson et al., 1999). Moreover, a poor nitrogen source or the addition of rapamycin promotes mitotic onset (Petersen et al., 2007). On the other hand, low doses of glucose can extend the chronological lifespan of fission yeast in the stationary phase by the activation of *sty1*. However, we do not know which function of *sty1* is necessary to maintain quiescence or to confer resistance against apoptosis. In my experiments, I used low-doses of glutamate as a source of nitrogen in glucose-rich medium (4%) to trigger cell exit from quiescence. The idea behind this experiment is to test whether the phenomenon that we have discovered depends on the nutrient source.

Table 7: Components of the medium and the concentration that could impact the fitness of the mutants and wild-type.

Experiment	Nutrition	Concentration
This study	glutamate	0.2 mM
		0.02 mM
	glucose	4%
Quiescnce exit	NH_4Cl	0.2 mM
		0.02 mM
	Yeast extract	0.2 mM
		0.02 mM
Quiescence exit and maintainence	glucose	2%
		0.2%
		0.02%

REFERENCES

6 REFERENCES

Ackermann, M. (2003). Senescence in a Bacterium with Asymmetric Division. Science *300*, 1920–1920.

Adam, A.P., George, A., Schewe, D.M., Bragado, P., Iglesias, B.V., Ranganathan, A.C., Kourtidis, A., Conklin, D.S., and Aguirre-Ghiso, J.A. (2009). Computational Identification of a p38SAPK-Regulated Transcription Factor Network Required for Tumor Cell Quiescence. Cancer Res. *69*, 5664–5672.

Aguirre-Ghiso, J.A. (2007). Models, mechanisms and clinical evidence for cancer dormancy. Nat. Rev. Cancer *7*, 834–846.

Aguirre-Ghiso, J.A., Estrada, Y., Liu, D., and Ossowski, L. (2003). ERK(MAPK) activity as a determinant of tumor growth and dormancy; regulation by p38(SAPK). Cancer Res. *63*, 1684–1695.

Al-Bana, B.H., Haddad, M.T., and Garduño, R.A. (2013). Stationary phase and mature infectious forms of Legionella pneumophilaproduce distinct viable but non-culturable cells. Environ. Microbiol. *16*, 382–395.

Alvarez, B., and Moreno, S. (2006). Fission yeast Tor2 promotes cell growth and represses cell differentiation. Journal of Cell Science *119*, 4475–4485.

Arcangioli, B., and Ben Hassine, S. (2009). Unrepaired oxidative DNA damage induces an ATR/ATM apoptotic-like response in quiescent fission yeast. Cell Cycle *8*, 2326–2331.

Arcangioli, B., 2006 Le réparosome-La replication de l'ADN: pour le meilleur comme pour le pire. Biofutur.

Argüello-Miranda, O., Liu, Y., Wood, N.E., Kositangool, P., and Doncic, A. (2018). Integration of Multiple Metabolic Signals Determines Cell Fate Prior to Commitment. Mol. Cell *71*, 733–744.e11.

Ashrafi, K., Sinclair, D.A., Gordon, J.I., and Guarente, L. (1999). Passage through stationary phase advances replicative aging in Saccharomyces cerevisiae. Pnas *96*, 9100–9105.

Ayrapetyan, M., Williams, T.C., and Oliver, J.D. (2015). Bridging the gap between viable but non-culturable and antibiotic persistent bacteria. Trends Microbiol. *23*, 7–13.

Baharoglu, Z., and Mazel, D. (2014). SOS, the formidable strategy of bacteria against aggressions. FEMS Microbiol. Rev. *38*, 1126–1145.

Banuett, F. (1998). Signalling in the yeasts: An informational cascade with links to the filamentous fungi. Microbiol. Mol. Biol. Rev. *62*, 249–.

Baranowska, H., Policińska, Z., and Jachymczyk, W.J. (1995). Effects of the Cdc2 Gene on Adaptive Mutation in the Yeast Saccharomyces-Cerevisiae. Curr. Genet. *28*, 521–525.

Barba, G., Soto, T., Madrid, M., Nunez, A., Vicente, J., Gacto, M., and Cansado, J. (2008). Activation of the cell integrity pathway is channelled through diverse signalling elements in fission yeast. Cell. Signal. *20*, 748–757.

Baskin, J.M., and Baskin, C.C. (2004). A classification system for seed dormancy. Seed Science Research *14*, 1–16.

Bearson, S., Benjamin, W.H., Swords, W.E., and Foster, J.W. (1996). Acid shock induction of RpoS is mediated by the mouse virulence gene mviA of Salmonella typhimurium. Journal of Bacteriology *178*, 2572–2579.

Beerman, I., Seita, J., Inlay, M.A., Weissman, I.L., and Rossi, D.J. (2014). Quiescent Hematopoietic Stem Cells Accumulate DNA Damage during Aging that Is Repaired upon Entry into Cell Cycle. Cell Stem Cell *15*, 37–50.

Bent, E.H., Gilbert, L.A., and Hemann, M.T. (2016). A senescence secretory switch mediated by PI3K/AKT/mTOR activation controls chemoprotective endothelial secretory responses. Genes Dev. *30*, 1811–1821.

Bernier, S.P., Lebeaux, D., DeFrancesco, A.S., Valomon, A., Soubigou, G., Coppée, J.-Y., Ghigo, J.-M., and Beloin, C. (2013). Starvation, Together with the SOS Response, Mediates High Biofilm-Specific Tolerance to the Fluoroquinolone Ofloxacin. PLoS Genet *9*, e1003144.

Berry, D.B., and Gasch, A.P. (2008). Stress-activated Genomic Expression Changes Serve a Preparative Role for Impending Stress in Yeast. Mol. Biol. Cell *19*, 4580–4587.

Bhagwat, A.S., and Lieb, M. (2002). Cooperation and competition in mismatch repair: very short-patch repair and methyl-directed mismatch repair in Escherichia coli. Mol. Microbiol. *44*, 1421–1428.

Bragado, P., Estrada, Y., Parikh, F., Krause, S., Capobianco, C., Farina, H.G., Schewe, D.M., and Aguirre-Ghiso, J.A. (2013). TGF-β2 dictates disseminated tumour cell fate in target organs through TGF-β-RIII and p38α/β signalling. Nat. Cell Biol. *15*, 1351–1361.

Bragado, P., Sosa, M.S., Keely, P., Condeelis, J., and Aguirre-Ghiso, J.A. (2012). Microenvironments Dictating Tumor Cell Dormancy. In Minimal Residual Disease and Circulating Tumor Cells in Breast Cancer, (Berlin, Heidelberg: Springer Berlin Heidelberg), pp. 25–39.

Branzei, D., and Foiani, M. (2005). The DNA damage response during DNA replication. Current Opinion in Cell Biology *17*, 568–575.

Brewster, J.L., and Gustin, M.C. (2014). Hog1: 20 years of discovery and impact. Science Signaling *7*, re7–re7.

Bulavin, D.V., and Fornace, A.J. (2004). p38 MAP kinase's emerging role as a tumor suppressor. Adv. Cancer Res. *92*, 95–118.

Bulavin, D.V., Amundson, S.A., and Fornace, A.J. (2002). p38 and Chk1 kinases: different conductors for the G(2)/M checkpoint symphony. Curr. Opin. Genet. Dev. *12*, 92–97.

Bulavin, D.V., Phillips, C., Nannenga, B., Timofeev, O., Donehower, L.A., Anderson, C.W., Appella, E., and Fornace, A.J. (2004). Inactivation of the Wip1 phosphatase inhibits mammary tumorigenesis through p38 MAPK–mediated activation of the p16Ink4a-p19Arf pathway. Nat. Genet. *36*, 343–350.

Cairns, J. (1975). Mutation selection and the natural history of cancer. Nature *255*, 197–200.

Cairns, J., and Foster, P.L. (1991). Adaptive Reversion of a Frameshift Mutation in Escherichia-Coli. Genetics *128*, 695–701.

Cairns, J., Overbaugh, J., and Miller, S. (1988). The origin of mutants. Nature *335*, 142–145.

Campisi, J. (1997). The biology of replicative senescence. European Journal of Cancer *33*, 703–709.

Campisi, J., and d'Adda di Fagagna, F. (2007). Cellular senescence: when bad things happen to good cells. Nat. Rev. Mol. Cell. Biol. *8*, 729–740.

Carey, H.V., Andrews, M.T., and Martin, S.L. (2003). Mammalian Hibernation: Cellular and Molecular Responses to Depressed Metabolism and Low Temperature. Physiological Reviews *83*, 1153–1181.

Carlson, C.R., Grallert, B., Stokke, T., and Boye, E. (1999). Regulation of the start of DNA replication in Schizosaccharomyces pombe. Journal of Cell Science *112*, 939–946.

Carnero, A. (2013). Markers of cellular senescence. Methods Mol. Biol. *965*, 63–81.

Caunt, C.J., and Keyse, S.M. (2012). Dual-specificity MAP kinase phosphatases (MKPs). FEBS Journal *280*, 489–504.

Chandeck, C., and Mooi, W.J. (2010). Oncogene-induced cellular senescence. Adv Anat Pathol *17*, 42–48.

Charlwood, J.D., Vij, R., and Billingsley, P.F. (2000). Dry season refugia of malaria-transmitting mosquitoes in a dry savannah zone of east Africa. Am. J. Trop. Med. Hyg. *62*, 726–732.

Chassot, A.-A., Lossaint, G., Turchi, L., Meneguzzi, G., Fisher, D., Ponzio, G., and Dulic, V. (2014). Confluence-induced cell cycle exit involves pre-mitotic CDK inhibition by p27Kip1 and cyclin D1 downregulation. Cell Cycle *7*, 2038–2046.

Chen, C., Liu, Y., Liu, R., Ikenoue, T., Guan, K.-L., Liu, Y., and Zheng, P. (2008). TSC–mTOR maintains quiescence and function of hematopoietic stem cells by repressing mitochondrial biogenesis and reactive oxygen species. J. Exp. Med. *205*, 2397–2408.

Chen, H. (2006). Feedback control of morphogenesis in fungi by aromatic alcohols. Genes Dev. *20*, 1150–1161.

Childs, B.G., Baker, D.J., Kirkland, J.L., Campisi, J., and van Deursen, J.M. (2014). Senescence and apoptosis: dueling or complementary cell fates? EMBO Rep. *15*, 1139–1153.

Cingolani, P., Platts, A., Wang, L.L., Coon, M., Nguyen, T., Wang, L., Land, S.J., Lu, X., and Ruden, D.M. (2014). A program for annotating and predicting the effects of single nucleotide polymorphisms, SnpEff. Fly *6*, 80–92.

Clarke, L., Baum, M., Marschall, L.G., Ngan, V.K., and Steiner, N.C. (1993). Structure and Function of *Schizosaccharomyces-pombe* Centromeres. Cold Spring Harb. Symp. Quant. Biol. *58*, 687–695.

Clotet, J., Escoté, X., Adrover, M.A., Yaakov, G., Garí, E., Aldea, M., de Nadal, E., and Posas, F. (2006). Phosphorylation of Hsl1 by Hog1 leads to a G2 arrest essential for cell survival at high osmolarity. Embo J. *25*, 2338–2346.

Colavitti, R., and Finkel, T. (2005). Reactive Oxygen Species as Mediators of Cellular Senescence. IUBMB Life (International Union of Biochemistry and Molecular Biology: Life) *57*, 277–281.

Collado, M., and Serrano, M. (2010). Senescence in tumours: evidence from mice and humans. Nat. Rev. Cancer *10*, 51–57.

Coller, H.A. (2011). Cell biology. The essence of quiescence. Science *334*, 1074–1075.

Colucci-D'Amato, L., Perrone-Capano, C., and di Porzio, U. (2003). Chronic activation of ERK and neurodegenerative diseases. Bioessays *25*, 1085–1095.

Cooper, T.F., Rozen, D.E., and Lenski, R.E. (2003). Parallel changes in gene expression after 20,000 generations of evolution in Escherichia coli. Pnas *100*, 1072–1077.

Coppe, J.P., Desprez, P.-Y., Krtolica, A., and Campisi, J. (2010). The Senescence-Associated Secretory Phenotype: The Dark Side of Tumor Suppression. Annu. Rev. Pathol. Mech. Dis. *5*, 99–118.

Corrêa, S.A.L., and Eales, K.L. (2012). The Role of p38 MAPK and Its Substrates in Neuronal Plasticity and Neurodegenerative Disease. Journal of Signal Transduction *2012*, 1–12.

Costa, K., Bacher, G., Allmaier, G., Dominguez-Bello, M.G., Engstrand, L., Falk, P., de Pedro, M.A., and García-del Portillo, F. (1999). The morphological transition of Helicobacter pylori cells from spiral to coccoid is preceded by a substantial modification of the cell wall. Journal of Bacteriology *181*, 3710–3715.

Courtois-Cox, S., Genther Williams, S.M., Reczek, E.E., Johnson, B.W., McGillicuddy, L.T., Johannessen, C.M., Hollstein, P.E., MacCollin, M., and Cichowski, K. (2006). A negative feedback signaling network underlies oncogene-induced senescence. Cancer Cell *10*, 459–472.

Crespo, J.L., and Hall, M.N. (2002). Elucidating TOR Signaling and Rapamycin Action: Lessons from Saccharomyces cerevisiae. Microbiol. Mol. Biol. Rev. *66*, 579–591.

Criscuolo, A., and Brisse, S. (2013). AlienTrimmer: a tool to quickly and accurately trim off multiple short contaminant sequences from high-throughput sequencing reads. Genomics *102*, 500–506.

Cuevas, B.D., Abell, A.N., and Johnson, G.L. (2007). Role of mitogen-activated protein kinase kinase kinases in signal integration. Oncogene *26*, 3159–3171.

Daniali, L., Benetos, A., Susser, E., Kark, J.D., Labat, C., Kimura, M., Desai, K.K., Granick, M., and Aviv, A. (2013). Telomeres shorten at equivalent rates in somatic tissues of adults. Nat Commun *4*, 640.

Dassow, von, P., and Montresor, M. (2010). Unveiling the mysteries of phytoplankton life cycles: patterns and opportunities behind complexity. Journal of Plankton Research *33*, 3–12.

Davis, B.D. (1989). Transcriptional bias: a non-Lamarckian mechanism for substrate-induced mutations. Proc. Natl. Acad. Sci. U.S.a. *86*, 5005–5009.

Demidov, O.N., Kek, C., Shreeram, S., Timofeev, O., Fornace, A.J., Appella, E., and Bulavin, D.V. (2006). The role of the MKK6/p38 MAPK pathway in Wip1-dependent regulation of ErbB2-driven mammary gland tumorigenesis. Oncogene *26*, 2502–2506.

Dhillon, A.S., Hagan, S., Rath, O., and Kolch, W. (2007). MAP kinase signalling pathways in cancer. Oncogene *26*, 3279–3290.

DiMauro, T., and David, G. (2010). Ras-Induced Senescence and its Physiological Relevance in Cancer. Current Cancer Drug Targets *10*, 869–876.

Ding, X., Bloch, W., Iden, S., Rüegg, M.A., Hall, M.N., Leptin, M., Partridge, L., and Eming, S.A. (2016). mTORC1 and mTORC2 regulate skin morphogenesis and epidermal barrier formation. Nat Commun *7*, 3021.

Dykhuizen, D.E. (1990). Experimental Studies of Natural Selection in Bacteria. Annu. Rev. Ecol. Syst. *21*, 373–398.

Erdogan, A., and Rao, S.S.C. (2015). Small Intestinal Fungal Overgrowth. Curr Gastroenterol Rep *17*, 495.

Errington, J. (2003). Regulation of endospore formation in Bacillus subtilis. Nat. Rev. Microbiol. *1*, 117–126.

Escoté, X., Miranda, M., Rodríguez-Porrata, B., Mas, A., Cordero, R., Posas, F., and Vendrell, J. (2011). The stress-activated protein kinase Hog1 develops a critical role after resting state. Mol. Microbiol. *80*, 423–435.

Ewald, J.A., Desotelle, J.A., Wilding, G., and Jarrard, D.F. (2010). Therapy-Induced Senescence in Cancer. JNCI: Journal of the National Cancer Institute *102*, 1536–1546.

Fabrizio, P., and Longo, V.D. (2003). The chronological life span of *Saccharomyces cerevisiae*. Aging Cell *2*, 73–81.

Fabrizio, P., and Longo, V.D. (2007). The chronological life span of Saccharomyces cerevisiae. *371*, 89–95.

Farlow, A., Long, H., Arnoux, S., Sung, W., Doak, T.G., Nordborg, M., and Lynch, M. (2015). The Spontaneous Mutation Rate in the Fission Yeast *Schizosaccharomyces pombe*. Genetics *201*, 737–744.

Finkel, S.E. (2006). Long-term survival during stationary phase: evolution and the GASP phenotype. Nat. Rev. Microbiol. *4*, 113–120.

Finkel, S.E., and Kolter, R. (1999). Evolution of microbial diversity during prolonged starvation. Pnas *96*, 4023–4027.

Finkel, S.E., and Kolter, R. (2001). DNA as a Nutrient: Novel Role for Bacterial Competence Gene Homologs. Journal of Bacteriology *183*, 6288–6293.

Finkelstein, R., Reeves, W., Ariizumi, T., and Steber, C. (2008). Molecular Aspects of Seed Dormancy. Annu. Rev. Plant Biol. *59*, 387–415.

Fitzgerald, D.M., Hastings, P.J., and Rosenberg, S.M. (2017). Stress-Induced Mutagenesis: Implications in Cancer and Drug Resistance. Annu Rev Cancer Biol *1*, 119–140.

Florea, M. (2017). Aging and immortality in unicellular species. Mechanisms of Ageing and Development *167*, 5–15.

Fontana, L., Partridge, L., and Longo, V.D. (2010). Extending Healthy Life Span--From Yeast to Humans. Science *328*, 321–326.

Foster, P.L. (1999). Mechanisms of stationary phase mutation: a decade of adaptive mutation. Annu. Rev. Genet. *33*, 57–88.

Foster, P.L., and Trimarchi, J.M. (1994). Adaptive Reversion of a Frameshift Mutation in Escherichia-Coli by Simple Base Deletions in Homopolymeric Runs. Science *265*, 407–409.

Foster, P.L. (2007). Stress-induced mutagenesis in bacteria. Crit. Rev. Biochem. Mol. Biol. *42*, 373–397.

Fox, E.J., Reid-Bayliss, K.S., Emond, M.J., and Loeb, L.A. (2014). Accuracy of Next Generation Sequencing Platforms. Next Gener Seq Appl *1*.

Fridlyanskaya, I., Alekseenko, L., and Nikolsky, N. (2015). Senescence as a general cellular response to stress: A mini-review. Experimental Gerontology *72*, 124–128.

Friedmann-Morvinski, D., and Verma, I.M. (2014). Dedifferentiation and reprogramming: origins of cancer stem cells. EMBO Rep. *15*, 244–253.

Fung, D.K.C., Chan, E.W.C., Chin, M.L., and Chan, R.C.Y. (2010). Delineation of a Bacterial Starvation Stress Response Network Which Can Mediate Antibiotic Tolerance Development. Antimicrob. Agents Chemother. *54*, 1082–1093.

Furuyama, S., and Biggins, S. (2007). Centromere identity is specified by a single centromeric nucleosome in budding yeast. Pnas *104*, 14706–14711.

Gaits, F., Degols, G., Shiozaki, K., and Russell, P. (1998). Phosphorylation and association with the transcription factor Atf1 regulate localization of Spc1/Sty1 stress-activated kinase in fission yeast. Genes Dev. *12*, 1464–1473.

Ganai, R.A., and Johansson, E. (2016). DNA Replication—A Matter of Fidelity. Mol. Cell *62*, 745–755.

Gangloff, S., and Arcangioli, B. (2017). DNA repair and mutations during quiescence in yeast. FEMS Yeast Res. *17*.

Gangloff, S., Achaz, G., Francesconi, S., Villain, A., Miled, S., Denis, C., and Arcangioli, B. (2017). Quiescence unveils a novel mutational force in fission yeast. Elife *6*, 149.

Gao, X., Zhang, M., Tang, Y., and Liang, X.-H. (2017). Cancer cell dormancy: mechanisms and implications of cancer recurrence and metastasis. Ott *Volume 10*, 5219–5228.

Gasch, A.P., Spellman, P.T., Kao, C.M., Carmel-Harel, O., Eisen, M.B., Storz, G., Botstein, D., and Brown, P.O. (2000). Genomic Expression Programs in the Response of Yeast Cells to Environmental Changes. Mol. Biol. Cell *11*, 4241–4257.

Gefen, O., and Balaban, N.Q. (2009). The importance of being persistent: heterogeneity of bacterial populations under antibiotic stress. FEMS Microbiol. Rev. *33*, 704–717.

Gengenbacher, M., and Kaufmann, S.H.E. (2012). Mycobacterium tuberculosis: success through dormancy. FEMS Microbiol. Rev. *36*, 514–532.

Gensler, H.L., and Bernstein, H. (1981). Dna Damage as the Primary Cause of Aging. Q Rev Biol *56*, 279–303.

Gentry, D.R., Hernandez, V.J., Nguyen, L.H., Jensen, D.B., and Cashel, M. (1993). Synthesis of the Stationary-Phase Sigma-Factor Sigma(S) Is Positively Regulated by ppGpp. Journal of Bacteriology *175*, 7982–7989.

Germain, E., Roghanian, M., Gerdes, K., and Maisonneuve, E. (2015). Stochastic induction of persister cells by HipA through (p)ppGpp-mediated activation of mRNA endonucleases. Pnas *112*, 5171–5176.

Glickman, M.S., and Sawyers, C.L. (2012). Converting Cancer Therapies into Cures: Lessons from Infectious Diseases. Cell *148*, 1089–1098.

Goffeau, A., Barrell, B.G., Bussey, H., Davis, R.W., Dujon, B., Feldmann, H., Galibert, F., Hoheisel, J.D., Jacq, C., Johnston, M., et al. (1996). Life with 6000 genes. Science *274*, 546–&.

Gomis, R.R., and Gawrzak, S. (2017). Tumor cell dormancy. Mol Oncol *11*, 62–78.

Grabiner, B.C., Nardi, V., Birsoy, K., Possemato, R., Shen, K., Sinha, S., Jordan, A., Beck, A.H., and Sabatini, D.M. (2014). A Diverse Array of Cancer-Associated MTOR Mutations Are Hyperactivating and Can Predict Rapamycin Sensitivity. Cancer Discov *4*, 554–563.

Gray-Schopfer, V.C., Cheong, S.C., Chong, H., Chow, J., Moss, T., Abdel-Malek, Z.A., Marais, R., Wynford-Thomas, D., and Bennett, D.C. (2006). Cellular senescence in naevi and immortalisation in melanoma: a role for p16? Br. J. Cancer *95*, 496–505.

Greene, C.N., and Jinks-Robertson, S. (1999). Comparison of spontaneous and adaptive mutation spectra in yeast. J. Genet. *78*, 51–55.

Grigg, G.W., and Stuckey, J. (1966). The reversible suppression of stationary phase mutation in Escherichia coli by caffeine. Genetics *53*, 823–834.

Gruber, T.M., and Gross, C.A. (2003). Multiple Sigma Subunits and the Partitioning of Bacterial Transcription Space. Annu. Rev. Microbiol. *57*, 441–466.

Grunstein, M., and Gasser, S.M. (2013). Epigenetics in Saccharomyces cerevisiae. Cold Spring Harb Perspect Biol *5*, a017491–a017491.

Guo, F., Zhang, S., Grogg, M., Cancelas, J.A., Varney, M.E., Starczynowski, D.T., Du, W., Yang, J.Q., Liu, W., Thomas, G., et al. (2013). Mouse gene targeting reveals an essential role of mTOR in hematopoietic stem cell engraftment and hematopoiesis. Haematologica *98*, 1353–1358.

Hall, B.G. (1992). Selection-Induced Mutations Occur in Yeast. Proc. Natl. Acad. Sci. U.S.a. *89*, 4300–4303.

Haller, S., Kapuria, S., Riley, R.R., O'Leary, M.N., Schreiber, K.H., Andersen, J.K., Melov, S., Que, J., Rando, T.A., Rock, J., et al. (2017). mTORC1 Activation during Repeated Regeneration Impairs Somatic Stem Cell Maintenance. Cell Stem Cell *21*, 806–818.e5.

Hanawalt, P.C. (2008). Emerging links between premature ageing and defective DNA repair. Mechanisms of Ageing and Development *129*, 503–505.

Harms, A., Maisonneuve, E., and Gerdes, K. (2016). Mechanisms of bacterial persistence during stress and antibiotic exposure. Science *354*, aaf4268.

Hartman, N.W., Lin, T.V., Zhang, L., Paquelet, G.E., Feliciano, D.M., and Bordey, A. (2013). mTORC1 Targets the Translational Repressor 4E-BP2, but Not S6 Kinase 1/2, to Regulate Neural Stem Cell Self-Renewal In Vivo. Cell Rep *5*, 433–444.

Haseltine, W.A., and Block, R. (1973). Synthesis of Guanosine Tetraphosphate and Pentaphosphate Requires Presence of a Codon-Specific, Uncharged Transfer Ribonucleic-Acid in Acceptor Site of Ribosomes - (Stringent Control Ppgpp (Msi) and Pppgpp (Msii) Protein Synthesis Escherichia-Coli). Pnas *70*, 1564–1568.

Hay, N. (2004). Upstream and downstream of mTOR. Genes Dev. *18*, 1926–1945.

Hayashi, T., Teruya, T., Chaleckis, R., Morigasaki, S., and Yanagida, M. (2018). S-Adenosylmethionine Synthetase Is Required for Cell Growth, Maintenance of G0 Phase, and Termination of Quiescence in Fission Yeast. iScience *5*, 38–51.

Hayflick, L. (1965). The limited in vitro lifetime of human diploid cell strains. Exp. Cell Res. *37*, 614–636.

Hayflick, L., and Moorhead, P.S. (1961). The serial cultivation of human diploid cell strains. Exp. Cell Res. *25*, 585–621.

Heidenreich, E. (1998). Replication-dependent and selection-induced mutations in respiration-competent and respiration-deficient strains of Saccharomyces cerevisiae. Mol. Gen. Genet. *260*, 395–400.

Heidenreich, E., and Wintersberger, U. (1997). Starvation for a specific amino acid induces high frequencies of rho(-) mutants in Saccharomyces cerevisiae. Curr. Genet. *31*, 408–413.

Heidenreich, E., and Wintersberger, U. (2001). Adaptive reversions of a frameshift mutation in arrested Saccharomyces cerevisiae cells by simple deletions in mononucleotide repeats. Mutation Research/Fundamental and … *473*, 101–107.

Hengge-Aronis, R. (2002). Signal Transduction and Regulatory Mechanisms Involved in Control of the S (RpoS) Subunit of RNA Polymerase. Microbiol. Mol. Biol. Rev. *66*, 373–395.

Herbig, U. (2006). Cellular Senescence in Aging Primates. Science *311*, 1257–1257.

Hernandez-Segura, A., Nehme, J., and Demaria, M. (2018). Hallmarks of Cellular Senescence. Trends Cell Biol. *28*, 436–453.

Herskowitz, I. (1988). Life-Cycle of the Budding Yeast Saccharomyces-Cerevisiae. Microbiol. Rev. *52*, 536–553.

Hitomi, M., and Stacey, D.W. (1999). Cyclin D1 production in cycling cells depends on Ras in a cell-cycle-specific manner. Curr. Biol. *9*, 1075–1084.

Iyama, T., and Wilson, D.M., III (2013). DNA repair mechanisms in dividing and non-dividing cells. DNA Repair (Amst.) *12*, 620–636.

Jeffares, D.C. (2018). The natural diversity and ecology of fission yeast. Yeast *35*, 253–260.

Jeffares, D.C., Rallis, C., Rieux, A., Speed, D., Převorovský, M., Mourier, T., Marsellach, F.X., Iqbal, Z., Lau, W., Cheng, T.M.K., et al. (2015). The genomic and phenotypic diversity of *Schizosaccharomyces pombe*. Nat. Genet. *47*, 235–241.

Jiang, Y., Gram, H., Zhao, M., New, L., Gu, J., Feng, L., Di Padova, F., Ulevitch, R.J., and Han, J. (1997). Characterization of the structure and function of the fourth member of p38 group mitogen-activated protein kinases, p38delta. J. Biol. Chem. *272*, 30122–30128.

Jishage, M. (2002). Regulation of sigma factor competition by the alarmone ppGpp. Genes Dev. *16*, 1260–1270.

Joh, R.I., Khanduja, J.S., Calvo, I.A., Mistry, M., Palmieri, C.M., Savol, A.J., Ho Sui, S.J., Sadreyev, R.I., Aryee, M.J., and Motamedi, M. (2016). Survival in Quiescence Requires the Euchromatic Deployment of Clr4/SUV39H by Argonaute-Associated Small RNAs. Mol. Cell *64*, 1088–1101.

Johnston, G.C., Singer, R.A., and Werner-Washburne, M. (2004). “Sleeping beauty”: quiescence in Saccharomyces cerevisiae. Microbiol. Mol. Biol. Rev. *68*, 187–206.

Kato, T., Okazaki, K., Murakami, H., Stettler, S., Fantes, P.A., and Okayama, H. (1996). Stress signal, mediated by a HOG1-like MAP kinase, controls sexual development in fission yeast. FEBS Lett. *378*, 207–212.

Kidger, A.M., and Keyse, S.M. (2016). The regulation of oncogenic Ras/ERK signalling by dual-specificity mitogen activated protein kinase phosphatases (MKPs). Semin. Cell Dev. Biol. *50*, 125–132.

Kiel, M.J., He, S., Ashkenazi, R., Gentry, S.N., Teta, M., Kushner, J.A., Jackson, T.L., and Morrison, S.J. (2007). Haematopoietic stem cells do not asymmetrically segregate chromosomes or retain BrdU. Nature *449*, 238–242.

Kim, E.K., and Choi, E.-J. (2010). Pathological roles of MAPK signaling pathways in human diseases. Biochimica Et Biophysica Acta (BBA) - Molecular Basis of Disease *1802*, 396–405.

Kim, J.-S., Chowdhury, N., Yamasaki, R., and Wood, T.K. (2018). Viable but non-culturable and persistence describe the same bacterial stress state. Environ. Microbiol. *20*, 2038–2048.

Klosinska, M.M., Crutchfield, C.A., Bradley, P.H., Rabinowitz, J.D., and Broach, J.R. (2011). Yeast cells can access distinct quiescent states. Genes Dev. *25*, 336–349.

Knoechel, B., Roderick, J.E., Williamson, K.E., Zhu, J., Lohr, J.G., Cotton, M.J., Gillespie, S.M., Fernandez, D., Ku, M., Wang, H., et al. (2014). An epigenetic mechanism of resistance to targeted therapy in T cell acute lymphoblastic leukemia. Nat. Genet. *46*, 364–370.

Kobayashi, A., Okuda, H., Xing, F., Pandey, P.R., Watabe, M., Hirota, S., Pai, S.K., Liu, W., Fukuda, K., Chambers, C., et al. (2011). Bone morphogenetic protein 7 in dormancy and metastasis of prostate cancer stem-like cells in bone. J. Exp. Med. *208*, 2641–2655.

Koboldt, D.C., Chen, K., Wylie, T., Larson, D.E., McLellan, M.D., Mardis, E.R., Weinstock, G.M., Wilson, R.K., and Ding, L. (2009). VarScan: variant detection in massively parallel sequencing of individual and pooled samples. Bioinformatics *25*, 2283–2285.

Kohanski, M.A., Dwyer, D.J., and Collins, J.J. (2010). How antibiotics kill bacteria: from targets to networks. Nat. Rev. Microbiol. *8*, 423–435.

Kondoh, K., and Nishida, E. (2007). Regulation of MAP kinases by MAP kinase phosphatases. Biochimica Et Biophysica Acta (BBA) - Molecular Cell Research *1773*, 1227–1237.

Koštál, V. (2006). Eco-physiological phases of insect diapause. Journal of Insect Physiology *52*, 113–127.

Krause, S.A., and Gray, J.V. (2002). The protein kinase C pathway is required for viability in quiescence in Saccharomyces cerevisiae. Curr. Biol. *12*, 588–593.

Kruman, I.I. (2004). Why do neurons enter the cell cycle? Cell Cycle *3*, 769–773.

Lehmann, A.R. (1996). Molecular biology of DNA repair in the fission yeast Schizosaccharomyces pombe. Mutat. Res. *363*, 147–161.

Leija-Salazar, M., Piette, C., and Proukakis, C. (2018). Review: Somatic mutations in neurodegeneration. Neuropathol. Appl. Neurobiol. *44*, 267–285.

Lengwinat, T., and Meyer, H. (1996). Investigations of BrdU incorporation in roe deer blastocysts in vitro. Anim. Reprod. Sci. *45*, 103–107.

Lennon, J.T., and Jones, S.E. (2011). Microbial seed banks: the ecological and evolutionary implications of dormancy. Nat. Rev. Microbiol. *9*, 119–130.

Lewis, D.L., and Gattie, D.K. (1991). The ecology of quiescent microbes. ASM News *57*, 27–32.

Lewis, K. (2007). Persister cells, dormancy and infectious disease. Nat. Rev. Microbiol. *5*, 48–56.

Li, H., Handsaker, B., Wysoker, A., Fennell, T., Ruan, J., Homer, N., Marth, G., Abecasis, G.R., Durbin, R., 1000 Genome Project Data Processing Subgroup (2009). The Sequence Alignment/Map format and SAMtools. Bioinformatics *25*, 2078–2079.

Li, H., and Durbin, R. (2009). Fast and accurate short read alignment with Burrows-Wheeler transform. Bioinformatics *25*, 1754–1760.

Li, L., Mendis, N., Trigui, H., Oliver, J.D., and Faucher, S.P. (2014). The importance of the viable but non-culturable state in human bacterial pathogens. Front. Microbiol. *5*, 130.

Lindner, A.B., Madden, R., Demarez, A., Stewart, E.J., and Taddei, F. (2008). Asymmetric segregation of protein aggregates is associated with cellular aging and rejuvenation. Pnas *105*, 3076–3081.

Liu, Y., Schröder, J., and Schmidt, B. (2013). Musket: a multistage k-mer spectrum-based error corrector for Illumina sequence data. Bioinformatics *29*, 308–315.

Lloyd, A.C. (2013). The Regulation of Cell Size. Cell *154*, 1194–1205.

Lodato, M.A., Rodin, R.E., Bohrson, C.L., Coulter, M.E., Barton, A.R., Kwon, M., Sherman, M.A., Vitzthum, C.M., Luquette, L.J., Yandava, C.N., et al. (2018). Aging and neurodegeneration are associated with increased mutations in single human neurons. Science *359*, 555–559.

Loewith, R., Jacinto, E., Wullschleger, S., Lorberg, A., Crespo, J.L., Bonenfant, D., Oppliger, W., Jenoe, P., and Hall, M.N. (2002). Two TOR complexes, only one of which is rapamycin sensitive, have distinct roles in cell growth control. Mol. Cell *10*, 457–468.

Loffredo, F.S., Steinhauser, M.L., Jay, S.M., Gannon, J., Pancoast, J.R., Yalamanchi, P., Sinha, M., Dall'Osso, C., Khong, D., Shadrach, J.L., et al. (2013). Growth Differentiation Factor 11 Is a Circulating Factor that Reverses Age-Related Cardiac Hypertrophy. Cell *153*, 828–839.

Lombard, D.B., Chua, K.F., Mostoslavsky, R., Franco, S., Gostissa, M., and Alt, F.W. (2005). DNA repair, genome stability, and aging. Cell *120*, 497–512.

Luria, S.E., and Delbrück, M. (1943). Mutations of Bacteria from Virus Sensitivity to Virus Resistance. Genetics *28*, 491–511.

Lustig, A.J., and Petes, T.D. (1986). Identification of Yeast Mutants with Altered Telomere Structure. Pnas *83*, 1398–1402.

Ma, X.M., and Blenis, J. (2009). Molecular mechanisms of mTOR-mediated translational control. Nat. Rev. Mol. Cell. Biol. *10*, 307–318.

Macintyre, G., Pitsikas, P., and Cupples, C.G. (1999). Growth phase-dependent regulation of Vsr endonuclease may contribute to 5-methylcytosine mutational hot spots in Escherichia coli. Journal of Bacteriology *181*, 4435–4436.

MacLean, M., Harris, N., and Piper, P.W. (2001). Chronological lifespan of stationary phase yeast cells; a model for investigating the factors that might influence the ageing of postmitotic tissues in higher organisms. Yeast *18*, 499–509.

Maestroni, L., Audry, J., Matmati, S., Arcangioli, B., Géli, V., and Coulon, S. (2017). Eroded telomeres are rearranged in quiescent fission yeast cells through duplications of subtelomeric sequences. Nat Commun *8*, 1684.

Magnusson, L.U., Farewell, A., and Nyström, T. (2005). ppGpp: a global regulator in Escherichia coli. Trends Microbiol. *13*, 236–242.

Magoč, T. (2011). FLASH: fast length adjustment of short reads to improve genome assemblies. Bioinformatics *27*, 2957–2963.

Mamdani, F., Rollins, B., Morgan, L., Myers, R.M., Barchas, J.D., Schatzberg, A.F., Watson, S.J., Akil, H., Potkin, S.G., Bunney, W.E., et al. (2016). Erratum: Variable telomere length across post-mortem human brain regions and specific reduction in the hippocampus of major depressive disorder. Transl Psychiatry *6*, e969–e969.

Marches, R., Scheuermann, R., and Uhr, J. (2006). Cancer Dormancy from Mice to Man: A Review. Cell Cycle *5*, 1772–1778.

Marguerat, S., Schmidt, A., Codlin, S., Chen, W., Aebersold, R., and Bähler, J. (2012). Quantitative analysis of fission yeast transcriptomes and proteomes in proliferating and quiescent cells. Cell *151*, 671–683.

Marthandan, S., Priebe, S., Hemmerich, P., Klement, K., and Diekmann, S. (2014). Long-Term Quiescent Fibroblast Cells Transit into Senescence. PLoS ONE *9*, e115597.

Martienssen, R.A., Zaratiegui, M., and Goto, D.B. (2005). RNA interference and heterochromatin in the fission yeast Schizosaccharomyces pombe. Trends in Genetics *21*, 450–456.

Matson, J.P., and Cook, J.G. (2016). Cell cycle proliferation decisions: the impact of single cell analyses. Febs J. *284*, 362–375.

Matsuo, T., Otsubo, Y., Urano, J., Tamanoi, F., and Yamamoto, M. (2007). Loss of the TOR Kinase Tor2 Mimics Nitrogen Starvation and Activates the Sexual Development Pathway in Fission Yeast. Mol. Cell. Biol. *27*, 3154–3164.

Matsuoka, K., Kiyokawa, N., Taguchi, T., Matsui, J., Suzuki, T., Mimori, K., Nakajima, H., Takenouchi, H., Weiran, T., Katagiri, Y.U., et al. (2002). Rum1, an inhibitor of cyclin-dependent kinase in fission yeast, is negatively regulated by mitogen-activated protein kinase-mediated phosphorylation at Ser and Thr residues. Eur. J. Biochem. *269*, 3511–3521.

May, A., Abeln, S., Buijs, M.J., Heringa, J., Crielaard, W., and Brandt, B.W. (2015). NGS-eval: NGS Error analysis and novel sequence VAriant detection tooL. Nucleic Acids Res. *43*, W301–W305.

McDowall, M.D., Harris, M.A., Lock, A., Rutherford, K., Staines, D.M., Bähler, J., Kersey, P.J., Oliver, S.G., and Wood, V. (2014). PomBase 2015: updates to the fission yeast database. Nucleic Acids Res. *43*, D656–D661.

McKenna, A., Hanna, M., Banks, E., Sivachenko, A.Y., Cibulskis, K., Kernytsky, A., Garimella, K., Altshuler, D.M., Gabriel, S., Daly, M., et al. (2010). The Genome Analysis Toolkit: A MapReduce framework for analyzing next-generation DNA sequencing data. Genome Res. *20*, 1297–1303.

Menon, S., and Manning, B.D. (2009). Common corruption of the mTOR signaling network in human tumors. Oncogene *27*, S43–S51.

Mertens, S., Craxton, M., and Goedert, M. (1996). SAP kinase-3, a new member of the family of mammalian stress-activated protein kinases. FEBS Lett. *383*, 273–276.

Minoche, A.E., Dohm, J.C., and Himmelbauer, H. (2011). Evaluation of genomic high-throughput sequencing data generated on Illumina HiSeq and Genome Analyzer systems. Genome Biol *12*, R112.

Mitchison, J.M., and Creanor, J. (1971). Further Measurements of Dna Synthesis and Enzyme Potential During Cell Cycle of Fission Yeast Schizosaccharomyces-Pombe. Exp. Cell Res. *69*, 244–.

Mitra, M., Ho, L.D., and Coller, H.A. (2018). An In Vitro Model of Cellular Quiescence in Primary Human Dermal Fibroblasts. Methods Mol. Biol. *1686*, 27–47.

Mochida, S., and Yanagida, M. (2006). Distinct modes of DNA damage response in *S. pombe* G0 and vegetative cells. Genes Cells *11*, 13–27.

Morrison, D.K. (2012). MAP Kinase Pathways. Cold Spring Harb Perspect Biol *4*, a011254–a011254.

Mortimer, R.K., and Johnston, J.R. (1959). Life span of individual yeast cells. Nature *183*, 1751–1752.

Muffler, A., Traulsen, D.D., Lange, R., and Hengge-Aronis, R. (1996). Posttranscriptional osmotic regulation of the sigma(s) subunit of RNA polymerase in Escherichia coli. Journal of Bacteriology *178*, 1607–1613.

Munakata, N., and Ikeda, Y. (1968). A mutant of Bacillus subtilis producing ultraviolet-sensitive spores. Biochem. Biophys. Res. Commun. *33*, 469–475.

Munakata, N., and Rupert, C.S. (1975). Effects of DNA-polymerase-defective and recombination-deficient mutations on the ultraviolet sensitivity of Bacillus subtilis spores. Mutat. Res. *27*, 157–169.

Munro, J., Steeghs, K., Morrison, V., Ireland, H., and Parkinson, E.K. (2001). Human fibroblast replicative senescence can occur in the absence of extensive cell division and short telomeres. Oncogene *20*, 3541–3552.

Murakami, M., Ichisaka, T., Maeda, M., Oshiro, N., Hara, K., Edenhofer, F., Kiyama, H., Yonezawa, K., and Yamanaka, S. (2004). mTOR Is Essential for Growth and Proliferation in Early Mouse Embryos and Embryonic Stem Cells. Mol. Cell. Biol. *24*, 6710–6718.

Nakamura, T.M., Morin, G.B., Chapman, K.B., Weinrich, S.L., Andrews, W.H., Lingner, J., Harley, C.B., and Cech, T.R. (1997). Telomerase catalytic subunit homologs from fission yeast and human. Science *277*, 955–959.

Newcombe, H.B. (1949). Origin of bacterial variants. Nature *164*, 150.

Nicholson, W.L., Munakata, N., Horneck, G., Melosh, H.J., and Setlow, P. (2000). Resistance of Bacillus endospores to extreme terrestrial and extraterrestrial environments. Microbiol. Mol. Biol. Rev. *64*, 548–.

NISC Comparative Sequencing Program, Huang, H.W., Mullikin, J.C., and Hansen, N.F. (2015). Evaluation of variant detection software for pooled next-generation sequence data. BMC Bioinformatics *16*, 210.

Nishiyama, T., Akutsu, N., Horii, I., Nakayama, Y., Ozawa, T., and Hayashi, T. (1991). Response to Growth-Factors of Human Dermal Fibroblasts in a Quiescent State Owing to Cell-Matrix Contact Inhibition. Matrix *11*, 71–75.

Nurse, P. (1975). Genetic control of cell size at cell division in yeast. Nature *256*, 547–551.

Nurse, P., Thuriaux, P., and Nasmyth, K. (1976). Genetic control of the cell division cycle in the fission yeast Schizosaccharomyces pombe. Mol. Gen. Genet. *146*, 167–178.

Nyström, T. (2004). Stationary-Phase Physiology. Annu. Rev. Microbiol. *58*, 161–181.

Osisami, M., and Keller, E. (2013). Mechanisms of Metastatic Tumor Dormancy. Jcm *2*, 136–150.

Ou, J., Wang, Y.X., Zhu, L.J., Ou, M.J., and GenomicAlignments, I. (2019). Package "trackViewer."

Pardee, A.B. (1974). A restriction point for control of normal animal cell proliferation. Pnas *71*, 1286–1290.

Payen, C., Sunshine, A.B., Ong, G.T., Pogachar, J.L., Zhao, W., and Dunham, M.J. (2016). High-Throughput Identification of Adaptive Mutations in Experimentally Evolved Yeast Populations. PLoS Genet *12*, e1006339.

Pearson, G., Robinson, F., Beers Gibson, T., Xu, B.-E., Karandikar, M., Berman, K., and Cobb, M.H. (2001). Mitogen-Activated Protein (MAP) Kinase Pathways: Regulation and Physiological Functions 1. Endocrine Reviews *22*, 153–183.

Petersen, J., Nurse, P., and Nurse, P. (2007). TOR signalling regulates mitotic commitment through the stress MAP kinase pathway and the Polo and Cdc2 kinases. Nat. Cell Biol. *9*, 1263–1272.

Poelchau, M.F., Reynolds, J.A., Elsik, C.G., Denlinger, D.L., and Armbruster, P.A. (2013). Deep sequencing reveals complex mechanisms of diapause preparation in the invasive mosquito, Aedes albopictus. Proc. Biol. Sci. *280*, 20130143–20130143.

Potapov, V., and Ong, J.L. (2017). Correction: Examining Sources of Error in PCR by Single-Molecule Sequencing. PLoS ONE *12*, e0181128.

Powell, J.A. (2001). Longest Insect Dormancy: Yucca Moth Larvae (Lepidoptera: Prodoxidae) Metamorphose After 20, 25, and 30 Years in Diapause. An *94*, 677–680.

Price, C., Boltz, K.A., Chaiken, M.F., Stewart, J.A., Beilstein, M.A., and Shippen, D.E. (2014). Evolution of CST function in telomere maintenance. Cell Cycle *9*, 3177–3185.

Rallis, C., Codlin, S., and Bähler, J. (2013). TORC1 signaling inhibition by rapamycin and caffeine affect lifespan, global gene expression, and cell proliferation of fission yeast. Aging Cell *12*, 563–573.

Ranganathan, A.C., Adam, A.P., and Aguirre-Ghiso, J.A. (2006). Opposing Roles of Mitogenic and Stress Signaling Pathways in the Induction of Cancer Dormancy. Cell Cycle *5*, 1799–1807.

Rhind, N., Chen, Z., Yassour, M., Thompson, D.A., Haas, B.J., Habib, N., Wapinski, I., Roy, S., Lin, M.F., Heiman, D.I., et al. (2011). Comparative Functional Genomics of the Fission Yeasts. Science *332*, 930–936.

Risson, V., Mazelin, L., Roceri, M., Sanchez, H., Moncollin, V., Corneloup, C., Richard-Bulteau, H., Vignaud, A., Baas, D., Defour, A., et al. (2009). Muscle inactivation of mTOR causes metabolic and dystrophin defects leading to severe myopathy. J Cell Biol *187*, 859–874.

Rittershaus, E.S.C., Baek, S.-H., and Sassetti, C.M. (2013). The Normalcy of Dormancy: Common Themes in Microbial Quiescence. Cell Host & Microbe *13*, 643–651.

Robinson, J.T., Thorvaldsdóttir, H., Winckler, W., Guttman, M., Lander, E.S., Getz, G., and Mesirov, J.P. (2011). Integrative genomics viewer. Nat. Biotechnol. *29*, 24–26.

Roche, B., Arcangioli, B., Martienssen, R.A., and Martienssen, R.A. (2016). RNA interference is essential for cellular quiescence. Science *354*.

Rodier, F., and Campisi, J. (2011). Four faces of cellular senescence. J Cell Biol *192*, 547–556.

Rosenberg, S.M., Longerich, S., Gee, P., and Harris, R.S. (1994). Adaptive Mutation by Deletions in Small Mononucleotide Repeats. Science *265*, 405–407.

Ryan, F.J. (1955). Spontaneous Mutation in Non-Dividing Bacteria. Genetics *40*, 726–738.

Saint-Ruf, C., Garfa-Traore, M., Collin, V., Cordier, C., Franceschi, C., and Matic, I. (2014). Massive Diversification in Aging Colonies of Escherichia coli. Journal of Bacteriology *196*, 3059–3073.

Sajiki, K., Hatanaka, M., Nakamura, T., Takeda, K., Shimanuki, M., Yoshida, T., Hanyu, Y., Hayashi, T., Nakaseko, Y., and Yanagida, M. (2009). Genetic control of cellular quiescence in *S. pombe*. Journal of Cell Science *122*, 1418–1429.

Sajiki, K., Pluskal, T., Shimanuki, M., and Yanagida, M. (2013). Metabolomic analysis of fission yeast at the onset of nitrogen starvation. Metabolites *3*, 1118–1129.

Sanso, M., Vargas-Perez, I., García, P., Ayté, J., and Hidalgo, E. (2011). Nuclear roles and regulation of chromatin structure by the stress-dependent MAP kinase Sty1 of Schizosaccharomyces pombe. Mol. Microbiol. *82*, 542–554.

Sapieha, P., and Mallette, F.A. (2018). Cellular Senescence in Postmitotic Cells: Beyond Growth Arrest. Trends Cell Biol. *28*, 595–607.

Sato, T., Nakashima, A., Guo, L., Coffman, K., and Tamanoi, F. (2010). Single amino-acid changes that confer constitutive activation of mTOR are discovered in human cancer. Oncogene *29*, 2746–2752.

Schewe, D.M., and Aguirre-Ghiso, J.A. (2008). ATF6 -Rheb-mTOR signaling promotes survival of dormant tumor cells in vivo. Pnas *105*, 10519–10524.

Schroering, A.G., Edelbrock, M.A., Richards, T.J., and Williams, K.J. (2007). The cell cycle and DNA mismatch repair. Exp. Cell Res. *313*, 292–304.

Schüller, C., Brewster, J.L., Alexander, M.R., Gustin, M.C., and Ruis, H. (1994). The Hog Pathway Controls Osmotic Regulation of Transcription via the Stress-Response Element (STRE) of the *Saccharomyces-cerevisiae CTT1* Gene. Embo J. *13*, 4382–4389.

Sell, S. (1993). Cellular origin of cancer: dedifferentiation or stem cell maturation arrest? Environ. Health Perspect. *101 Suppl 5*, 15–26.

Sellathurai, J., Cheedipudi, S., Dhawan, J., and Schroder, H.D. (2013). A Novel In Vitro Model for Studying Quiescence and Activation of Primary Isolated Human Myoblasts. PLoS ONE *8*, e64067.

Sengar, A.S., Markley, N.A., Marini, N.J., and Young, D. (1997). Mkh1, a MEK kinase required for cell wall integrity and proper response to osmotic and temperature stress in Schizosaccharomyces pombe. Mol. Cell. Biol. *17*, 3508–3519.

Serra, D.O., Richter, A.M., Klauck, G., Mika, F., and Hengge, R. (2013). Microanatomy at Cellular Resolution and Spatial Order of Physiological Differentiation in a Bacterial Biofilm. MBio *4*, 95–13.

Serrano, M., Lin, A.W., McCurrach, M.E., Beach, D., and Lowe, S.W. (1997). Oncogenic ras provokes premature cell senescence associated with accumulation of p53 and p16INK4a. Cell *88*, 593–602.

Setlow, B., and Setlow, P. (1996). Role of DNA repair in Bacillus subtilis spore resistance. Journal of Bacteriology *178*, 3486–3495.

Shapiro, J.A. (1984). Observations on the formation of clones containing araB-lacZ cistron fusions. Mol. Gen. Genet. *194*, 79–90.

Shimanuki, M., Chung, S.-Y., Chikashige, Y., Kawasaki, Y., Uehara, L., Tsutsumi, C., Hatanaka, M., Hiraoka, Y., Nagao, K., and Yanagida, M. (2007). Two-step, extensive alterations in the transcriptome from G0 arrest to cell division in Schizosaccharomyces pombe. Genes Cells *12*, 677–692.

Shiozaki, K., and Russell, P. (1996). Conjugation, meiosis, and the osmotic stress response are regulated by Spc1 kinase through Atf1 transcription factor in fission yeast. Genes Dev. *10*, 2276–2288.

Shiozaki, K., and Russell, P. (1995). Cell-cycle control linked to extracellular environment by MAP kinase pathway in fission yeast. Nature *378*, 739–743.

Sibirny, A.A. (2016). Yeast peroxisomes: structure, functions and biotechnological opportunities. FEMS Yeast Res. *16*, fow038.

Sideri, T., Rallis, C., Bitton, D.A., Lages, B.M., Suo, F., Rodríguez-López, M., Du, L.-L., and Bähler, J. (2014). Parallel profiling of fission yeast deletion mutants for proliferation and for lifespan during long-term quiescence. G3 (Bethesda) *5*, 145–155.

Sledjeski, D.D., Gupta, A., and Gottesman, S. (1996). The small RNA, DsrA, is essential for the low temperature expression of RpoS during exponential growth in Escherichia coli. Embo J. *15*, 3993–4000.

Smith, C.L., Matsumoto, T., Niwa, O., Klco, S., Fan, J.B., Yanagida, M., and Cantor, C.R. (1987). An Electrophoretic Karyotype for Schizosaccharomyces-Pombe by Pulsed Field Gel-Electrophoresis. Nucleic Acids Res. *15*, 4481–4489.

Smith, D.A. (2002). The Srk1 Protein Kinase Is a Target for the Sty1 Stress-activated MAPK in Fission Yeast. J. Biol. Chem. *277*, 33411–33421.

Soeda, A., Lathia, J., Williams, B.J., Wu, Q., Gallagher, J., Androutsellis-Theotokis, A., Giles, A.J., Yang, C., Zhuang, Z., Gilbert, M.R., et al. (2017). The p38 signaling pathway mediates quiescence of glioma stem cells by regulating epidermal growth factor receptor trafficking. Oncotarget *8*, 33316–33328.

Sosa, M.S., Avivar-Valderas, A., Bragado, P., Wen, H.-C., and Aguirre-Ghiso, J.A. (2011). ERK1/2 and p38α/β Signaling in Tumor Cell Quiescence: Opportunities to Control Dormant Residual Disease. Clin. Cancer Res. *17*, 5850–5857.

Spitzer, E.D., Spitzer, S.G., Freundlich, L.F., and Casadevall, A. (1993). Persistence of Initial Infection in Recurrent Cryptococcus-Neoformans Meningitis. Lancet *341*, 595–596.

Spivey, E.C., Jones, S.K., Jr, Rybarski, J.R., Saifuddin, F.A., and Finkelstein, I.J. (2017). An aging-independent replicative lifespan in a symmetrically dividing eukaryote. Elife *6*, 1751.

Sprague, G.F. (2006). Eukaryotes learn how to count: quorum sensing by yeast. Genes Dev. *20*, 1045–1049.

Steele, D.F., and Jinks-Robertson, S. (1992). An Examination of Adaptive Reversion in *Saccharomyces-cerevisiae*. Genetics *132*, 9–21.

Stern, B., and Nurse, P. (1996). A quantitative model for the cdc2 control of S phase and mitosis in fission yeast. Trends Genet. *12*, 345–350.

Stewart, E.J., Madden, R., Paul, G., and Taddei, F. (2005). Aging and Death in an Organism That Reproduces by Morphologically Symmetric Division. PLoS Biol. *3*, e45.

Stewart, P.S., Franklin, M.J., Williamson, K.S., Folsom, J.P., Boegli, L., and James, G.A. (2015). Contribution of Stress Responses to Antibiotic Tolerance in Pseudomonas aeruginosa Biofilms. Antimicrob. Agents Chemother. *59*, 3838–3847.

Storey, K.B., and Storey, J.M. (2012). Aestivation: signaling and hypometabolism. Journal of Experimental Biology *215*, 1425–1433.

Takeda, K., and Yanagida, M. (2010). In quiescence of fission yeast, autophagy and the proteasome collaborate for mitochondrial maintenance and longevity. Autophagy *6*, 564–565.

Tanaka, K., and Yanagida, M. (1996). A nitrogen starvation-induced dormant G0 state in fission yeast: the establishment from uncommitted G1 state and its delay for return to proliferation. Journal of Cell Science *109 (Pt 6)*, 1347–1357.

Toda, T., Dhut, S., Superti-Furga, G., Gotoh, Y., Nishida, E., Sugiura, R., and Kuno, T. (1996). The fission yeast *pmk1*+ gene encodes a novel mitogen-activated protein kinase homolog which regulates cell integrity and functions coordinately with the protein kinase C pathway. Mol. Cell. Biol. *16*, 6752–6764.

Tom, J.A., Reeder, J., Forrest, W.F., Graham, R.R., Hunkapiller, J., Behrens, T.W., and Bhangale, T.R. (2017). Identifying and mitigating batch effects in whole genome sequencing data. BMC Bioinformatics *18*, 351.

Traxler, M.F., Summers, S.M., Nguyen, H.-T., Zacharia, V.M., Hightower, G.A., Smith, J.T., and Conway, T. (2008). The global, ppGpp-mediated stringent response to amino acid starvation in Escherichia coli. Mol. Microbiol. *68*, 1128–1148.

van Deursen, J.M. (2014). The role of senescent cells in ageing. Nature *509*, 439–446.

Velappan, Y., Signorelli, S., and Considine, M.J. (2017). Cell cycle arrest in plants: what distinguishes quiescence, dormancy and differentiated G1? Ann. Bot. *120*, 495–509.

Vézina, C., Kudelski, A., and Sehgal, S.N. (1975). Rapamycin (AY-22,989), a new antifungal antibiotic. I. Taxonomy of the producing streptomycete and isolation of the active principle. J. Antibiot. *28*, 721–726.

Vonlaufena, A., Phillipsa, P.A., Yanga, L., Xua, Z., Fiala-Beera, E., Zhanga, X., Pirola, R.C., Wilson, J.S., and Apte, M.V. (2010). Isolation of Quiescent Human Pancreatic Stellate Cells: A Promising in vitro Tool for Studies of Human Pancreatic Stellate Cell Biology. Pancreatology *10*, 434–443.

Wajapeyee, N., Serra, R.W., Zhu, X., Mahalingam, M., and Green, M.R. (2008). Oncogenic BRAF Induces Senescence and Apoptosis through Pathways Mediated by the Secreted Protein IGFBP7. Cell *132*, 363–374.

Weisman, R., Choder, M., and Koltin, Y. (1997). Rapamycin specifically interferes with the developmental response of fission yeast to starvation. Journal of Bacteriology *179*, 6325–6334.

Wilkinson, M.G., Samuels, M., Takeda, T., Toone, W.M., Shieh, J.C., Toda, T., Millar, J., and Jones, N. (1996). The Atf1 transcription factor is a target for the Sty1 stress-activated MAP kinase pathway in fission yeast. Genes Dev. *10*, 2289–2301.

Wood, V., Gwilliam, R., Rajandream, M.-A., Lyne, M., Lyne, R., Stewart, A., Sgouros, J., Peat, N., Hayles, J., Baker, S., et al. (2002). The genome sequence of Schizosaccharomyces pombe. Nature *415*, 871–880.

Wood, V., Harris, M.A., McDowall, M.D., Rutherford, K., Vaughan, B.W., Staines, D.M., Aslett, M., Lock, A., Bahler, J., Kersey, P.J., et al. (2011). PomBase: a comprehensive online resource for fission yeast. Nucleic Acids Res. *40*, D695–D699.

Woollard, A., and Nurse, P. (1995). G1 regulation and checkpoints operating around START in fission yeast. Bioessays *17*, 481–490.

Wright, J., Dungrawala, H., Bright, R.K., and Schneider, B.L. (2013). A growing role for hypertrophy in senescence. FEMS Yeast Res. *13*, 2–6.

Wullschleger, S., Loewith, R., and Hall, M.N. (2006). TOR Signaling in Growth and Metabolism. Cell *124*, 471–484.

Wuyts, J., Van Dijck, P., and Holtappels, M. (2018). Fungal persister cells: The basis for recalcitrant infections? PLoS Pathog. *14*, e1007301.

Xu, H.S., Roberts, N., Singleton, F.L., Attwell, R.W., Grimes, D.J., and Colwell, R.R. (1982). Survival and viability of nonculturable *Escherichia coli* and *Vibrio cholerae* in the estuarine and marine environment. Microb. Ecol. *8*, 313–323.

Yaakov, G., Lerner, D., Lerner, D., Bentele, K., Steinberger, J., Steinberger, J., and Barkai, N. (2017). Coupling phenotypic persistence to DNA damage increases genetic diversity in severe stress. Nat Ecol Evol *1*, 0016.

Yanagida, M. (2009). Cellular quiescence: are controlling genes conserved? Trends Cell Biol. *19*, 705–715.

Yao, G. (2014). Modelling mammalian cellular quiescence. Interface Focus *4*, 20130074–20130074.

Yeiser, B., Pepper, E.D., Goodman, M.F., and Finkel, S.E. (2002). SOS-induced DNA polymerases enhance long-term survival and evolutionary fitness. Pnas *99*, 8737–8741.

Yennek, S., and Tajbakhsh, S. (2013). DNA asymmetry and cell fate regulation in stem cells. Semin. Cell Dev. Biol. *24*, 627–642.

Zambrano, M.M., Siegele, D.A., Almirón, M., Tormo, A., and Kolter, R. (1993). Microbial competition: *Escherichia coli* mutants that take over stationary phase cultures. Science *259*, 1757–1760.

Zhu, X., Smith, M.A., Perry, G., Wang, Y., Ross, A.P., Zhao, H.W., LaManna, J.C., and Drew, K.L. (2005). MAPKs are differentially modulated in arctic ground squirrels during hibernation. J. Neurosci. Res. *80*, 862–868.

Zhu, Y.O., Siegal, M.L., Hall, D.W., and Petrov, D.A. (2014). Precise estimates of mutation rate and spectrum in yeast. Proc. Natl. Acad. Sci. U.S.a. *111*, E2310–E2318.

Zinser, E.R., and Kolter, R. (1999). Mutations enhancing amino acid catabolism confer a growth advantage in stationary phase. Journal of Bacteriology *181*, 5800–5807.

Zinser, E.R., and Kolter, R. (2000). Prolonged stationary-phase incubation selects for lrp mutations in Escherichia coli K-12. Journal of Bacteriology *182*, 4361–4365.

Zinser, E.R., and Kolter, R. (2004). *Escherichia coli* evolution during stationary phase. Res. Microbiol. *155*, 328–336.

Zinser, E.R., Schneider, D., Blott, M., and Kolter, R. (2003). Bacterial evolution through the selective loss of beneficial genes: Trade-offs in expression involving two loci. Genetics *164*, 1271–1277.

Zuin, A., Carmona, M., Morales-Ivorra, I., Gabrielli, N., Ayté, J., and Hidalgo, E. (2010). Lifespan extension by calorie restriction relies on the Sty1 MAP kinase stress pathway. Embo J. *29*, 981–991.